Title
Host Pathogen Interaction Regulating the Replication of Bromoviridae Family

Permalink
https://escholarship.org/uc/item/0sj2r01t

Author
CHATURVEDI, SONALI

Publication Date
2014

Peer reviewed|Thesis/dissertation

UNIVERSITY OF CALIFORNIA
RIVERSIDE

Host Pathogen Interaction Regulating the Replication of Bromoviridae Family

A Dissertation submitted in partial satisfaction
of the requirements for the degree of

Doctor of Philosophy

in

Plant Pathology

by

Sonali Anilkumar Chaturvedi

December 2014

Dissertation Committee:
        Prof. A.L.N. Rao, Chairperson
        Prof. Shou-Wei Ding
        Prof. James Ng

The Dissertation of Sonali Anilkumar Chaturvedi is approved:

_____

_____

_____

Committee Chairperson

University of California, Riverside

ACKNOWLEDGEMENTS

me to chase my dreams. Also, I would like to thank my siblings, and extended family for always believing in me, and motivating me.

And at last, I would like to take an opportunity to thank God for blessing me with such a beautiful life with wonderful people around.

Dedication

To my loving grandparents

ABSTRACT OF THE DISSERTATION

Host Pathogen Interaction Regulating the Replication of Bromoviridae Family

by

Sonali Anilkumar Chaturvedi

Doctor of Philosophy, Graduate Program in Plant Pathology
University of California, Riverside, December 2014
Dr. A.L.N. Rao, Chairperson

Positive sense RNA viruses play a central role in the field of virology in general and agriculture in particular. Cucumber mosaic virus (CMV) is a positive sense RNA virus, playing an important role in agriculture because of its broad host range, as it can infect over 1200 species of plants. CMV is sometime accompanied by satellite RNA, a 336 nucleotides long noncoding RNA, which can either ameliorate or intensify symptom expression by the virus. CMV is a multipartite virus, requiring a constellation of three virion particles to initiate a successful infection. **Chapter 1** of this dissertation focuses on optimization the *Agrobacterium* cell concentration of three genomic RNA agroconstructs of Brome mosaic virus (BMV), a widely used model system to study replication, recombination and packaging in positive sense RNA viruses. In this chapter, the focus is made on understanding effect of optical density (O.D$_{600}$) of *Agrobacterium* cell cultures on synchronized infection followed viral gene expression. **Chapter 2** is largely focused on understanding the mechanism

regulating nuclear import of satellite RNA (satRNA) in the presence and absence of CMV. It was identified that Bromodomain containing RNA binding protein (BRP1), an ortholog of which has been previously documented to play an important role in the life cycle of *Potato Spindle Tuber Viroid (*PSTVd), plays a crucial role in the nuclear import of satRNA. Information garnered in this chapter helped bridging the evolutionary gap between satellite RNA and PSTVd. In **chapter 3,** an attempt is made to understand the proteome interacting with BRP1, whose functionality in a plant is yet unknown. By using proteomic approaches, we were able to understand proteome interacting with BRP1 by itself, or in the presence of CMV or satellite RNA in *Nicotiana benthamiana* plants. **Chapter 4** is an extension of chapter 3, where single gene knockout lines of *Arabidopsis thaliana* of short listed host proteins from chapter 3 were tested for their role in CMV replication, and specificaly the role of Glyceraldehyde 3 phosphate dehydrogenase (GAPDH) in replicase complex assembly/stability was studied. Understanding the shift in proteome of host in case of a satRNA is a daunting task (due to the inability of satRNA to code for proteins), hence, we employed riboproteomic approach in **chapter 5** to short list host proteins interacting with satellite RNA in plus- or minus- sense, in the presence or absence of CMV. Viral protein-protein interactions play an important role in the replication of positive sense RNA viruses. **Chapter 6, and 7** focus on comparative study of protein protein interactions for two important members of Bromoviridae family. In chapter 6, live cell imaging using BiFC analysis helped us

visualize protein protein interactions and subcellular localization of BMV proteins.. Finally, in **Chapter 7**, we provide an extensive protein-protein interaction study of CMV viral proteins in vivo using Bimolecular Fluorescence complementation (BiFC) assay.

TABLE OF CONTENTS

CHAPTER 1

Effect of optical density of agroconstructs in the expression of a multipartite positive sense RNA virus genome

CHAPTER 2

A Bromodomain-Containing Host Protein Mediates the Nuclear Importation of a Satellite RNA of *Cucumber Mosaic Virus*

CHAPTER 3

A shift in plant proteome profile for a <u>B</u>romodomain containing <u>RNA</u> binding <u>P</u>rotein (BRP1) in plants infected with Cucumber mosaic virus or its satellite RNA

CHAPTER 4

Evaluating the role of BRP1 and GAPDH in CMV replication

CHAPTER 5

Application of riboproteomics for the identification of RNA-Protein interaction network in a Satellite RNA

CHAPTER 6

Live Cell Imaging of Interactions Between Replicase and Capsid Protein of Brome Mosaic Virus using Bimolecular Fluorescence Complementation: Implications for Replication and Genome Packaging

CHAPTER 7

Protein-Protein Interaction in Cucumber Mosaic Virus

LIST OF TABLES

LIST OF FIGURES

of CMV or satRNA determined by MASCOT.

CHAPTER 4

CHAPTER 7

INTRODUCTION

Positive-strand RNA viruses cause serious diseases in humans, animals and plants. Bromoviridae family is one of the most important families of plant viruses. Its wide host range makes it agronomically important virus family to study (Palukaitis and Garcia-Arenal, 2003). It is characterized by a non-enveloped, icosahedral shape and multipartite virion. Genera like Alfamovirus, Anulavirus, Bromovirus, Cucumovirus, Ilarvirus and Oleavirus belong to Bromoviridae family (Codoner et al., 2005). In this thesis, *Brome mosaic virus* (BMV) or *Cucumber mosaic virus* (CMV) is used to understand the underlying mechanism of the replication of members of Bromoviridae family.

BROME MOSAIC VIRUS

Brome Mosaic Virus (BMV) is a model system to study replication, recombination and encapsidation of positive sense RNA viruses (Ahlquist et al., 1984; Annamalai and Rao, 2007; Bujarski and Dzianott, 1991). Genome of BMV is divided into three different RNAs, where RNA 1 encodes for methyl transferase and helicase domains, RNA 2 encodes for RNA dependent RNA polymerase, and RNA 3 is dicistronic, where 5' end encodes for movement protein and 3' end encodes for subgenomic coat protein (Fig. 1). Most of the studies performed on Brome mosaic virus are carried out to understand the replication (Ahlquist et al.,

1984), genome packaging (Annamalai and Rao, 2006) or to understand the role of cellular membranes in the life cycle of a positive sense RNA virus (Bamunusinghe et al., 2011).

CUCUMBER MOSAIC VIRUS

In the agricultural industry, CMV is of economic importance because of the severity of disease it causes. It exhibits a broad host range comprising over 1200 plant species which include many important crops such as celery, cowpea, cucurbits, lettuce, pepper, tomato, banana, pasture legumes and ornamentals (Jacquemond, 2012; Palukaitis and Garcia-Arenal, 2003b).

It was first reported as a causal agent of a disease in cucumber and muskmelon in Michigan in the year 1916, and since then it has been observed to be a causal agent of several disease epidemics throughout the world (Jacquemond, 2012; Palukaitis and Garcia-Arenal, 2003b). CMV is an icosahedral virus with $T=3$ quasismymmetry (Smith et al., 2000). Virion consists of 180 identical subunits of capsid protein forming a shell around viral RNA, which constitutes 18% of total volume (Smith et al., 2000). It is a tripartite virus, with three morphologically indistinguishable virus particles encapsidating three genomic (RNAs 1, 2 and 3) and a single subgenomic RNA (RNA4) (Fig. 2) (Jacquemond, 2012; Palukaitis and Garcia-Arenal, 2003b). The genome of CMV

2

consists of three 5'-capped positive-strand RNAs. RNA1 and -2 encode nonstructural proteins p1a and p2a, respectively, and form a functional replication complex (Jacquemond, 2012; Palukaitis and Garcia-Arenal, 2003b). RNA2 also encodes another nonstructural protein 2b, a well-characterized suppressor of RNA silencing (Ding et al., 1994). RNA3 is dicistronic, encoding two proteins, a movement protein (MP) and a coat protein (CP), that are involved in cell-to-cell and long-distance movement of the virus (Canto et al., 1997; Schmitz and Rao, 1998). Both MP and CP are dispensable for RNA replication but are required for whole-plant infection (Boccard and Baulcombe, 1993). CMV capsid protein is a determinant of transmission by aphid vectors (Ali et al., 2006). Evolution of capsid protein in different subgroups of CMV leads to the difference in selection pressure on transmissibility by aphids, and in turn affects the evolution of the virus (Moury, 2004). Previous data has demonstrated that CMV CP is the key factor for aphid transmission, as the transmission of CMV virion from inoculum containing CMV RNA 3 from one strain, and RNAs 1 and 2 from a different strain was demonstrated to be specific for the strain of RNA 3 (Mossop and Francki, 1977). CMV strains are classified into subgroups I and II (Jacquemond, 2012; Palukaitis and Garcia-Arenal, 2003b). A notable feature that distinguishes CMV strains of subgroup II from those of subgroup I is the presence of an additional RNA species, referred to as RNA5 (de Wispelaere and Rao, 2009). Molecular characterization of RNA5 revealed that it is a mixture of

the 3'-terminal 307- and 304-nt regions of CMV RNA2 and 3 respectively and is produced in replication-independent manner (de Wispelaere and Rao, 2009).

CMV is transmitted from one plant to another in a non-persistent manner (where the retention time of the virus is very short) by aphids (Palukaitis et al., 1992). More than 80 species of aphids can transmit CMV. Specifically, *Myzus persicae* and *Aphis gossypii* are considered to be most efficient aphids to transmit CMV (Ali et al., 2006). In addition to encapsidate viral genome, multifunctional capsid protein of CMV mediates virus movement in, and between, plants (Palukaitis and Garcia-Arenal, 2003a). Transmissibility of CMV by aphid vectors is stable under the conditions of repeated mechanical passaging. In case of *M persicae* and *A. gossypii*, the virion was successfully transmitted even after 24 mechanical passages (Ng, 1999). Aphid transmission of CMV is determined by amino acids of capsid protein either exposed on the outer surface of the virion, or buried in the virion structure (Smith et al., 2000). In case of *A. gossypii,* amino acids at position 129 and 162 (Perry et al., 1994), and for *M. persicase*, amino acids at position 25, 129, 168, 169 and 214 are considered to play an important role in vector-mediated transmission of the virus (Perry et al., 1998).

SUBVIRAL PATHOGENS

Subviral pathogens can be classified as (a) virus dependent or (b) virus independent subviral pathogen. Satellite RNA and human *Hepatitis Delta Virus* (HDV) fall in virus dependent category, and viroids fall in virus independent category.

(A) SATELLITE RNA AND VIRUSES

Some plant viruses are associated with a small molecular parasite, sometimes being commensal or even beneficial, and are among the simplest life forms, namely, satellite RNAs (satRNAs) and satellite viruses (Hu et al., 2009). These satRNAs are short RNA molecules, usually 200-1,500 nt, that depend on cognate helper viruses for replication, encapsidation, movement, and transmission, but most share little or no sequence homology to the helper viruses (Hu et al., 2009). In contrast, satellite viruses are satRNAs that encode and are encapsidated in their own capsid proteins (Hu et al., 2009). satRNAs have gained a special interest in the field of plant virology due to their ability to modulate symptom induction by their helper virus in plants. (Hu et al., 2009).

(i) SATELLITE RNA ASSOCIATED WITH CMV

satRNAs associated with CMV are among the earliest found and well-studied subviral pathogens (Hu et al., 2009). CMV satRNAs have 5'-capped, noncoding, single-stranded RNA genomes of 330 to 405 nucleotides (nt) (Fig. 3, 4)(Hu et al., 2009). They exhibit a high secondary structure with 50% intramolecular base pairing, sharing little or no sequence homology with their HV (Hu et al., 2009). During replication by HV, Cucumovirus satRNAs have been shown to generate multimers of dimeric and tetrameric forms (Kuroda et al., 1997; Seo et al., 2013). Some satRNAs (i.e., Nepovirus and Sobemovirus satRNAs) generate multimeric intermediates by a rolling-circle mechanism and produce monomeric progeny by autocatalytic cleavage (Forster and Symons, 1987). However, this is unlikely to be applicable to multimeric forms of Cucumovirus satRNAs since no circular intermediates have been detected (Linthorst and Kaper, 1984). Although it was suggested that CMV satRNAs can produce dimeric forms by self-ligation of double- stranded RNA (dsRNA) monomeric forms (Roossinck et al., 1992) , the mechanism involved in the production of multimeric forms is not well understood. Interestingly, CMV satRNA has been shown to survive for up to 25 days without its HV (Mossop and Francki, 1978). However, the molecular basis of this abnormal long-term survival of CMV satRNA remains obscure although their high secondary structure was envisioned to contribute to this HV-independent survival (Roossinck et al., 1992). However,

a more recent cell-biology based evidence suggested that the stability of satRNA could be due to its propensity to localize in the nucleus (Choi et al., 2012).

OTHER SUBVIRAL PATHOGENS

Properties that distinguish satRNA from HDV and viroid are schematically shown in Fig.4. Based on phylogenetic studies done by Elena *et al*, all three subviral pathogens are considered to be evolutionarily related (Elena et al., 1991). Viroid was discovered in the year 1971(Diener, 1971). It is a small, circular, single stranded, noncoding RNA, having a high secondary structure, and unlike satellite RNA they are neither replicated or encapsidated by a virus (Ding, 2009). They autonomously replicate in the nucleus of a cell using host transcriptional machinery (DNA dependent RNA polymerase II (pol II)) by rolling-circle mechanism (Ding, 2009). Third subviral pathogen, HDV was first discovered in the year 1977 in the nucleus of hepatocytes from patients infected with hepatitis B virus (HBV) (Rizzetto et al., 1980). It has a small circular RNA genome with only ~1700 nucleotides and uses HBV's replication machinery to replicate its own genome by using rolling circle mechanism and the only functional ORF encoded by HDV is delta antigen (Chang et al., 2008).

VIRUS-HOST PROTEIN INTERACTIONS

A successful infection by any RNA virus includes entry into a host, translation of replicase proteins followed by RNA replication, genome packaging, short and long distance movement in a host, and release into the environment. Viruses use an ingenious approach to overcome their inability to code for large number of proteins by usurping host organelles, proteins and metabolites in their life cycle (Laliberte and Sanfacon, 2010; Verchot, 2011). It is well documented that several viruses use different cellular compartments for replicating their genome, endoplasmic reticulum as in case of *Polio virus* (Schlegel et al., 1996) and *Brome mosaic virus*, mitochondria as in case of *Flock house virus* and peroxisomes as in case of *Tomato bushy stunt virus* (Denison, 2008). Literature is replete with enumerating the role of host proteins in positive sense RNA virus life cycle, where these proteins are observed to orchestrate different steps in viral replication (Table 1) (Nagy and Pogany, 2012). For example, eukaryotic EF1α is observed to be involved in RNA recruitment and (-) sense RNA synthesis in case of *West Nile Virus,* and viral replicase complex assembly is carried out by HSP90 for *Hepatitis C Virus* (Nagy and Pogany, 2012). Viruses induce membrane remodeling to facilitate replication of its genome. It has been observed that in *Polio virus*, viral replication organelle is formed by host encoded ARF1-GTPase and its guanine nucleotide exchange factor-GBF1 (Nagy and Pogany, 2012). Virus can utilize host machinery to shuttle its proteins from one organelle to

another, as in the case of *Tomato bushy stunt virus* (TBSV), host Pex 19p is observed to transport viral replicase protein (p33) to the site of viral replication (i.e., Peroxisomes) (Nagy and Pogany, 2012).

Figure 1. Genome organization of Brome mosaic virus
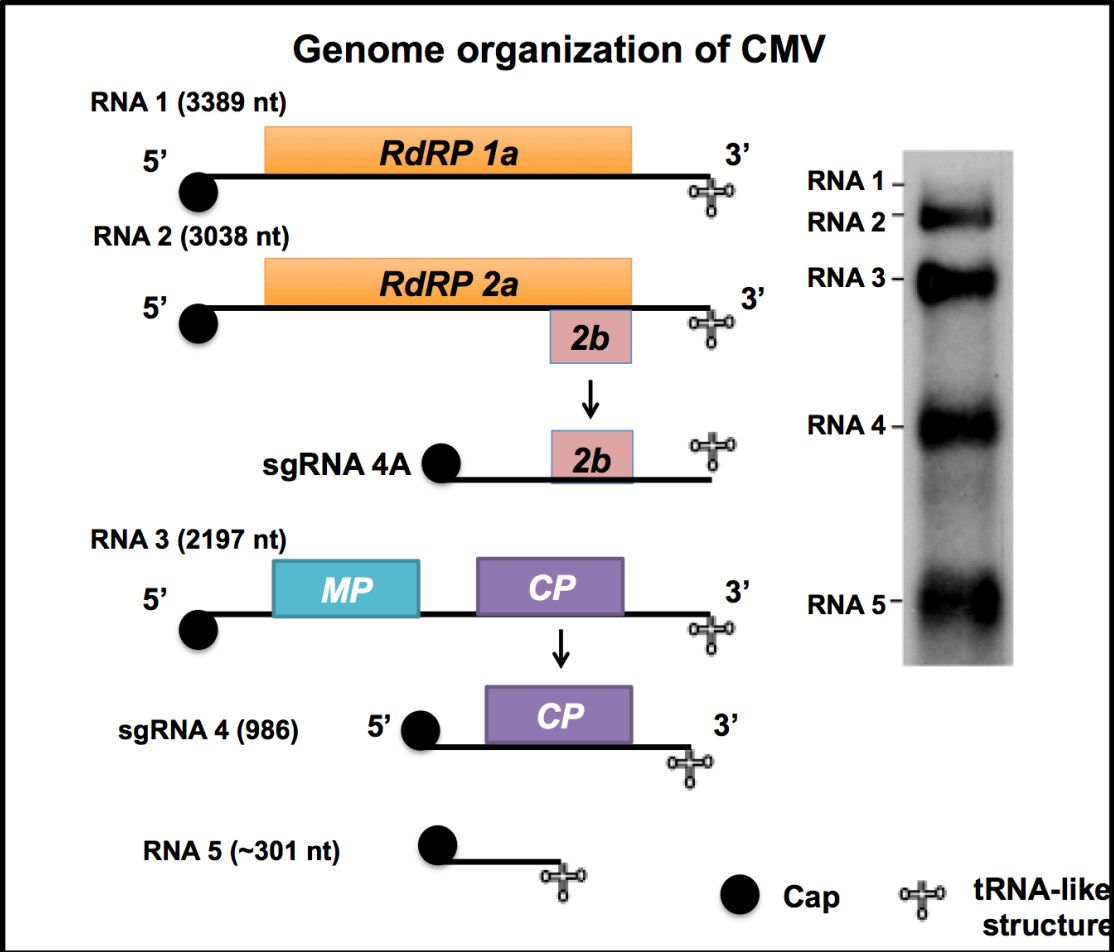
Figure 2. Genome organization of Cucumber mosaic virus

SatRNA (336 nt)
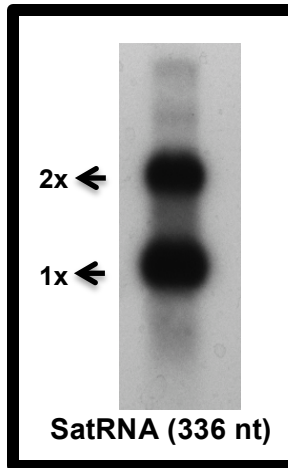
Figure 3. Genome organization of Satellite RNA associated with Cucumber mosaic virus

Figure 4. Distribution and properties of subviral pathogens
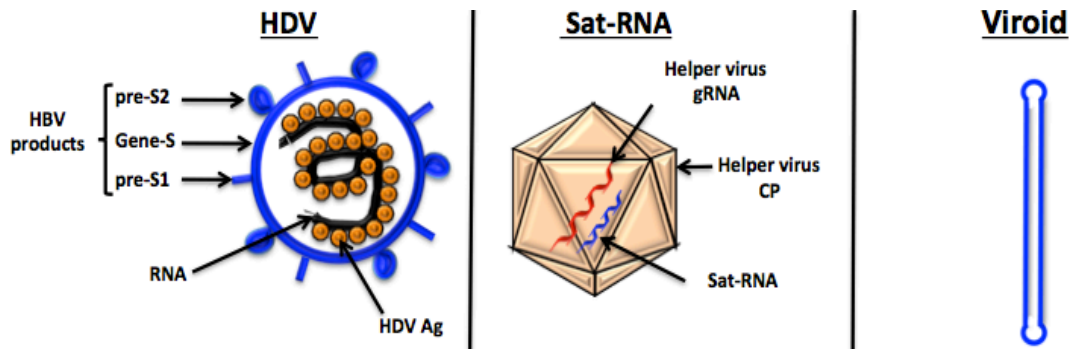
Trait	HDV	Sat-RNA	Viroid (eg. PSTVd)
Host	Humans	Plants	Plants
Helper Virus (HV)	Hepatitis B virus (HBV)	Cucumber mosaic virus (CMV)	None
Genome	RNA	RNA	RNA
Replication	RNA polymerase II	Helper virus replicase	RNA polymerase II
Site of replication	Nucleus	Cytoplasm	Nucleus
Coding capacity	Delta antigen	None	None
Encapsidation	HBV envelope	HV capsid protein	None

Host factors	Viruses	Function
RNA- binding proteins		
eEF1α	Tomato Bushy Stunt Virus, West Nile Virus	RNA recruitment and (-) RNA synthesis
Cellular chaperones		
HSP90	Flock House Virus, Hepatitis C Virus	Viral Replicase complex assembly or activation
Protein targeting		
TOM1 and TOM3	Tomato mosaic virus	Replication protein targeting, and anchoring to membranes
Membrane remodelling and lipid synthesis		
ARF1, GBF1	Polio virus	Viral replicase and organelle formation
Cellular lipids		
Phospholipids	Tomato bushy stunt virus, Flock house virus	Viral replicase complex formation
Membrane shaping proteins		
Reticulons	Brome mosaic virus	Viral replicase complex formation
Other host proteins		
PMR1, ECA1 and ECA3	Tomato bushy stunt virus	Viral replicase complex activity and RNA recombination

Table 1. Example of host proteins playing an important role in the replication of positive sense RNA viruses (adapted from

REFERENCE

1.   **Ahlquist, P., Dasgupta, R., Kaesberg, P., 1984.** Nucleotide sequence of the brome mosaic virus genome and its implications for viral replication. Journal of molecular biology 172, 369-383.

2.   **Ali, A., Li, H., Schneider, W.L., Sherman, D.J., Gray, S., Smith, D., Roossinck, M.J., 2006.** Analysis of genetic bottlenecks during horizontal transmission of Cucumber mosaic virus. Journal of virology 80, 8345-8350.

3.   **Annamalai, P., Rao, A.L., 2006.** Packaging of brome mosaic virus subgenomic RNA is functionally coupled to replication-dependent transcription and translation of coat protein. Journal of virology 80, 10096-10108.

4,   **Annamalai, P., Rao, A.L., 2007.** In vivo packaging of brome mosaic virus RNA3, but not RNAs 1 and 2, is dependent on a cis-acting 3' tRNA-like structure. Journal of virology 81, 173-181.

5.   **Bamunusinghe, D., Seo, J.K., Rao, A.L., 2011.** Subcellular localization and rearrangement of endoplasmic reticulum by Brome mosaic virus capsid protein. Journal of virology 85, 2953-2963.

6.   **Boccard, F., Baulcombe, D., 1993.** Mutational analysis of cis-acting sequences and gene function in RNA3 of cucumber mosaic virus. Virology 193, 563-578.

7.   **Bujarski, J.J., Dzianott, A.M., 1991.** Generation and analysis of nonhomologous RNA-RNA recombinants in brome mosaic virus: sequence complementarities at crossover sites. Journal of virology 65, 4153-4159.

8.   **Canto, T., Prior, D.A., Hellwald, K.H., Oparka, K.J., Palukaitis, P., 1997.** Characterization of cucumber mosaic virus. IV. Movement protein and coat protein are both essential for cell-to-cell movement of cucumber mosaic virus. Virology 237, 237-248.

9.   **Chang, J., Nie, X., Chang, H.E., Han, Z., Taylor, J., 2008.** Transcription of hepatitis delta virus RNA by RNA polymerase II. Journal of virology 82, 1118-1127.

10.   **Choi, S.H., Seo, J.K., Kwon, S.J., Rao, A.L., 2012.** Helper virus-independent transcription and multimerization of a satellite RNA associated with cucumber mosaic virus. Journal of Virology 86, 4823-4832.

11.   **Codoner, F.M., Cuevas, J.M., Sanchez-Navarro, J.A., Pallas, V., Elena, S.F., 2005.** Molecular evolution of the plant virus family Bromoviridae based on RNA3-encoded proteins. Journal of molecular evolution 61, 697-705.

12.   **de Wispelaere, M., Rao, A.L., 2009.** Production of cucumber mosaic virus RNA5 and its role in recombination. Virology 384, 179-191.

13.   **Denison, M.R., 2008.** Seeking membranes: positive-strand RNA virus replication complexes. PLoS biology 6, e270.

14.   **Diener, T.O., 1971.** Potato spindle tuber "virus". IV. A replicating, low molecular weight RNA. Virology 45, 411-428.

15.   **Ding, B., 2009.** The biology of viroid-host interactions. Annual review of phytopathology 47, 105-131.

16.   **Ding, S.W., Anderson, B.J., Haase, H.R., Symons, R.H., 1994.** New overlapping gene encoded by the cucumber mosaic virus genome. Virology 198, 593-601.

17.   **Elena, S.F., Dopazo, J., Flores, R., Diener, T.O., Moya, A., 1991.** Phylogeny of viroids, viroidlike satellite RNAs, and the viroidlike domain of

hepatitis delta virus RNA. Proceedings of the National Academy of Sciences of the United States of America 88, 5631-5634.

18.   **Forster, A.C., Symons, R.H., 1987.** Self-cleavage of plus and minus RNAs of a virusoid and a structural model for the active sites. Cell 49, 211-220.

19.   **Hu, C.-C., Hsu, Y.-H., Lin, N.-S., 2009.** Satellite RNAs and Satellite Viruses of Plants. Viruses 1, 1325-1350.

20.   **Jacquemond, M., 2012.** Cucumber mosaic virus. Advances in virus research 84, 439-504.

21.   **Kuroda, T., Natsuaki, T., Wang, W.Q., Okuda, S., 1997.** Formation of multimers of cucumber mosaic virus satellite RNA. The Journal of general virology 78 (Pt 4), 941-946.

22.   **Laliberte, J.F., Sanfacon, H., 2010.** Cellular remodeling during plant virus infection. Annual review of phytopathology 48, 69-91.

23.   **Linthorst, H.J., Kaper, J.M., 1984.** Replication of peanut stunt virus and its associated RNA 5 in cowpea protoplasts. Virology 139, 317-329.

24. **Martin, B., Collar, J.L., Tjallingii, W.F., Fereres, A., 1997.** Intracellular ingestion and salivation by aphids may cause the acquisition and inoculation of non-persistently transmitted plant viruses. The Journal of general virology 78 (Pt 10), 2701-2705.

25. **Mossop, D.W., Francki, R.I., 1977.** Association of RNA 3 with aphid transmission of cucumber mosaic virus. Virology 81, 177-181.

26. **Mossop, D.W., Francki, R.I., 1978.** Survival of a satellite RNA in vivo and its dependence on cucumber mosaic virus for replication. Virology 86, 562-566.

27. **Moury, B., 2004.** Differential selection of genes of cucumber mosaic virus subgroups. Molecular biology and evolution 21, 1602-1611.

28. **Nagy, P.D., Pogany, J., 2012.** The dependence of viral RNA replication on co-opted host factors. Nature reviews. Microbiology 10, 137-149.

29. **Ng, J., and Perry, K.L, 1999.** Stability of the aphid transmission phenotype in cucumber mosaic virus. Plant Pathol 48, 388-394.

30. **Palukaitis, P., Garcia-Arenal, F., 2003.** Cucumoviruses. Advances in virus research 62, 241-323.

31.   **Palukaitis, P., Roossinck, M.J., Dietzgen, R.G., Francki, R.I., 1992.** Cucumber mosaic virus. Advances in virus research 41, 281-348.

32.   **Perry, K.L., Zhang, L., Palukaitis, P., 1998.** Amino acid changes in the coat protein of cucumber mosaic virus differentially affect transmission by the aphids Myzus persicae and Aphis gossypii. Virology 242, 204-210.

33.   **Perry, K.L., Zhang, L., Shintaku, M.H., Palukaitis, P., 1994.** Mapping determinants in cucumber mosaic virus for transmission by Aphis gossypii. Virology 205, 591-595.

34.   **Rizzetto, M., Shih, J.W., Gerin, J.L., 1980.** The hepatitis B virus-associated delta antigen: isolation from liver, development of solid-phase radioimmunoassays for delta antigen and anti-delta and partial characterization of delta antigen. Journal of immunology 125, 318-324.

35.   **Roossinck, M.J., Sleat, D., Palukaitis, P., 1992.** Satellite RNAs of plant viruses: structures and biological effects. Microbiol Rev 56, 265-279.

36.   **Schlegel, A., Giddings, T.H., Jr., Ladinsky, M.S., Kirkegaard, K., 1996.** Cellular origin and ultrastructure of membranes induced during poliovirus infection. Journal of virology 70, 6576-6588.

37.   **Schmitz, I., Rao, A.L., 1998.** Deletions in the conserved amino-terminal basic arm of cucumber mosaic virus coat protein disrupt virion assembly but do not abolish infectivity and cell-to-cell movement. Virology 248, 323-331.

38.   **Seo, J.K., Kwon, S.J., Chaturvedi, S., Ho Choi, S., Rao, A.L., 2013.** Functional significance of a hepta nucleotide motif present at the junction of Cucumber mosaic virus satellite RNA multimers in helper-virus dependent replication. Virology 435, 214-219.

39.   **Smith, T.J., Chase, E., Schmidt, T., Perry, K.L., 2000.** The structure of cucumber mosaic virus and comparison to cowpea chlorotic mottle virus. Journal of virology 74, 7578-7586.

40.   **Verchot, J., 2011.** Wrapping membranes around plant virus infection. Curr Opin Virol 1, 388-395.

CHAPTER 1

Effect of optical density of agroculture in the expression of a multipartite

positive sense RNA virus genome

ABSTRACT

Agrobacterium mediated transient expression of genes, because of its efficiency in delivering all the components to a single cell, is the most widely used approach for studying life cycle of multipartite viruses. Overexpression of one component of virus to understand how a particular protein will affect overall replication of the virus is an important area to study. Infiltrating higher optical density (OD_{600}) of bacterial cell suspension can be used to achieve higher protein expression. An attempt is made to analyze the effect of optical density in understanding the role of one protein in overall replication process. It was observed that transiently expressed coat protein was different from replication derived coat protein. Moreover, the replication of BMV was down-regulated in samples with 1.0 and 2.0 OD_{600} of agroculture containing coat protein (CP), but similar effect was also observed in case of Empty vector (EV). These results suggest that the down-regulation was an effect of high cell density of agrocultures containing CP or EV. Further, it was observed (OD_{600}) more than 0.5 leads to senescence in leaves, which might affect viral replication.

23

INTRODUCTION

Study of genome replication is cardinal for understanding the life cycle of any virus pathogenic to humans, animals and plants. Immense research has been carried out to understand the mechanism underlying replication process in positive sense RNA viruses pathogenic to eukaryotic cells (Annamalai et al., 2008a; Baumstark and Ahlquist, 2001; Dinant et al., 1993). Plant viruses have been used as model systems for advancing our knowledge on replication mechanisms in positive sense RNA viruses. There are different systems in which a plant virus replication can be studied. Some of these include plant protoplasts, yeast or whole plant systems (Annamalai et al., 2008a; Garcia-Ruiz and Ahlquist, 2006; Watts et al., 1987). In case of plant viruses, a study of viral replication, or movement, if carried out in an intact plant, mimics resulting processes close to natural settings.

There are two standardized methods by which viral genes are delivered into plants: (a) Mechanical inoculation, (b) *Agrobacterium* mediated transient expression (Agroinfiltration) (Bamunusinghe et al., 2011a; Chaturvedi et al., 2012b). Mechanical inoculation is routinely used to deliver viral RNAs into leaves (Hull, 2009). Although, the technique is efficient enough to initiate infection for mono-component viruses like TMV but not for multicomponent RNA viruses such as CMV, where initiation of virus infection requires presence of all three genomic

RNA components in the same cell. This inherent requirement can be circumvented by agroinfiltration that allows more than 90% of cells synchronously receive up to 5 plasmids to the same cell as outlined by Annamalai and Rao (2005b). Furthermore, agroinfiltration is ideal for expressing higher or lower mounts of a given protein by altering OD_{600} of corresponding agroculture (Yi et al., 2009a). Although the effect of increasing concentration of a given agroculture on the host and *trans*-gene expression was previously investigated (Wroblewski**,**et al.*,* 2005) , but not in viral replication.

Consequently, we initiated a project to standardize various parameters of agroinfiltration that affect overall virus replication and gene expression. We approached this issue by using agroconstructs of BMV (Annamalai and Rao, 2005b). BMV is a tripartite virus, where three genomic RNAs are encapsidated into an individual virus particle (Bamunusinghe et al., 2011a). Two non-structural proteins encoded by RNAs 1 and 2 constitute the functional replicase complex. Dicistronic RNA 3 encodes for a non-structural movement protein (MP), and a structural capsid protein (CP) translated from a subgenomic RNA 4 synthesized via internal initiation from progeny (-) RNA3. Our study revealed that agrocultures exceeding cell density more than 1.0 (OD_{600}) had negative effect on host, gene expression and ultimately viral replication.

MATERIALS AND METHODS

Agroinfiltration

Agroinfiltration was performed in *N. benthamiana* plants. Construction and characterization of T-DNA based plasmids for expression of full length BMV genomic RNAs and BMV CP (BCP) has been previously described (Annamalai and Rao, 2005b), along with CP variant BCPKO (^{1251}AUG^{1253} to ^{1251}AUA^{1253} and ^{1275}AUG^{1277} to ^{1275}AUA^{1277}) (de Wispelaere et al., 2011) and 35S-B3/ΔCP-eGFP (Annamalai and Rao, 2005a). Infiltration of empty vector (EV) Pcass-RZ served as a control. Agroinfiltration procedure was performed as described previously (Chaturvedi et al., 2012b). Agrocultures of BMV RNA 1, RNA 2, RNA 3 and BCPKO were infiltrated at a concentration of 0.1 OD$_{600}$ while the cell concentrations of EV or BCP varied in each experiment as specified under figure legends (Fig. 1.1, 1.2, 1.3).

Progeny analysis

Total RNA was isolated from 4 days post infiltration (dpi) leaf samples using Trizol (Sigma, U.S.A). Northern blot analysis of total RNA (10 μg) was performed and probed using ^{32}P B3 TLS as described previously (Annamalai et al., 2008a). Total protein from infiltrated leaf samples was extracted as follows.

Briefly, the leaf tissue was ground in liquid nitrogen, and was re-suspended in 500 µl of protein extraction buffer (50mM Tris-HCl at pH 8.0, 150mM NaCl, 0.5% Triton X-100, 0.2% 2-mercaptoethanol, 5% glycerol and proteinase inhibitor cocktail [Sigma, USA]). The resulting leaf extract was centrifuged at 10,000 rpm for 5 minutes, and supernatant was used as soluble protein fraction for subsequent western blot analysis. Total protein was subjected to SDS-PAGE followed by immunoblot analysis using anti-CP antibodies (Bamunusinghe et al., 2013b).

RESULTS

Difference between the replication derived coat protein and transiently expressed coat protein

To understand the difference between expression level of replication derived coat protein and transiently expressed coat protein, 0.5 OD_{600} of BMV RNA1+ RNA2+ RNA3 or BMV RNA1+ RNA2+ B3CPKO (B3 coat protein knockout) + B4a agrocultures were infiltrated to *N. benthamiana* leaves. Total protein was extracted at 2dpi and 4dpi, and subjected to western blot analysis for detection of coat protein. It was observed that the transiently expressed coat protein was 59% of the replication derived coat protein in case of day two and was 71% in case of day 4 compared to replication derived coat protein (Fig. 1.1A). Taken together, these results suggest that the replication derived coat protein is different in terms of expression level as compared to the transiently expressed coat protein.

Further, expression level of B4 was monitored at different $O.D_{600}$ in planta. To that end, agrocultures carrying B4 construct was infiltrated to *N. benthamiana* leaves and at 4dpi, total protein was extracted, and was subjected to western blot analysis using antibody against coat protein (CP) (Fig. 1.1B). It

was observed that B4 started appearing at 0.5 OD_{600} of agroculture against coat protein.

Taken together, it was observed that the transiently expressed coat protein was not expressed to the level as replication derived coat protein (Fig 1.1 A), suggesting that coat protein coming via replication is more efficient than transiently expressed coat protein. Moreover, when coat protein was expressed by itself, there was a gradual increase in the expression of coat protein with the increase in OD_{600} of B4 agroculture (Fig. 1.1 B), suggesting that the transcripts synthesized in case of transient expression of coat protein are subjected to translation, and are comparable to the concentration of input agroculture.

Effect of increasing OD of B4 on the replication of BMV

To determine the effect of B4 on replication of BMV, (0.1 OD_{600}) of B1+B2+B3 with increasing concentration of B4 (0 OD_{600} or 0.03 OD_{600}, or 0.1 OD_{600}, or 0.2 OD_{600} or 0.5 OD_{600} or 1.0 OD_{600} or 2.0 OD_{600}) were infiltrated to *N. benthamiana* leaves. At 4 dpi, total RNA and protein was extracted. RNA was further subjected to northern blot analysis and probed for B3 TLS, whereas protein was subjected to western blot analysis to detect coat protein. As demonstrated in the result (Fig. 1.2, 1.3), it was observed that increasing the concentration of coat protein didn't alter the expression level of coat protein

tremendously. Though, the northern blot analysis demonstrate that the replication of BMV was highest when all the components were infiltrated at the same OD_{600} (ie., 0.1 OD_{600}), whereas increasing the OD_{600} to 2.0, affected replication of BMV tremendously.

Effect of increasing OD_{600} of Empty vector (EV) on the replication of BMV

To determine if transiently expressed coat protein affects the replication of BMV, or it was the high cell concentration which affected the replication of the virus, agrocultures of B1+B2+B3 (0.1 OD_{600}) with increasing concentration of EV (0 OD_{600} or 0.03 OD_{600}, or 0.1 OD_{600}, or 0.2 OD_{600} or 0.5 OD_{600} or 1.0 OD_{600} or 2.0 OD_{600}) were infiltrated to *N. benthamiana* leaves. At 4 dpi, total RNA and protein was subjected to Northern and western blot analysis. As demonstrated in results (Fig. 1.4, 1.5), it was observed that increasing the concentration of EV didn't alter the expression level of coat protein. In case of RNA accumulation, it was observed that as the concentration of EV increased, the RNA accumulation of BMV decreased, suggesting the role of cell density in the expression level of viral genome.

Effect of high cell density on the leaf phenotype

Further, effect of increase in cell density of empty vector on the phenotype of leaf was studied. Increasing OD_{600} of EV was infiltrated to 4 weeks old *N. benthamiana* leaf, and at 8 dpi, phenotypes of the infiltrated leaf was studied. Senescence was observed on leaves infiltrated with 1.0 or 2.0 OD_{600} of EV (Fig. 1.6). Above result suggests that the concentration of agrobacterium higher than 0.5 OD_{600} is detrimental to the cell, and it might affect the replication of virus.

DISCUSSION

Capsid protein of a positive sense RNA virus plays a pivotal role not only in providing the structure to a virus, but also in the replication of viral genome. It has been previously demonstrated that adding CP exogenously to genomic RNAs of Alfalfa Mosaic Virus (AMV) increased the infectivity of virus in protoplasts (Houwing and Jaspars, 2000). In case of BMV, observation that replication is intricately associated with packaging re-evaluates the role of CP in the replication of positive sense RNA virus (Annamalai and Rao, 2006c). Understanding the effect of higher concentration of CP would help evaluate the role of CP in a concentration dependent manner. Yi et.al has previously demonstrated the negative effect of high concentration of CP on the replication of BMV (Yi et al., 2009a), where it has been observed that increasing the OD_{600} of CP down regulated the replication of BMV, though there no demonstration of increase in CP synthesized by infiltrating higher OD_{600} of agroculture containing BMV CP was provided (Yi et al., 2009a). Hence, in this piece of data, we extensively evaluated various factors that might affect the replication of BMV by keeping CP in the center.

It has been suggested previously that increasing the concentration of CP by transiently expressing CP genome under 35S promoter affects the replication of virus compared to the replication derived CP (Yi et al., 2009a). To compare the

expression level of replication derived CP to transiently expressed one, transient expression of CP in the presence of RNA 1, 2 and 5' region of RNA 3 (encoding for MP) was carried out, and compared to the wild type BMV CP (coming via replication) (Fig. 1.1A). Whereas, increasing the OD_{600} of CP for transient expression of CP suggests a gradual increase in the level of detectable CP suggesting successful synthesis of viral protein in a concentration dependent manner (Fig. 1.1B), though increasing OD_{600} of agroculture of transiently expressing CP in the presence of CP coming via replication, didn't represent similar pattern of increase in CP synthesis (Fig. 1.2B, 1.3). Recycling of mRNA for the accumulation of CP in more or less same concentration suggests that CP accumulation reaches a plateau and did not increase further even when higher OD_{600} of transiently expressed CP was added to the sample. In case of replication, viral RNA replication increases to an extent when 0.1 OD_{600} of transiently expressed CP was added, but decreased as the OD_{600} increased to 2.0. This decrease in the replication of viral RNAs is a demonstration of phenomena other than previously speculated negative feedback of replication of viral genome by CP.

In this systematic evaluation of various factors, including concentration of CP to optical density of agro-constructs, effect of higher OD_{600} of agroculture is studied. From results, it is observed that by increasing OD_{600} of empty vector, replication of viral genome decreases (Fig. 1.4A, 1.5), though protein expression

33

remains unaltered (Fig. 1.4B, 1.5). This suggests that higher cell density was responsible for previously observed down-regulation of viral RNA synthesis.

Optical density is known to play an important role in the transient expression of genes. It has been previously demonstrated that the optimal cell density of agrobacterium for GV3101 cells is ~0.6 for the transient expression of GUS gene, and with increase in the cell density, the expression level of GUS decreased (Kim et al., 2009). Also, yellowing of leaves have been previously observed on infiltrating bacterial culture above OD_{600} to be 1.0 (Wroblewski et al., 2005). To this end, increasing concentration of agrobacterium suspension containing empty vector (pCASS) was infiltrated to 4 weeks old *N. benthamiana* leaves. At 8 dpi, yellowing of leaves was observed in case of leaves with OD_{600} 1.0 or OD_{600} 2.0 (Fig. 1.6). This suggests that downregulation observed in the replication level of viral genome could be a result of leaf senescence, and not a feedback inhibition of weak transient expression of CP. It is imperative to optimize optical density of agrobacterium containing viral genome for studying the replication of a multipartite viral genome. It is necessary to device an approach to overexpress a viral protein without increasing the optical density of agrobacterium carrying that particular gene more than 1.0 OD_{600}, as the resultant effect of higher optical density could be an indicative of stress induced in case of higher density of agrobacterium.
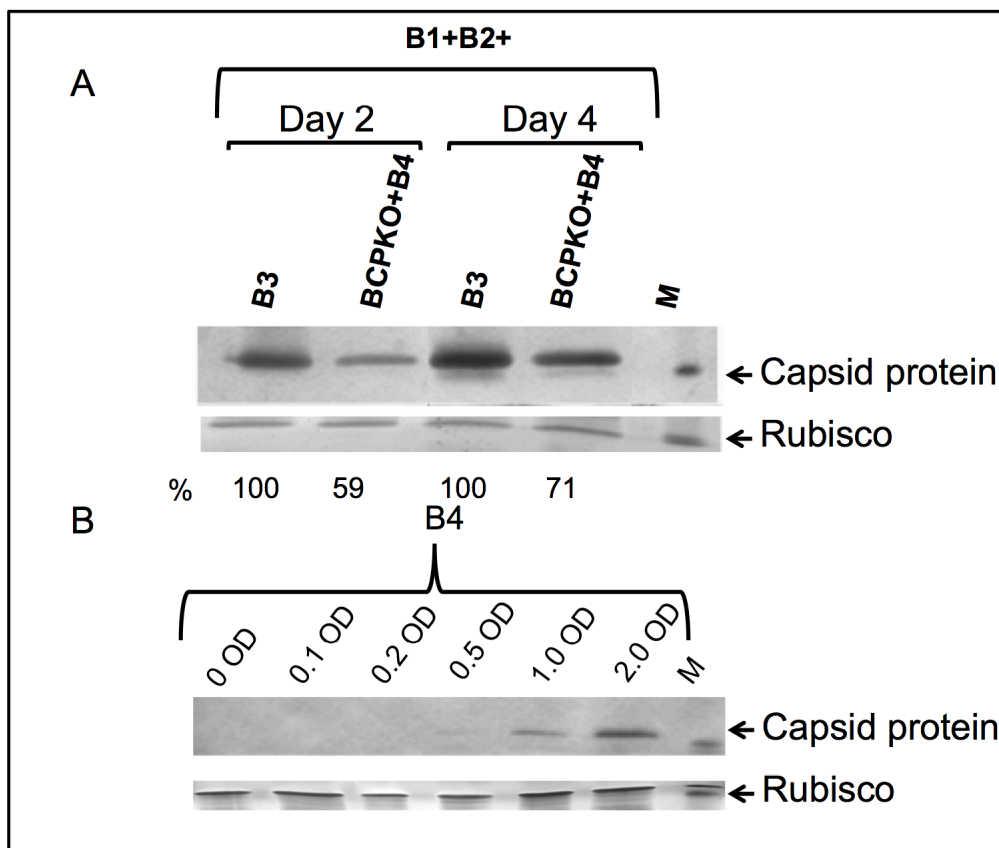
Figure 1.1 Difference between the replication derived coat protein and transiently expressed coat protein. (A) *N benthamiana* leaves were infiltrated with 0.5 OD$_{600}$ of B1+B2+B3 or B1+B2+ BCPKO+B4. At 2 dpi or 4dpi, total protein was extracted from the leaves and western blot analysis was performed using antibodies against CP. (B) Capsid protein was transiently expressed at different cell concentration (as mentioned in the figure), and at 4dpi western blot analysis was performed on total protein to detect CP.
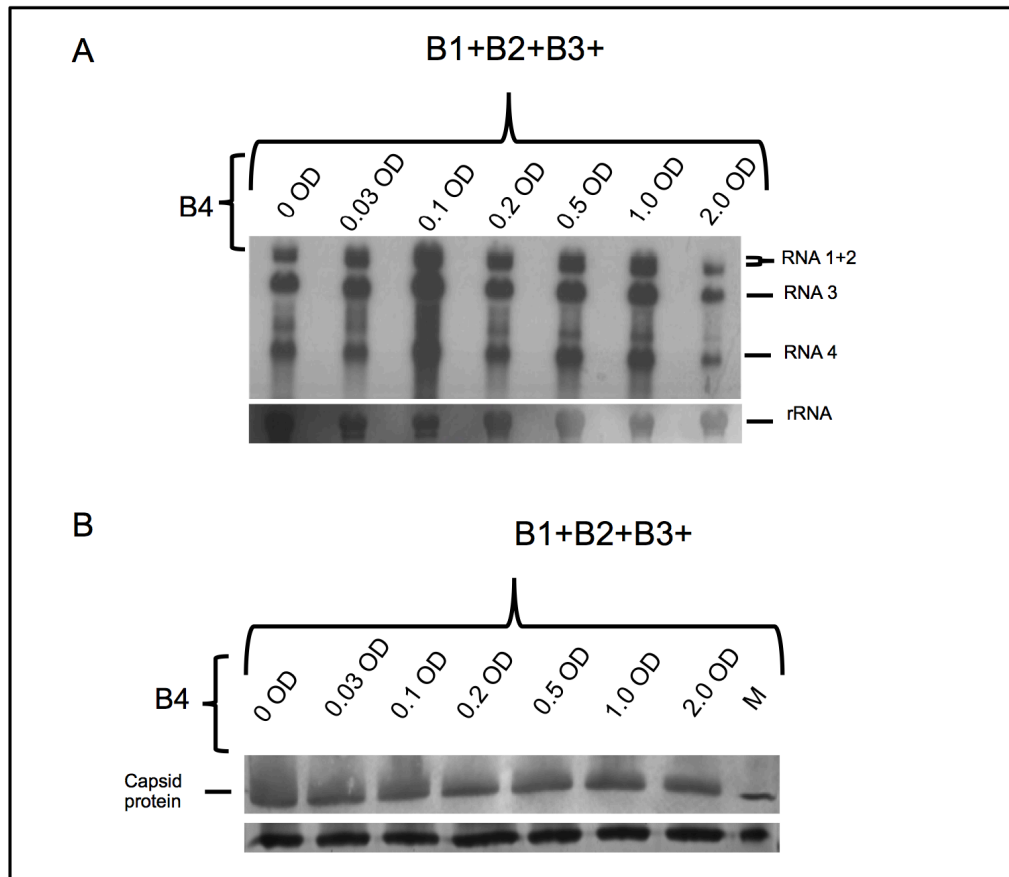
Figure 1.2 Effect of increasing OD of B4 on the replication of BMV. *N benthamiana* leaves were infiltrated with 0.1 OD_{600} of B1+B2+B3 and increasing OD_{600} of B4 (as mentioned in the figure). At 4dpi, total RNA and protein was extracted from the infiltrated leaves and subjected to northern blot and western blot analysis to detect the progeny RNA and CP.
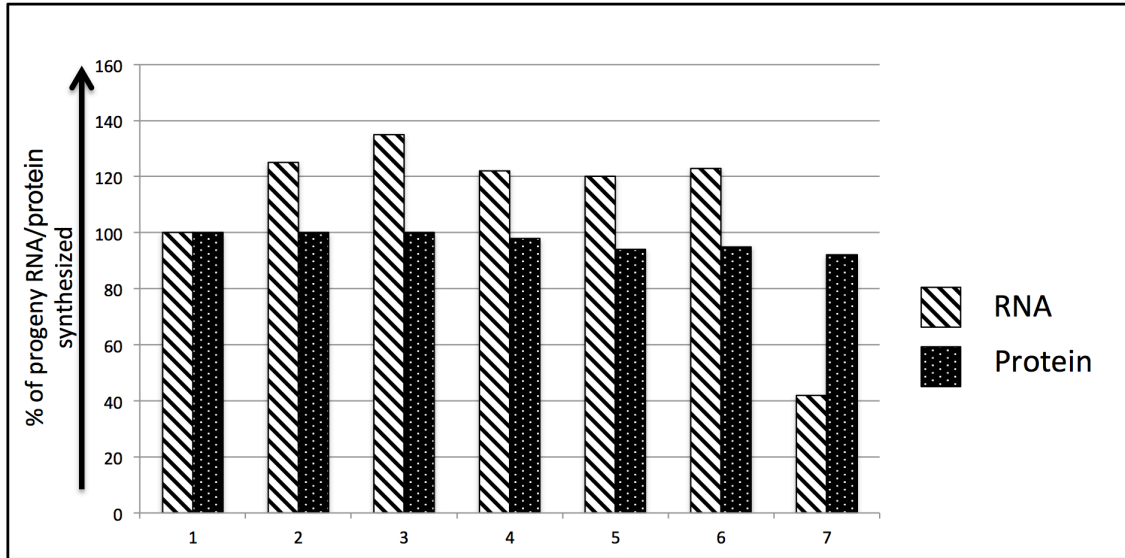
Figure 1.3 Quantification of RNA and protein expression levels to study the effect of increasing OD_{600} of B4 on the replication of BMV. Number of pixels in constant size from samples in figure 2 were counted using U.V trans-illuminator and were plotted as a graph using Microsoft Excel.
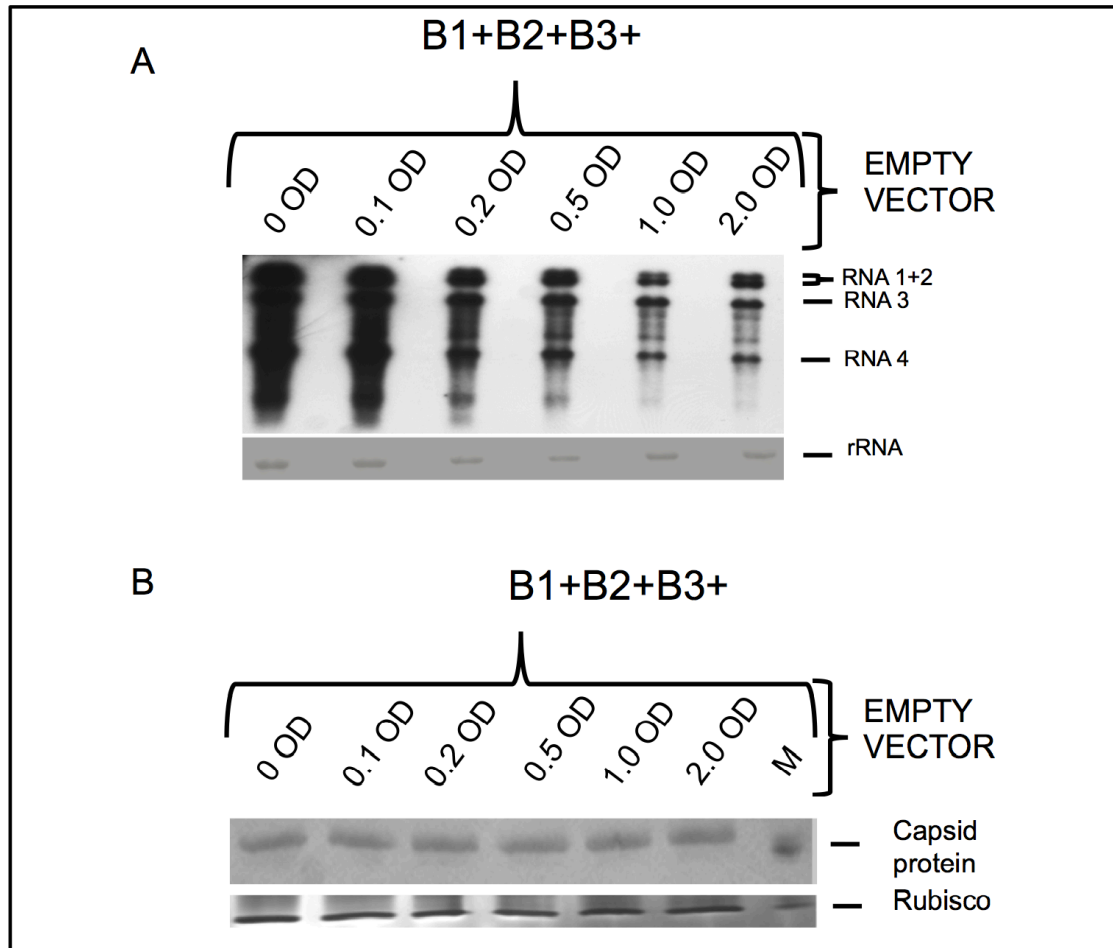
Figure 1.4 Effect of increasing OD_{600} of Empty vector (EV) on the replication of BMV. *N benthamiana* leaves were infiltrated with 0.1 OD_{600} of B1+B2+B3 and increasing OD_{600} of EV (as mentioned in the figure). At 4dpi, total RNA and protein was extracted from the infiltrated leaves and subjected to northern blot and western blot analysis to detect the progeny RNA and CP.
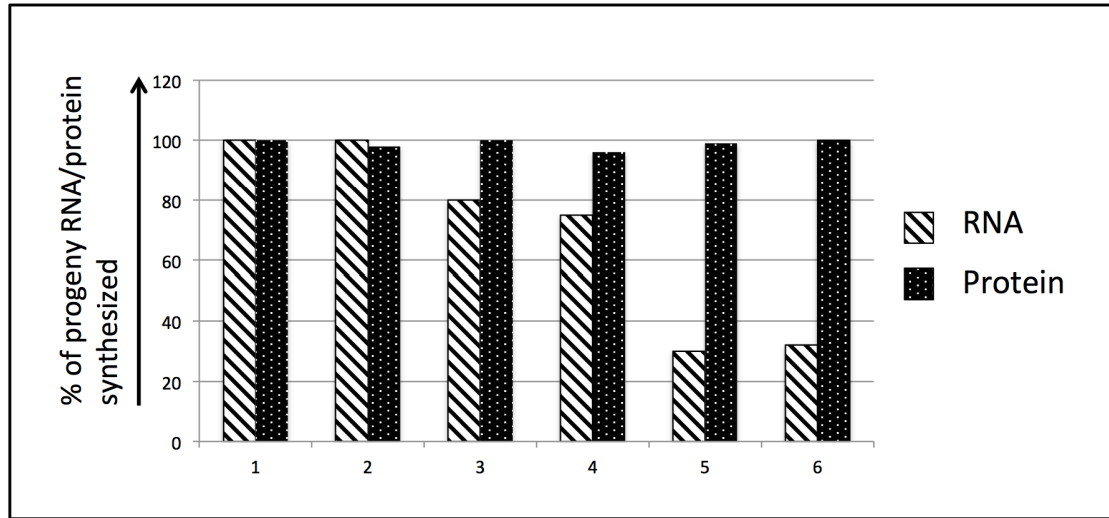
Figure 1.5 Quantification of RNA and protein expression level for studying the effect of increasing OD_{600} of EV on the replication of BMV. Number of pixels in constant size from samples in figure 4 were counted using U.V trans-illuminator and were plotted as a graph using Microsoft Excel.
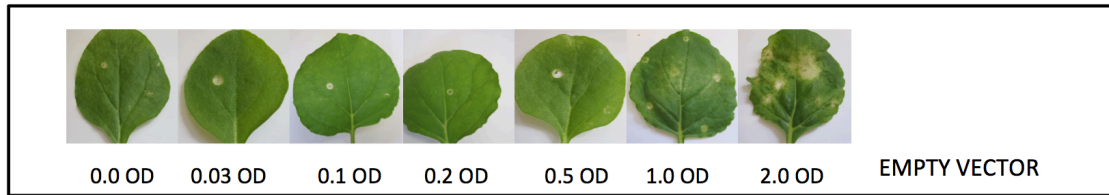
Figure 1.6 Effect of high cell density on leaf phenotype. Different OD_{600} of agrocultures containing empty vector was infiltrated to 4 weeks old *N. benthamiana* leaves, and at 8dpi, images of infiltrated leaves were taken.

REFERENCE

1.   **Annamalai, P., Rao, A.L., 2005a.** Dispensability of 3' tRNA-like sequence for packaging cowpea chlorotic mottle virus genomic RNAs. Virology 332, 650-658.

2.   **Annamalai, P., Rao, A.L., 2005b**. Replication-independent expression of genome components and capsid protein of brome mosaic virus in planta: a functional role for viral replicase in RNA packaging. Virology 338, 96-111.

3.   **Annamalai, P., Rao, A.L., 2006**. Packaging of brome mosaic virus subgenomic RNA is functionally coupled to replication-dependent transcription and translation of coat protein. Journal of virology 80, 10096-10108.

4.   **Annamalai, P., Rao, A.L., 2007**. In vivo packaging of brome mosaic virus RNA3, but not RNAs 1 and 2, is dependent on a cis-acting 3' tRNA-like structure. Journal of virology 81, 173-181.

5. **Annamalai, P., Rofail, F., Demason, D.A., Rao, A.L., 2008**. Replication-coupled packaging mechanism in positive-strand RNA viruses: synchronized coexpression of functional multigenome RNA components of an animal and a

plant virus in Nicotiana benthamiana cells by agroinfiltration. Journal of virology 82, 1484-1495.

6.   **Bamunusinghe, D., Seo, J.K., Rao, A.L., 2011.** Subcellular localization and rearrangement of endoplasmic reticulum by Brome mosaic virus capsid protein. Journal of virology 85, 2953-2963.

7.   **Baumstark, T., Ahlquist, P., 2001.** The brome mosaic virus RNA3 intergenic replication enhancer folds to mimic a tRNA TpsiC-stem loop and is modified in vivo. Rna 7, 1652-1670.

8.   **Bujarski, J.J., Nagy, P.D., 1994**. Targeting of the site of nonhomologous genetic recombination in brome mosaic virus. Archives of virology. Supplementum 9, 231-238.

9.   **Chaturvedi, S., Jung, B., Gupta, S., Anvari, B., Rao, A.L., 2012.** Simple and robust in vivo and in vitro approach for studying virus assembly. Journal of visualized experiments : JoVE.

10.   **de Wispelaere, M., Chaturvedi, S., Wilkens, S., Rao, A.L., 2011.** Packaging and structural phenotype of brome mosaic virus capsid protein with altered N-terminal beta-hexamer structure. Virology 419, 17-23.

11.   **Dinant, S., Janda, M., Kroner, P.A., Ahlquist, P., 1993.** Bromovirus RNA replication and transcription require compatibility between the polymerase- and helicase-like viral RNA synthesis proteins. Journal of virology 67, 7181-7189.

12.   **Garcia-Ruiz, H., Ahlquist, P., 2006**. Inducible yeast system for Viral RNA recombination reveals requirement for an RNA replication signal on both parental RNAs. Journal of virology 80, 8316-8328.

13.   **Houwing, C.J., Jaspars, E.M., 2000.** Activation of the alfalfa mosaic virus genome by viral coat protein in non-transgenic plants and protoplasts. The protection model biochemically tested. Archives of virology 145, 13-35.

14.   **Hull, R., 2009.** Mechanical inoculation of plant viruses. Current protocols in microbiology Chapter 16, Unit 16B 16.

15.   **Kim, M.J., Baek, K., Park, C.M., 2009**. Optimization of conditions for transient Agrobacterium-mediated gene expression assays in Arabidopsis. Plant cell reports 28, 1159-1167.

16.   **Watts, J.W., King, J.M., Stacey, N.J., 1987**. Inoculation of protoplasts with viruses by electroporation. Virology 157, 40-46.

17.   **Wroblewski, T., Tomczak, A., Michelmore, R., 2005**. Optimization of Agrobacterium-mediated transient assays of gene expression in lettuce, tomato and Arabidopsis. Plant biotechnology journal 3, 259-273.

18.   **Yi, G., Letteney, E., Kim, C.H., Kao, C.C., 2009**. Brome mosaic virus capsid protein regulates accumulation of viral replication proteins by binding to the replicase assembly RNA element. Rna 15, 615-626.

Chapter 2

A Bromodomain-Containing Host Protein Mediates the Nuclear Importation of a Satellite RNA of *Cucumber Mosaic Virus*

Reprinted from Journal of Virology, 88, 1890-96 (2014). Chaturvedi, S, Kalantidis, K and A.L.N Rao. A Bromodomain containing host protein mediates the nuclear import of a satellite RNA of Cucumber Mosaic Virus.

ABSTRACT

The replication of satellite RNAs of *Cucumber mosaic virus* (CMV) is dependent on replicase proteins encoded by their helper virus. However, we recently demonstrated that, like *Potato spindle tuber viroid* (PSTVd), a satellite RNA (satRNA) associated with CMV strain Q (Q-satRNA) has a propensity to localize in the nucleus and generate multimers that subsequently serve as templates for HV-dependent replication. But the mechanism regulating the nuclear importation of Q-satRNA is unknown. Here we show that, the nuclear import of Q-sat RNA is mediated by a bromodomain containing host protein (BRP1), which is also apparently involved in the nuclear localization of PSTVd. A comparative analysis of nuclear and cytoplasmic fractions from *Nicotiana benthamiana* plants co-infected with Q-satRNA and its HV confirmed the association of Q-satRNA, but not HV, with nuclear compartment. Application of a RNA tagging assay in conjunction with confocal microscopy demonstrated that the nuclear localization of Q-satRNA was completely blocked in transgenic lines of *Nicotiana benthamiana* (ph5.2nb) that are defective in BRP1 expression. This defect, however, was restored when the ph5.2nb lines of *N. benthamiana* were *trans*-complemented by ectopically expressing BRP1 protein. The binding specificity of BRP1 with Q-satRNA was confirmed *in vivo* and *in vitro* by co-immunoprecipitation and electrophoretic mobility shift assays, respectively. Finally, infectivity assays involving co-expression of Q-satRNA and its HV in wild type and ph5.2nb lines of *N. benthamiana* accentuated a biological role for BRP1

46

in Q-satRNA infection cycle. The significance of these results in relation to a possible evolutionary relationship to viroids is discussed.

INTRODUCTION

Cucumber Mosaic Virus (CMV) is the type member of the genus Cucumovirus and belongs to the Bromoviridae family of plant viruses (Palukaitis and Garcia-Arenal, 2003a). CMV is a tripartite RNA virus and its genome is divided among three single stranded, positive-sense RNAs. Genomic RNAs 1 and 2 encode two non-structural proteins, 1a and 2a, respectively that are required for replication (Boccard and Baulcombe, 1993). Genomic RNA2 also encodes another protein, 2b (that is expressed as a subgenomic RNA4A) and is the designated suppressor of post-transcriptional gene silencing (Brigneti et al., 1998; Ding et al., 1994). Genomic RNA3 is dicistronic: a nonstructural movement protein (MP) ORF encoded in the 5′ half is translated directly from RNA3. Whereas, the 3′ ORF of the dicistronic RNA3 encoding coat protein (CP) is synthesized from another subgenomic RNA4 generated *de novo* from progeny minus-sense RNA3 (Boccard and Baulcombe, 1993). Both MP and CP are dispensable for CMV replication but are required for whole plant infection (Boccard and Baulcombe, 1993; Canto et al., 1997; Schmitz and Rao, 1998).

In addition to genomic and subgenomic RNAs, some strains of CMV have been shown to encapsidate a 5'-capped, non-coding, linear, single stranded RNAs of 330 to 405 nucleotides (nt) (Garcia-Arenal and Palukaitis, 1999b; Hu et al., 2009). These small RNAs are classified as satellites (Q-satRNA), since they are incapable of self-replication and completely dependent on the replication

machinery encoded by its helper virus (HV), i.e. CMV (Garcia-Arenal and Palukaitis, 1999b; Hu et al., 2009). Although Q-satRNA has no appreciable sequence homology with the HV genome, it significantly interferes with HV genome replication and either attenuates or intensifies symptom expression *in planta* (Hu et al., 2009; Shimura et al., 2011a; Smith et al., 2011b). Consequently, a majority of studies have focused on characterizing various strains of Q-satRNA, their relationship to HV, symptom expression and origin (Escriu et al., 2000; Hu et al., 2009; Shimura et al., 2011a; Smith et al., 2011b; Wang et al., 2004). Because of the inherent dependency on HV, most research on Sat-RNA replication to date has been performed in the presence of HV using mechanical inoculation of either virion RNA or *in vitro* transcripts (Shimura et al., 2011a; Smith et al., 2011b; Wang et al., 2004).

Recent application of molecular and cell-biology approaches showed that, when expressed in the absence of CMV Q strain, its Sat- RNA (Q-satRNA) has propensity to localize in the nucleus and transcribed to generate multimers of genomic and anti-genomic strands (Choi et al., 2012b; Seo et al., 2013b). This previously unrecognized novel feature could account for the persistent survival of CMV Q-satRNA in the absence of HV (Mossop and Francki, 1979; Palukaitis and Garcia-Arenal, 2003a). Furthermore, mutations engineered to evaluate the significance of Q-satRNA multimers generated in the nucleus exemplified that nuclear phase is functionally active and obligatory for HV-dependent replication (Seo et al., 2013b). Since Q-satRNA has no nuclear localization signals, the

49

question that needs to be addressed would be: *How does Q-satRNA reach the nucleus?*

In 1992, a novel class of bromodomains, isolated from *Drosophila melanogaster* brahma protein, was identified as a primary amino acid sequence present in some proteins that have chromatin or transcription function (Haynes et al., 1992). Since then, many bromodomain-containing proteins (BRP) are found in transcription complexes, where they perform scaffolding functions (Denis et al., 2010). The bromodomain is a structural domain of 110 amino acids that is conserved through yeast through mammals. With regards to the implication of bromodomain containing proteins in viral pathology, they have been found to play an important role in the transcription of HIV (Zhou et al., 2009), Epstein-Barr virus (Lin et al., 2008) and in the inhibition of E2 protein that is involved in the replication of human papillomavirus (Gagnon et al., 2009) and more recently in *Potato spindle tuber viroid* (PSTVd), a subviral pathogen of plants. Bromodomain containing protein-1 (BRP-1), is present in different tissues of healthy plants and was the first bromodomain containing host protein isolated from tomato plants (Martinez de Alba et al., 2003a). Orthologs of BRP-1 have been found in various *Solanaceae* species (*Lycopersicon esculentum, Nicotiana tabaccum and N. benthamiana*) as well as in *Arabidopsis thaliana* (Martinez de Alba et al., 2003a). BRP-1 of *N. benthamiana* is 615 amino acids long containing some functional domains specifying RNA binding and nuclear and vacuole localization signals (Martinez de Alba et al., 2003a). Suppression of BRP-1 in *N. benthamiana* plants

through RNA silencing failed to induce PSTVd infection, suggesting a role for BRP-1 in the PSTVd infection cycle (Kalantidis et al., 2007a).

In this study, using molecular, genetic and cell biology based approaches we sought to examine the mechanism regulating the nuclear import of Q-satRNA. The results show that, analogous to PSTVd, nuclear import of Q-satRNA is mediated by BRP-1.

MATERIALS AND METHODS

Virus strains, agrotransformants, antibodies: The construction and characteristic features of agroconstructs of QCMV genomic RNA, Q-satRNA and Q5 was described previously (Choi et al., 2012b; de Wispelaere and Rao, 2009). The construction and characteristic features of agroconstructs of BRP1-FLAG and BRP1-GFP were as described (Kalantidis et al., 2007a). BRP1-HIS was constructed by amplifying a PCR product of BRP1 using a forward primer (5' ATCTCGAGATGGCATCCGCCGTCTT 3') and a reverse primer (5' ACGCGGTACCTCAAGAGTGTGCATCATC 3'). The resulting product was digested with *Xho*1 and *Kpn*1 and ligated into a similarly treated pRSET-1a vector. Generation of BRP1 suppressed transgenic lines of *N. benthamiana* (ph5.2nb) was as described previously(Kalantidis et al., 2007a).

Agroinfiltration and progeny analysis: All agrotransformants used in the study were transformed into GV3101 agrobacterium cells and infiltrated into the abaxial side of either wild type or transgenic lines of *N. benthamiana* leaves as described previously (Annamalai and Rao, 2006a). The total RNAs from either agroinfiltrated or mechanically inoculated plants were extracted using Trizol reagent (Invitrogen). Q-satRNA progeny was analyzed by Northern hybridization with (+)-strand specific ^{32}P-labeled as described previously (Seo et al., 2013b).

RNA tagging assay and confocal microscopy: The bacteriophage MS2-CP RNA tagging assay to localize the Q-satRNA in wild type and *N. benthamiana* lines of ph5.2nb was performed as described previously (Choi et al., 2012b). Prior to performing confocal microscopy using Leica TCS SP2, at 2dpi, the leaves were infiltrated with 1:1000 dilution of DAPI in PBS buffer.

Subcellular fractionation: The nuclear and cytoplasmic fractionation was performed with slight modifications as described (Eini et al., 2009). Briefly, 5 g *N. benthamiana* leaves were ground in liquid nitrogen and emulsified with 10 ml of extraction buffer [(50 mM Tris-cl(pH 7.5), 5 mM $MgCL_2$, 0.1 mM EDTA, 1mM DTT, 0.3 M sucrose, 15 mM KCl, 0.2 mM phenylmethylsulphyl fluoride (PMSF) and 10 mg of protease inhibitor-Sigma)]. The resulting homogenate was filtered twice through Miracloth and centrifuged at 5000 rpm for 10 minutes at 4^oC. Supernatant containing the cytoplasmic fraction was retained separately while the pellet containing nuclear fractions was washed two times with chilled extraction buffer. Total RNA was extracted from the nuclear and cytoplasmic fractions using Trizon reagent. RNA was subjected to RT-PCR using M-MuLV Reverse transcriptase and Vent polymerase using a set of primers specific for either Q-satRNA (forward primer: 5' GTTTTGTTTGTTAGAGAATTG 3' and reverse primer 5'GGGTCCTGGTAGGGAATGATA 3') or QCMV RNA 1 (forward primer 5' AGGATCCGATGGCAACGTCCTCATTC 3' and reverse primer 5'ACGGTACCTCAGACTAACGGAATACAAT 3').

Coimmunoprecipitation assay: Coimmunoprecipitation assay was performed as described previously (Azevedo et al., 2010) and modified as follows. Wild type *N. benthamiana* leaves were infiltrated independently with agrocultures containing the following mixture of inocula: BRP1-FLAG+Q-satRNA; BRP1-FLAG+Q-satRNA+HV; BRP1-FLAG+Q5 RNA; Q-satRNA; Q-satRNA+HV and Q5RNA. At 4 dpi, leaves were collected and ground in liquid nitrogen, and proteins were extracted in 3ml/g of extraction buffer (20mM Tris-Cl; pH 7.5, 300mM NaCl, 5 mM MgCl2, 5 mM DTT, 1% plant protease inhibitor mixture (Sigma). Insoluble material was pelleted by centrifugation for 15 minutes at 12,000 rpm at 4°C, and the supernatant was filtered through a 0.22 µm filter. The supernatant was subjected to immunoprecipitation for 4 hours at 4°C by adding 25 µl of FLAG M2 agarose beads (Sigma) per gram of starting material with gentle shaking. Then, the agarose beads were washed three times with extraction buffer followed by a short spin at 2000 rpm at 4°C. RNA bound to agarose beads was extracted with Trizol (Sigma). The resulting RNA was subjected to RT-PCR using sequence specific primers for Q-satRNA and Q5 RNA.

Northwestern blot and EMSA: The Northwestern assay was performed as described (Zaidi and Malter, 1995). Briefly, BRP1-His or His (induced or uninduced by IPTG) were resolved on 12% SDS-polyacrylamide gels and transferred to nitrocellulose membrane. Proteins immobilized on the nitrocellulose membrane were renatured overnight in a buffer containing 15 mM

HEPES; pH 8.0, 10 mM KCl, 10% glycerol, and 1 mM dithiothreitol at 4°C. Membranes were then hybridized with ^{32}P-Q-satRNA or ^{32}P-Q5 RNA for 1 hour at room temperature in the renaturing buffer containing 2 mg/ml yeast tRNA. The membrane was washed twice with renaturing buffer at room temperature to remove any unbounded RNA followed by autoradiography. EMSA was performed as described previously (Martinez de Alba et al., 2003b) with minor modifications. For synthesizing ^{32}P-Q-satRNA transcripts, an *Hind*III linearized pT7/T3 Q-sat (Seo et al., 2013b) was subjected to *in vitro* transcription with T7 polymerase. For synthesizing ^{32}P-Q-PSTVd, an *Eco*RI linearized pHa106 plasmid (Tabler et al., 1992) transcripts was subjected to *in vitro* transcription with SP6 polymerase. Approximately 10 ng of ^{32}P-Q-satRNA transcript was mixed with different concentrations of BRP1-His in binding buffer [10 mM HEPES-NaOH (pH 8.0), 50mM KCl, 100 mM EDTA, and 5% glycerol] and 1 µg yeast tRNA in a final volume of 10 µl. The resulting RNA-BRP1-His protein mixture was incubated at 22°C for 30 minutes and subjected to electrophoresis on 1% agarose gel prepared and electrophoresed 1% TAE buffer followed by autoradiography. For binding specificity assay, either ^{32}P-Q-satRNA or ^{32}P-PSTVd transcripts were allowed to compete with 5-fold excess of either unlabeled competitors (transcripts of QsatRNA or PSTVd) or non-competitors (3' tRNA-like structure of BMV RNA or Q5RNA). The reaction products were analyzed by EMSA as described above.

RESULTS

Sub-cellular fractionation of Q-satRNA. We previously demonstrated that Q-saRNA has a propensity to enter nucleus in the presence and absence of its HV (Choi et al., 2012b). To shed light on the subcellular compartmentalization of Q-satRNA, we wanted to analyze the distribution of Q-satRNA in the presence and absence of HV during early time points. Since the replication of Q-satRNA or its HV does not involve DNA intermediates and the fact that T-DNA based transient RNA expression system is initiated in the nucleus (Annamalai and Rao, 2005b), use of agroinfiltration for delivery and expression of either Q-satRNA or its HV could complicate the interpretation of results of subcellular fraction experiments. Therefore, we preferred to analyze the subcellular compartmentalization of Q-satRNA in mechanically inoculated plants. Consequently, *N. benthamiana* plants were mechanically inoculated with either Q-satRNA alone or Q-satRNA+HV. Inoculated leaves were harvested at 2 and 4 days post inoculation (dpi) and nuclear and cytoplasmic fractions were collected followed by the detection of Q-satRNA by RT-PCR as described under Methods. Results are shown in Fig. 2.1. In plants inoculated only with Q-satRNA, at 2 dpi, Q-satRNA was localized exclusively in the nuclear fractions in plants inoculated only with Q-satRNA (Fig. 2.1A, lane 1). By 4 dpi, Q-satRNA was detected both in nuclear (Fig. 2.1A, lane 2) and cytoplasmic fractions ((Fig. 2.1B, lane 2). Whereas in plants inoculated with HV+Q-satRNA, nuclear and cytoplasmic fractions collected at 2 and 4 dpi contained Q-satRNA (see Discussion for explanation). As expected, at 2 and 4

dpi, HV was detected only in the cytoplasmic fractions of plants inoculated with HV (Fig. 2.1B, lanes 9, 10) and HV+Q-satRNA (Fig. 2.1B, lanes 11, 12). Taken together the results confirm our previous observations that Q-satRNA localizes to nucleus.

BRP1 suppressed _N. benthamiana_ plants inhibit nuclear localization of Q-satRNA. It was previously observed that the replication of PSTVd was severely inhibited when the plants were co-infected with CMV and Q-satRNA, whereas CMV alone had no affect on the replication of PSTVd (Montasser et al., 1991; Yang et al., 1996). Since PSTVd replicates in the nucleus and BRP1 plays major role in PSTVd infection (Kalantidis et al., 2007a), we hypothesize that the inhibition of PSTVd replication in plants co-infected with CMV and Q-satRNA is due to competition for BRP-1 by PSTVd and Q-satRNA. These observations formed the basis to hypothesize that BRP1 could be involved in the nuclear import of Q-staRNA. Thus, we performed a bacteriophage MS2-coat protein (MS2-CP) RNA-tagging assay that allows visualizing the subcellular location of Q-satRNA in living cells (Haim et al., 2007) in wild type (wt) and BRP-1 suppressed transgenic lines of _N. benthamiana_. Results are shown in Fig. 2.2. When _N. benthamiana_ leaves of wt and BRP-1 suppressed transgenic lines were infiltrated with control constructs of GFP, GFP-CP and GFP-NLS (Nuclear Localization Signal)-CP, fluorescent signals were detected in the expected subcellular compartments i.e. GFP and GFP-CP in the cytoplasm and GFP-

CNLS-CP in the nucleus (Fig. 2.2, top panels). Identical distribution patterns of GFP signals were observed when Q-satRNA was co-expressed with either GFP or GFP-CP or GFP-NLS-CP (Fig. 2.2, middle panel. As demonstrated recently by our group (Choi et al., 2012b) wt *N. benthamiana* cells co-expressing Q-satRNA-MS2 and GFP-CP, the GFP signals were observed in the nucleus (Fig. 2.2A, bottom panel). Whereas expression of similar constructs in BRP-1 suppressed transgenic lines, GFP signals were confined to cytoplasm (Fig. 2.2B, bottom panel). As expected, in both wt and BRP-1 suppressed transgenic lines GFP signals resulting from co-expression of control inocula containing Q-RNA5-MS2+GFP-CP were confined to cytoplasm while those for Q5RNA-MS2+GFP-NLS-CP were confined to nucleus. These results suggest that nuclear import of Q-satRNA is mediated by BRP-1, in a fashion similar to that of PSTVd (Kalantidis et al., 2007a).

Trans-complementation with BRP1 restores nuclear localization of Q-satRNA. To further authenticate the result shown in Fig. 2.2, BRP1 suppressed *N. benthamiana* lines infiltrated with Q-satRNA-MS2+GFP-CP were complemented with an agroconstruct designed to express BRP1. Control infiltrations were performed with Q5-MS2+CP-GFP. Results are shown in Fig. 2.3. Following infiltration of Q-satRNA-MS2+GFP-CP to wild-type plants, the distribution of fluorescent signals was confined to the nucleus and *trans*-complementation with BRP1 did not alter this pattern. By contrast, in BRP1

suppressed lines, fluorescent signals were predominantly localized to cytoplasm (Fig. 2.3C, left panel). However, *trans*-complementation with BRP1 restored the localization of fluorescent signal to nucleus (Fig. 2.3D, left pannel). *Trans*-complementation with BRP1 had no effect on the GFP distribution pattern for control samples Q5-MS2+CP-GFP. Collectively results shown in Figs 2.2 and 2.3 confirm that BRP1 is the primary host factor involved in the nuclear localization of Q-satRNA.

***In vitro* interaction between Q-satRNA and BRP1.** To verify the interaction between Q-satRNA and BRP1, we used two different assays. In the first Northwestern assay, BRP1 protein extracts from *E. coli* cells containing plasmids pHis-VIRP1 were separated on SDS–PAGE gels and transferred to a nitrocellulose membrane. A strong signal could be detected after the membrane was probed with radioactively labeled Q-satRNA positive-strand RNAs (Fig. 2.4A). No signal was visible when radiolabelled Q5 RNA was used as a hybridization probe (Fig. 2.4B).

In the second assay, the purified protein was used to test the interaction of BRP1 and Q-satRNA in solution by EMSA. The protein was incubated with radioactively labeled monomeric Q-satRNA positive-strand RNA in the presence of tRNA as a competitor and the resulting complexes were analyzed on native polyacrylamide gels (Fig. 2.5). Retardation of Q-satRNA was observed when the

concentration of BRP1 protein is more than 25 mM (Figs. 2.5A; 2.5B, lane 3). Similar EMSA was performed to assess the specificity of BRP1 binding to Q-satRNA and results are shown in Fig. 2.5B. In this assay, ^{32}P labeled PSTVd transcript served as positive control. As expected in the absence of BRP1, radiolabelled transcripts of Q-satRNA and PSTVd migrated to expected positions (Fig. 2.5B, lanes 1 and 2). As expected, a clear retardation of Q-satRNA and PSTVd was observed with BRP1 (Fig. 2.5B, lanes 3 and 4). When either unlabeled Q-satRNA or PSTVd was used as a competitor, the retardation of the radioactively labeled RNA in each case was be reversed (Fig. 2.5B, lanes 5, 6). No retardation of BRP1 was observed when either cold 3' tRNA-like stsructure from BMV RNA3 or Q5 RNA transcripts were used as negative controls (Fig. 2.5B, lanes 7, 8). Taken together, data shown in Fig. 2.5 A and B confirm that the interaction between BRP1 and Q-satRNA is specific.

Q-satRNA has high affinity to bind BRP1 *in vivo*. To further verify physical interaction between BRP1 and Q-satRNA in vivo, we performed a co-immunoprecipitation assay. For this, *N. benthamiana* plants were agroinfiltrated with BRP1 carrying FLAG epitope (Kalantidis et al., 2007a), and then mechanically inoculated with either Q-satRNA or HV+Q-satRNA or Q5 (control). At 4 dpi, leaf extracts were subjected to anti-FLAG immunoprecipitation. Results are shown in Fig. 2.4. Q-satRNA (Fig. 2.6A, B), but not Q5 (Fig. 2.6C), was specifically co-immunoprecipitated with anti-FLAG antibody. Since the interaction

sustained stringent washing conditions (see Methods), we conclude that BRP1 strongly interacts with Q-satRNA in vivo.

A defect in nuclear import phenotype significantly affects Q-satRNA replication. Results shown above clearly demonstrate that interaction of Q-satRNA with BRP1 promotes the nuclear import. In addition, we have previously shown that nuclear importation of Q-satRNA is a critical step for subsequent HV-dependent replication (Choi et al., 2012b; Seo et al., 2013b). To further shed light on the biological significance of the BRP1 mediated nuclear importation of Q-satRNA (Figs. 2.2 and 2.3), the relative HV-dependent replication competence and accumulation of Q-satRNA progeny was examined in wild type and BRP1 defective transgenic lines of *N. benthamiana*. Following agroinfiltration of HV and Q-satRNA, Northern blots containing total RNA recovered at 4 dpi were hybridized with Q-satRNA probe. As a control, wild type and BRP1 defective plants were infiltrated with a mixture of agrotransformants of brome mosaic virus (BMV). Results are shown in Fig. 2.7. Unlike in wild type control plants, the HV-dependent replication of Q-satRNA was down regulated by 55% (Fig. 2.7A lanes 1 and 2). This down regulation of Q-satRNA is not attributed to the genetic defects in transgenic lines, since no such down regulation in the replication of BMV was observed (Fig. 2.7B).

DISCUSSION

The premise for testing the role of BRP1 in importing Q-satRNA to the nucleus is as follows. The subcellular localization sites of Q-satRNA are not known. Since Q-satRNA is replicated by its HV replicase, virus-dependent Q-satRNA replication would be cytoplasmic. However, our recent molecular and cell biology based approaches clearly demonstrated that Q-satRNA has a propensity to localize in the nucleus (Choi et al., 2012b). But Q-satRNA has no recognizable nuclear localization signals (NLS). For viruses that replicate in the nucleus, proteins encoded by their genomes have been shown to contain NLS (Whittaker and Helenius, 1998). Although PSTVd has been shown to localize in the nucleus (Zhao et al., 2001) and replicate by Pol II (Schindler and Muhlbach, 1992), no signals responsible for nuclear localization have been identified. Thus, it has been suggested that some structural domains or a cellular counterpart, may exist in plants to localize PSTVd to the nucleus (Zhao et al., 2001). However, a host protein, identified as BRP-1 having a bipartite localization signal, was isolated from tomato plants and shown to promote nuclear localization of PSTVd (Martinez de Alba et al., 2003a). BRP-1 orthologs have been identified in other *Solanaceae* species including *N. benthamiana* (Martinez de Alba et al., 2003a). Interestingly, a satRNA of CMV was first isolated from tomato plants (Kaper and Waterworth, 1977). Since Q-satRNA, like PSTVd, lacks a NLS, we envisioned that analogous to PSTVd, nuclear import of Q-satRNA could be mediated

through its interaction with BRP-1. Furthermore, it was observed that the replication of PSTVd was severely inhibited when the plants were co-infected with CMV and Q-satRNA, whereas CMV alone had no affect on the replication of PSTVd (Montasser et al., 1991; Yang et al., 1996). Since both PSTVd and Q-satRNA have nuclear phase in their replication cycles, it is reasonable to speculate that replication of PSTVd in co-infected plants was abated by inhibiting PSTVd entry to nucleus. This has led us to believe that the host factor involved in the nuclear localization of PSTVd (i.e. BRP1) is commonly shared with Q-satRNA as well. Consequently these perceptions form the foundation for performing experiments shown in the present study.

BRP1 promotes nuclear import of Q-satRNA. Our subcellular fraction experiments provide additional supporting evidence of our previous observations (Choi et al., 2012b) that Q-satRNA encompasses a nuclear phase in its replication cycle. For example, Q-satRNA was successfully amplified by RT-PCR in the nuclear fractions (Fig. 2.1A, lane 1), but not in the cytoplasmic fractions (Fig. 2.1B, lane 1) collected at the earliest time point (i.e. 2 dpi) from leaves mechanically inoculated with Q-satRNA only. However, Q-satRNA was detected in both nuclear (Fig. 2.1A, lane 5) and cytoplasmic fractions (Fig. 2.1B, lane 5) collected at 2dpi from leaves mechanically inoculated with Q-satRNA+HV. A possible explanation for the detection of Q-satRNA in the cytoplasmic fractions could be that small portions of Q-satRNA multimers formed in the nucleus at 2

63

dpi enter the cytoplasm to serve as templates for replication by HV RdRp. Since we performed our inoculations with *in vitro* synthesized RNA transcripts, however, leaves inoculated with Q-satRNA+HV, Analyses of cytoplasmic fractions reveal that as early as 4 dpi some Q-satRNA could exit nucleus and enter cytoplasm (Fig. 2.1B, lane 2) to serve as template for HV-dependent replication. It was largely confined to the nucleus (Fig. 2.1A, lane 1) since it was not present in the cytoplasmic fractions (Fig. 2.1B, lane 1). By 4dpi, some Q-satRNA appears to leak into the cytoplasm (Fig. 2.1B, lane 2) we show that that BRP1 is the first host factor identified as being involved in the nuclear localization of Q-satRNA (Figs. 2.2-2.4). Also BRP1 is the first bromodomain containing host factor we identified having a prominent role in the replication cycle of a sub-viral pathogen associated with an RNA virus pathogenic to plants. Compelling evidence for the involvement of BRP1 in the nuclear localization of Q-satRNA comes from MS2-CP based RNA tagging assay performed in wt and BRP1 defective transgenic lines (Fig. 2.3).

Function of BRP1 in the infection cycle of Q-satRNA. With the aim of elucidating the biological significance of BRP1 mediated nuclear import of Q-satRNA, we tested the relative HV-dependent replication of Q-satRNA in wt and BRP1-supressed transgenic lines of *N. benthamiana.* Northern blot analyses revealed that the HV-dependent replication of Q-satRNA was severely down regulated in BRP1 suppressed lines (Fig. 2.7A). A low level of Q-satRNA

64

replication observed can be attributed to the fact that the transgenic lines of *N. benthamina* are not 100% devoid of BRP1 expression (Kalantidis et al., 2007a). Thus we hypothesize that, since BRP1 has a nuclear localization signal (Martinez de Alba et al., 2003b) and can specifically bind Q-satRNA (Figs. 2.4 and 2.5), upon binding one of its primary roles would be to promote the nuclear import of Q-satRNA. However we do not rule out the possible role of other host proteins in this active process. We recently collected a pool of host factors associated with Q-satRNA using riboproteomics approach and in the process of screening the likely roles played by prioritized host proteins (other than BRP1) in Q-satRNA infection cycle.

Results shown in Fig. 2.7 suggest a role for BRP1 in HV replication, since replication of HV was downregulated by 50% in BRP1-suppressed lines (Fig. 2.7). Support for this conjecture was recently obtained from an in vivo protein-protein interaction assay, which revealed that BRP1 does interact with HV replicase 1a. These observations suggest that BRP1 is an integral part of the HV replicase complex. We are performing additional experiments to substantiate the role of BRP1 in HV replication using Arabidopsis gene knockout lines of BRP1 orthologs. Results obtained from such studies are likely to provide valuable information concerning the role of BRP1 in the HV infection cycle.

In conclusion, as presented here, both PSTVd and Q-satRNA depend on BRP1

for nuclear importation. It is interesting that plants coinfected with Cucumber Mosaic Virus and its satRNA were resistant to PSTVd infection (Montasser, MS et al., 1991, Yang, X et al., 1996). It was suggested (Yang X et al., 1996) that base-pairing between satRNA and PSTVd interfered with PSTVd replication. However, results of this study provide a more convincing alternate reason for the observed PSTVd resistance in plants coinfected with Cucumber Mosaic Virus satRNA. Although PSTVd was found to compete with Q-satRNA in EMSA (Fig. 2.5B), in plants coinfected with PSTVd and Q-satRNA and its HV, the concentration of Q-satRNA would be significantly higher than that of PSTVd. Therefore, we hypothesize that in coinfected plants, a high concentration of satRNA would outcompete PSTVd for BRP1 binding, inhibiting PSTVd localization to the nucleus and preventing its replication. Additional experiments are in progress to substantiate this hypothesis.

ACKNOWLEDGMENTS
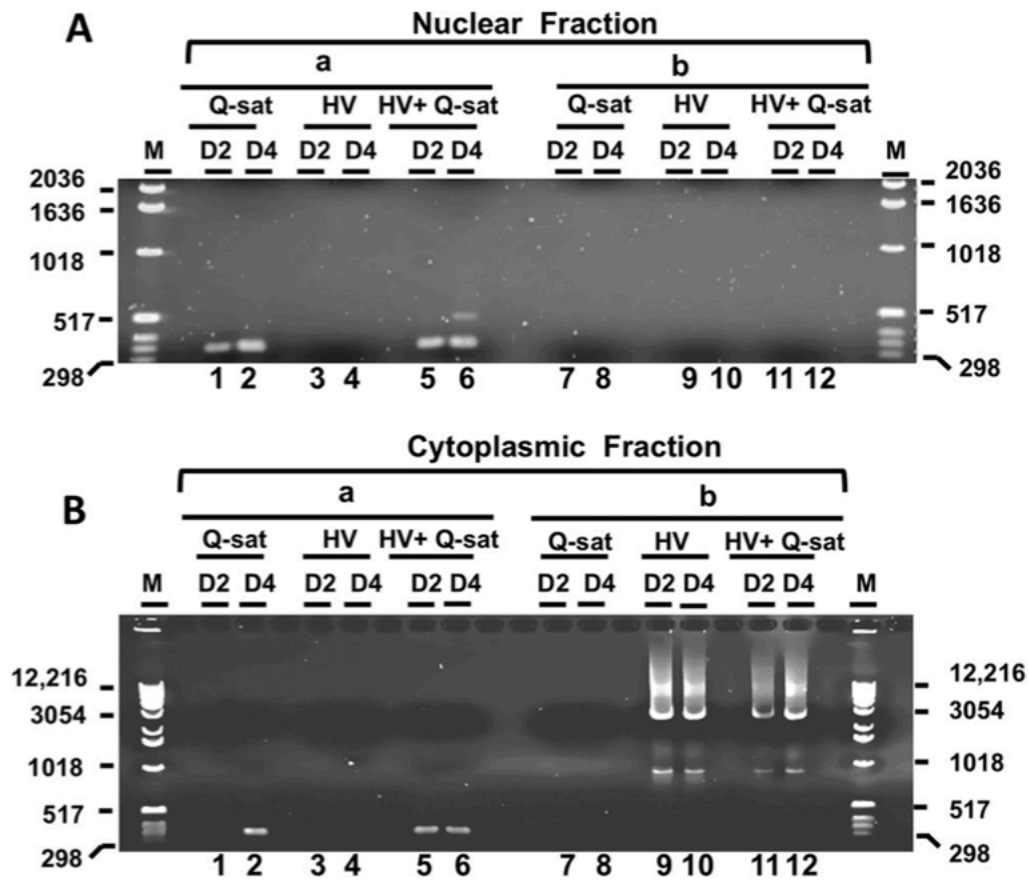
Figure 2.1   Distribution of Q-satRNA and HV RNA1 component in nuclear and cytoplasmic fractions. Agarose gel electrophoretic analysis of RT-PCR products of Q-satRNA in (A) nuclear and (B) cytoplasmic fractions of *N. benthamiana* leaves at 2 (D2) and 4 (D4) days post agroinfiltration with indicated inocula. Procedure used to obtain nuclear and cytoplasmic fractions and detection of Q-satRNA for fractions encompassing section "a" and HV RNA1 encompassing fractions "b" by RT-PCR was as described under Materials and Methods section. Size markers were shown on each side of the panels.
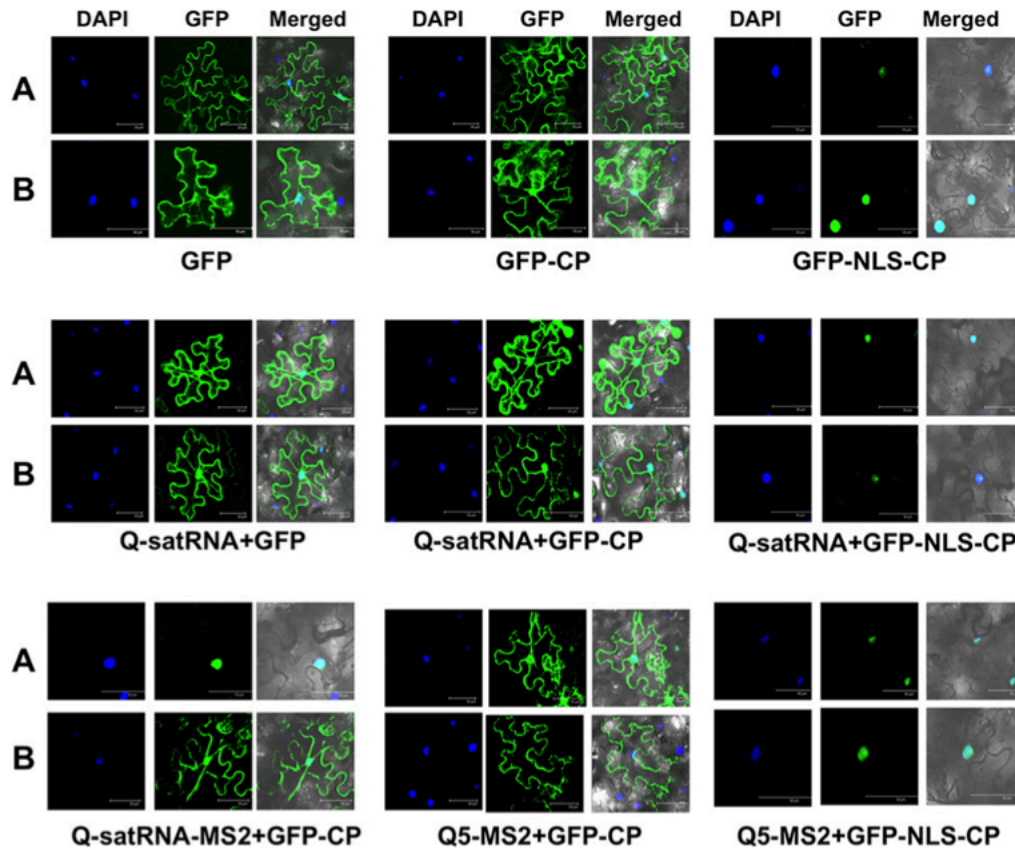
Figure 2.2 RNA tagging assay. Subcellular localization of Q-satRNA in (A) wild type and (B) BRP1 defective *N. benthamiana* leaves using MS2-CP based RNA tagging assay. Representative confocal microscopic images of *N.benthamiana* leaves agroinfiltrated with either single or pair wise combinations of the indicated agrocultures. Fluorescent signals were in epidermal cells at 3 dpi. To visualize the nuclei, leaves infiltrated with DAPI prior to viewing under confocal microscope. Agroconstructs to perform the MS2-CP based RNA tagging assay, experimental conditions and confocal microscopy procedure used are as described previously (Choi et al., 2012b).
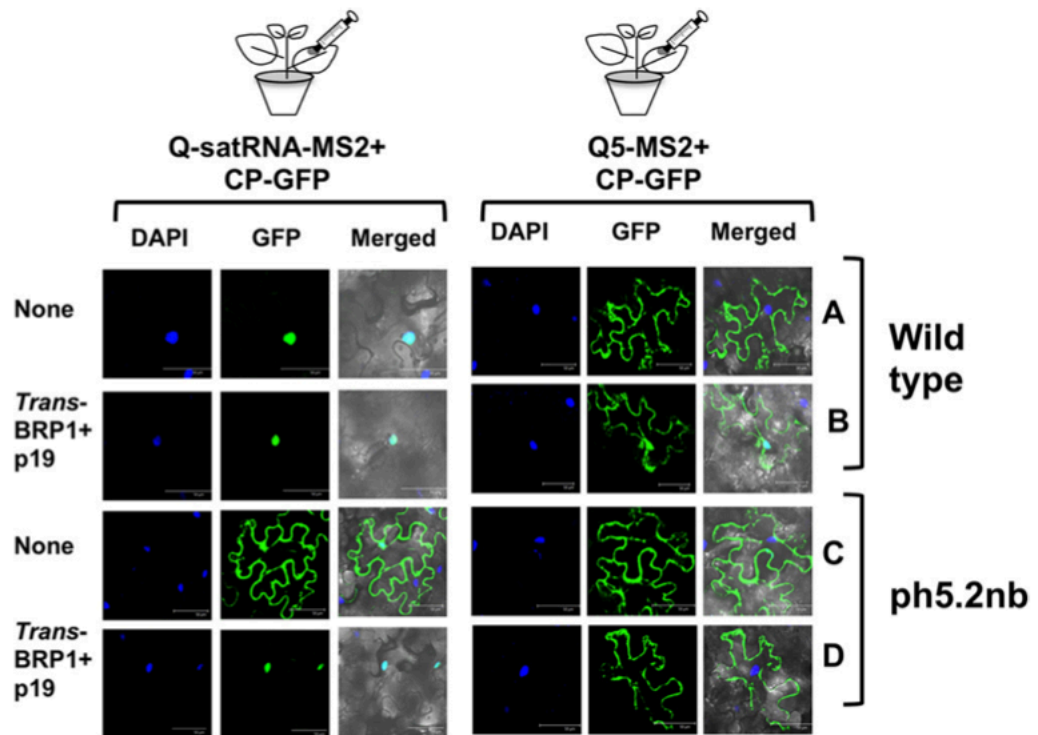
Figure 2.3 *Trans*-complementation with BRP1. One set of *N.benthamiana* plants (A, C) of wild type or ph5.2nb (defective in BRP1 expression) were infiltrated only with SatRNA-MS2-CP-GFP and while in the other set (B, D) BRP1 was *trans*-complemented by was additionally infiltrating an agrotransformant designed to ectopically express BRP1 along with p19, a suppressor of RNA silencing. Identical infiltrations performed into another set of plants with Q5-MS2+CP-GFP served as negative controls. Plants that are not *trans*-complemented with BRP1 were labeled as "None". Agroconstructs to perform the MS2-CP based RNA tagging assay, DAPI staining, experimental conditions and confocal microscopy procedure used are as described under Fig. 2.
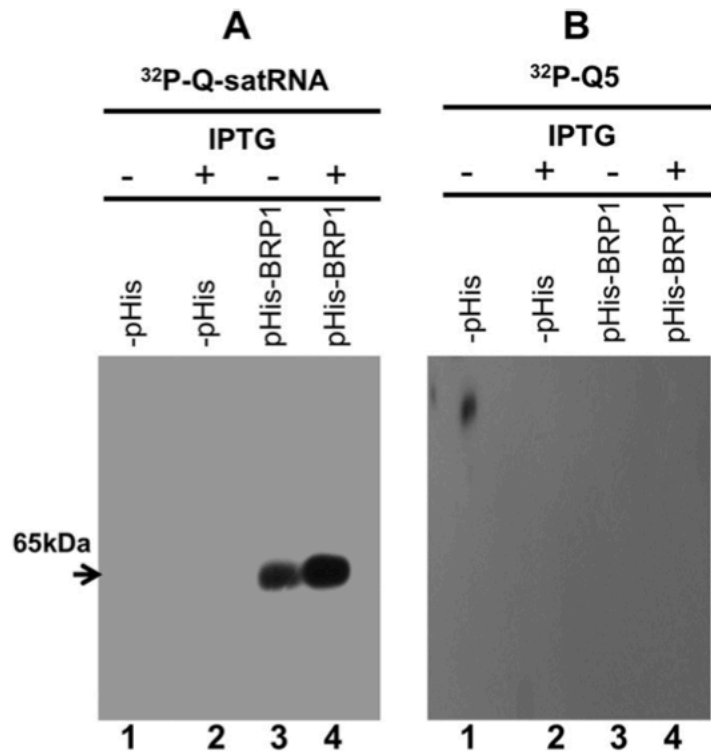
Figure 2.4 Northwestern blot analysis of BRP1 and Q-satRNA. Specificity of binding of BRP1 protein with Q-satRNA was confirmed by Northwestern assay. *E. coli* cells harboring either pHis, pHis-BRP1 were subjected to duplicate SDS–10% PAGE, transferred to nitrocellulose membranes and hybridized with ^{32}P-labeled transcripts of either (A) Q-satRNA or (B) Q5. Lanes 1 and 3, noninduced cells; lanes 2 and 4, IPTG-induced cells.
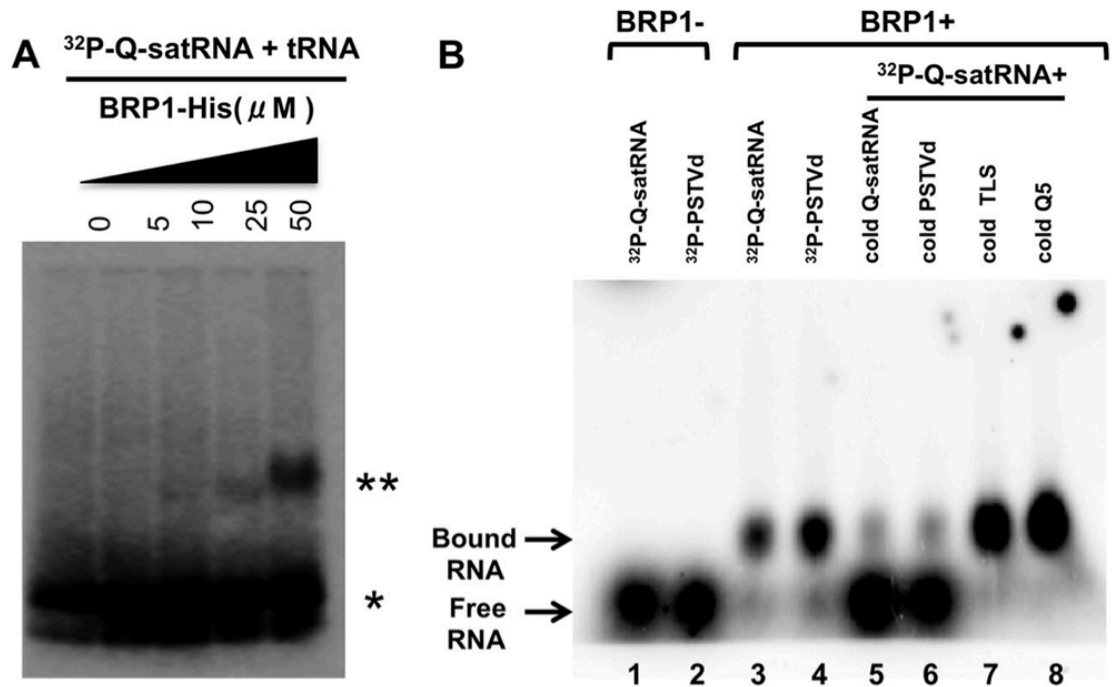
Figure 2.5 EMSA assay. (A) An autoradiograph of agarose gel showing electrophoretic mobility shift assay to demonstrate the binding of Q-satRNA with indicated concentrations of BRP1 protein. Single and double asterisks indicate positions of unbound RNAs and RNA-protein complex, respectively. (B) An autoradiograph of agarose gel showing the EMAS assay to demonstrate the binding specificity between Q-satRNA and BRP1 protein. ^{32}P-labeled indicated RNA transcripts were incubated with or without purified BRP1 protein for 60 min at room temperature. Mixtures were electrophoresed on 1.2% agarose gels and subjected to autoradiography. When either Q-satRNA (lane 1) or PSTVd RNA (lane 2, serving as positive control) was incubated with BRP1 protein (lanes 3 and 4), retardation due to RNA-protein complex formation could be observed, which could be competed for in the presence of 100-fold excess respective non-labeled RNAs (lanes 5 and 6). In contrast, when other RNA transcripts, TLS or Q5 (lanes 7 and 8) were used as competitors no such retardation was detected.
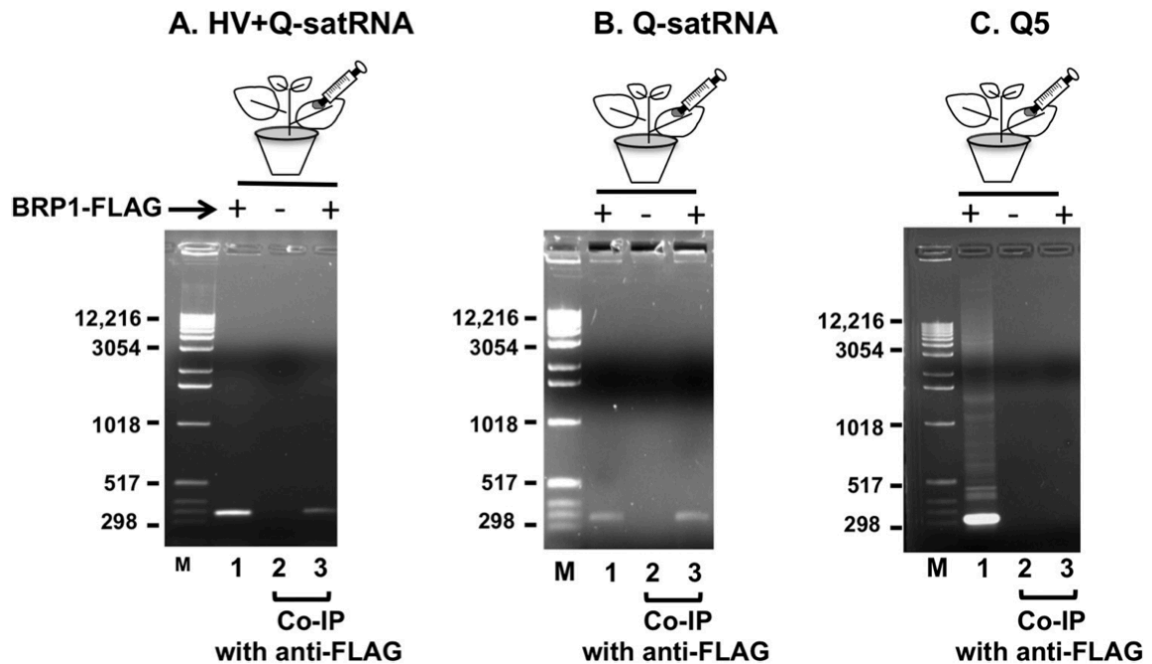
Figure 2.6 Analysis of *in vivo* binding of BRP1 protein with Q-satRNA using Co-immunoprecipitation (Co-IP) assay. Agarose gel electrophoretic analysis of RT-PCR products of Q-satRNA after Co-IP. *N. benthamiana* plants were agroinfiltrated with BRP1-FLAG and either (A) HV+Q-satRNA or (B) only Q-satRNA or (C) only Q5. Plant that did not receive BRP1-FLAG served as controls. At 4dpi, leaf extracts were subjected to co-immunoprecipitation with anti-FLAG agarose beads followed by extraction of eluted RNA as described under Materials and Methods. Samples that are not subjected to Co-IP served as controls (lane 1). In panels A and B, RNA samples in lanes 1-3 were subjected to RT-PCR using a set of forward and reverse primers specific for Q-satRNA. In panel C, RNA samples in lanes 1-3 were subjected to RT-PCR using a set of forward and reverse primers specific for Q5. M, Molecular weight marker lane.
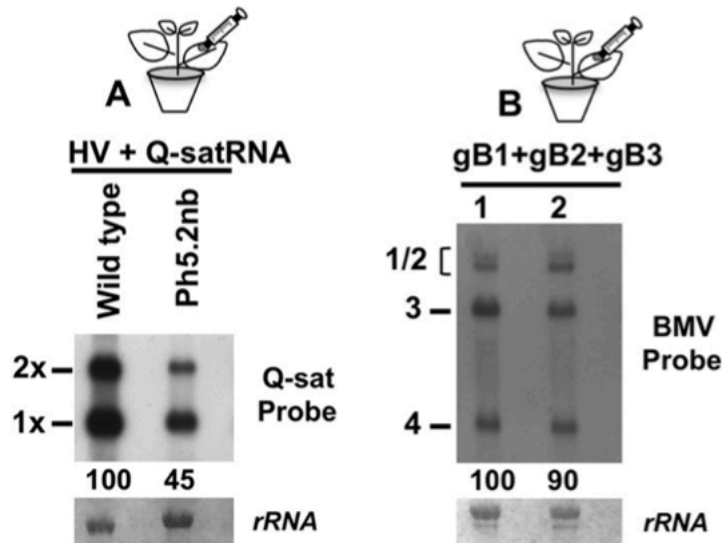
Figure 2.7 Biological significance of BRP1 to Q-satRNA and HV replication. Northern blot hybridization analysis of total RNA recovered from either (1) wild type or (2) BRP1 defective transgenic *N. benthamiana* leaves infiltrated with either (A) HV+Q-satRNA or (B) BMV (control). Multiple blots were generated and hybridized with indicated riboprobes shown to the right of each panel. Accumulation levels of HV and QsatRNA (in panel A) and BMV (in panel B) below each panel were normalized against respective samples in wild type plants as 100%. In panel A, the positions of HV progeny RNAs (RNAs 1-5) and Q-satRNA monomeric (1x) and dimeric (2x) forms and in panel B, the positions of progeny BMV RNA (RNAs 1-4) are shown to the left. Ribosomal RNA (rRNA) represents loading controls.

REFERENCE

1.   **Palukaitis P, Garcia-Arenal F.** 2003. Cucumoviruses. Advances in virus research **62:**241-323.

2.   **Boccard F, Baulcombe D.** 1993. Mutational analysis of cis-acting sequences and gene function in RNA3 of cucumber mosaic virus. Virology **193:**563-578.

3.   **Brigneti G, Voinnet O, Li WX, Ji LH, Ding SW, Baulcombe DC.** 1998. Viral pathogenicity determinants are suppressors of transgene silencing in Nicotiana benthamiana. EMBO J **17:**6739-6746.

4.   **Ding SW, Anderson BJ, Haase HR, Symons RH.** 1994. New overlapping gene encoded by the cucumber mosaic virus genome. Virology **198:**593-601.

5.   **Canto T, Prior DA, Hellwald KH, Oparka KJ, Palukaitis P.** 1997. Characterization of cucumber mosaic virus. IV. Movement protein and coat protein are both essential for cell-to-cell movement of cucumber mosaic virus. Virology **237:**237-248.

6.   **Schmitz I, Rao AL.** 1998. Deletions in the conserved amino-terminal basic arm of cucumber mosaic virus coat protein disrupt virion assembly but do not abolish infectivity and cell-to-cell movement. Virology **248:**323-331.

7.   **Garcia-Arenal F, Palukaitis P.** 1999. Structure and functional relationships of satellite RNAs of cucumber mosaic virus. Curr Top Microbiol Immunol **239:**37-63.

8.   **Hu C-C, Hsu Y-H, Lin N-S.** 2009. Satellite RNAs and Satellite Viruses of Plants. Viruses **1:**1325-1350.

9.   **Shimura H, Pantaleo V, Ishihara T, Myojo N, Inaba J, Sueda K, Burgyan J, Masuta C.** 2011. A viral satellite RNA induces yellow symptoms on tobacco by targeting a gene involved in chlorophyll biosynthesis using the RNA silencing machinery. PLoS Pathog **7:**e1002021.

10.   **Smith NA, Eamens AL, Wang MB.** 2011. Viral small interfering RNAs target host genes to mediate disease symptoms in plants. PLoS Pathog **7:**e1002022.

11.   **Escriu F, Fraile A, Garcia-Arenal F.** 2000. Evolution of Virulence in Natural Populations of the Satellite RNA of Cucumber mosaic virus. Phytopathology **90:**480-485.

12.   **Wang MB, Bian XY, Wu LM, Liu LX, Smith NA, Isenegger D, Wu RM, Masuta C, Vance VB, Watson JM, Rezaian A, Dennis ES, Waterhouse PM.** 2004. On the role of RNA silencing in the pathogenicity and evolution of viroids and viral satellites. Proceedings of the National Academy of Sciences of the United States of America **101:**3275-3280.

13.   **Choi SH, Seo JK, Kwon SJ, Rao AL.** 2012. Helper virus-independent transcription and multimerization of a satellite RNA associated with cucumber mosaic virus. Journal of Virology **86:**4823-4832.

14.   **Seo JK, Kwon SJ, Chaturvedi S, Ho Choi S, Rao AL.** 2013. Functional significance of a hepta nucleotide motif present at the junction of Cucumber mosaic virus satellite RNA multimers in helper-virus dependent replication. Virology **435:**214-219.

15.   **Mossop DW, Francki RI.** 1979. The stability of satellite viral RNAs in vivo and in vitro. Virology **94:**243-253.

16.   **Haynes SR, Dollard C, Winston F, Beck S, Trowsdale J, Dawid IB.** 1992. The bromodomain: a conserved sequence found in human, Drosophila and yeast proteins. Nucleic acids research **20:**2603.

17.   **Denis GV, Nikolajczyk BS, Schnitzler GR.** 2010. An emerging role for bromodomain-containing proteins in chromatin regulation and transcriptional control of adipogenesis. FEBS letters **584:**3260-3268.

18.   **Zhou M, Huang K, Jung KJ, Cho WK, Klase Z, Kashanchi F, Pise-Masison CA, Brady JN.** 2009. Bromodomain protein Brd4 regulates human immunodeficiency virus transcription through phosphorylation of CDK9 at threonine 29. Journal of Virology **83:**1036-1044.

19.   **Lin A, Wang S, Nguyen T, Shire K, Frappier L.** 2008. The EBNA1 protein of Epstein-Barr virus functionally interacts with Brd4. Journal of Virology **82:**12009-12019.

20.   **Gagnon D, Joubert S, Senechal H, Fradet-Turcotte A, Torre S, Archambault J.** 2009. Proteasomal degradation of the papillomavirus E2 protein is inhibited by overexpression of bromodomain-containing protein 4. Journal of Virology **83:**4127-4139.

21.   **Martinez de Alba AE, Sagesser R, Tabler M, Tsagris M.** 2003. A bromodomain-containing protein from tomato specifically binds potato spindle tuber viroid RNA in vitro and in vivo. J Virol **77:**9685-9694.

22.   **Kalantidis K, Denti MA, Tzortzakaki S, Marinou E, Tabler M, Tsagris M.** 2007. Virp1 is a host protein with a major role in Potato spindle tuber viroid infection in Nicotiana plants. Journal of Virology **81:**12872-12880.

23.   **de Wispelaere M, Rao AL.** 2009. Production of cucumber mosaic virus RNA5 and its role in recombination. Virology **384:**179-191.

24.   **Annamalai P, Rao AL.** 2006. Delivery and Expression of functional viral RNA genomes in planta by agroinfiltration, p. p2.1-2.15. *In* Downey T (ed.), Current Protocols in MIcrobiology, vol. Unit 16B. John Wiley & Sons, New York.

25.   **Eini O, Behjatnia SA, Dogra S, Dry IB, Randles JW, Rezaian MA.** 2009. Identification of sequence elements regulating promoter activity and replication of a monopartite begomovirus-associated DNA beta satellite. The Journal of general virology **90:**253-260.

26.   **Azevedo J, Garcia D, Pontier D, Ohnesorge S, Yu A, Garcia S, Braun L, Bergdoll M, Hakimi MA, Lagrange T, Voinnet O.** 2010. Argonaute quenching and global changes in Dicer homeostasis caused by a pathogen-encoded GW repeat protein. Genes Dev **24:**904-915.

27.   **Zaidi SH, Malter JS.** 1995. Nucleolin and heterogeneous nuclear ribonucleoprotein C proteins specifically interact with the 3'-untranslated region of

amyloid protein precursor mRNA. The Journal of biological chemistry **270:**17292-17298.

28.   **Martinez de Alba AE, Sagesser R, Tabler M, Tsagris M.** 2003. A bromodomain-containing protein from tomato specifically binds potato spindle tuber viroid RNA in vitro and in vivo. Journal of virology **77:**9685-9694.

29.   **Tabler M, Tzortzakaki S, Tsagris M.** 1992. Processing of linear longer-than-unit-length potato spindle tuber viroid RNAs into infectious monomeric circular molecules by a G-specific endoribonuclease. Virology **190:**746-753.

30.   **Annamalai P, Rao AL.** 2005. Replication-independent expression of genome components and capsid protein of brome mosaic virus in planta: a functional role for viral replicase in RNA packaging. Virology **338:**96-111.

31.   **Montasser MS, Kaper JM, Owens RA.** 1991. First report of potential biological control of potato spindle tuber viroid disease by virus-satellite combination. Plant Disease **75:**319.

32.   **Yang X, Kang L, Po T.** 1996. Resistance of tomato infected with cucumber mosaic virus satellite RNA to potato spindle tuber viroid. Ann appl Biol **130:**207-215.

33.   **Haim L, Zipor G, Aronov S, Gerst JE.** 2007. A genomic integration method to visualize localization of endogenous mRNAs in living yeast. Nat Methods **4:**409-412.

34.   **Whittaker GR, Helenius A.** 1998. Nuclear import and export of viruses and virus genomes. Virology **246:**1-23.

35.   **Zhao Y, Owens RA, Hammond RW.** 2001. Use of a vector based on Potato virus X in a whole plant assay to demonstrate nuclear targeting of Potato spindle tuber viroid. J Gen Virol **82:**1491-1497.

36.   **Schindler I-M, Muhlbach H-P.** 1992. Involvement of nuclear DNA-dependent RNA polymerases in potato spindle tuber viroid replication:a reevaluation. Plant science **84:**221-229.

37.   **Kaper JM, Waterworth HE.** 1977. Cucumber mosaic virus associated RNA 5: causal agent for tomato necrosis. Science **196:**429-431.

38.   **Linthorst HJ, Kaper JM.** 1984. Replication of peanut stunt virus and its associated RNA 5 in cowpea protoplasts. Virology **139:**317-329.

Chapter 3

A shift in plant proteome profile for a <u>B</u>romodomain containing <u>R</u>NA binding <u>P</u>rotein (BRP1) in plants infected with Cucumber mosaic virus or its satellite RNA

ABSTRACT

      Host proteins are the integral part of a successful infection caused by a given RNA virus pathogenic to plants. Therefore, identification of crucial host proteins playing an important role in establishing the infection process likely to help in devising approaches to curb disease spread. *Cucumber mosaic virus* (CMV), and its satellite RNA (satRNA) are important pathogens of many economically important crop plants worldwide. In a previous study, we demonstrated the biological significance of a <u>B</u>romodomain containing <u>R</u>NA binding <u>P</u>rotein (BRP1) in the infection cycle of satRNA, making BRP1 an important host protein to study. In this study, we demonstrate the importance of BRP1 in the replication of CMV followed by its out competence by satRNA over CMV. To further shed a light on the mechanistic role of BRP1 in the replication of CMV and satRNA, we analyzed the *Nicotiana benthamiana* host protein interactomes either for BRP1 alone or in the presence of CMV or satRNA. Co-immunoprecipitation, followed by LC MS/MS analysis of BRP1-FLAG on challenging with CMV or satRNA has led us observe a shift in the host protein interactome of BRP1. The significance of these results in relation to CMV and its satRNA infection cycle is discussed.

INTRODUCTION

Cucumber mosaic virus (CMV) is a member of *Bromoviridae* family belonging to the genus Cucumovirus(Palukaitis and Garcia-Arenal, 2003b). Considering its wide host range, CMV is an important plant virus to study. It is a tripartite virus, whose genome is composed of three RNAs: RNA 1 encodes for helicase and methyltransferase domains; RNA 2 encodes for RNA dependent RNA polymerase, along with a subgenomic RNA encoding for a post-transcriptional gene-silencing suppressor(Ding et al., 1994). RNA 3 is dicistronic. It encodes for a movement protein (MP), and a capsid protein (CP)(Choi et al., 2012a) expressed via subgenomic RNA4. RNA1 and RNA2 are packaged independently, while RNA3 and subgenomic RNA4 are co-packaged into a third virion(de Wispelaere and Rao, 2009). In addition to genomic and subgenomic RNAs, some strains of CMV are accompanied by a 336 nucleotides long noncoding satellite RNA (satRNA)(Hu et al., 2009). The replication of satRNA is entirely dependent on the RNA-dependent RNA polymerase (RdRP) encoded by the helper CMV(Hu et al., 2009). satRNA can either ameliorate or intensify symptom expression by CMV (Hu et al., 2009; Seo et al., 2013a).

The subcellular localization of CMV and its satRNA has been considered to be cytoplasmic until a recent discovery(Choi et al., 2012a), that satRNA (in the presence or absence of CMV) has a propensity to enter the nucleus of a plant

cell and form multimers due to the addition of a unique hepta-nucleotide sequence GGGAAAA (Choi et al., 2012a). More recently, it was demonstrated that a Bromodomain containing RNA binding protein (BRP1) mediates the nuclear localization of satRNA(Chaturvedi et al., 2014). Interestingly, BRP1 (previous referred to Viroid RNA binding Protein) has been demonstrated to play an important role in the infectivity of *Potato spindle tuber virod* (PSTVd) by transporting PSTVd to nucleus, the subcellular site of PSTVd replication(Kalantidis et al., 2007b).

A widely expanding approach of proteomics has provided an insight in delineating pivotal role(s) of several host proteins in the infectivity of RNA viruses, be it the role of HSP-70 in the replication of Tombusvirus(Serva and Nagy, 2006), a putative Rab-GTPase activation protein in the intracellular movement of *Bamboo mosaic virus*(Huang et al., 2013), or others. Replication of RNA viruses pathogenic eukaryotic organisms is dependent on plethora of host proteins forming a network during viral infection(Nagy and Pogany, 2012b). There have been several reports demonstrating the role of host proteins in promoting the replication of a virus, along with many acting in the defense mechanism of plant against virus(Nagy and Pogany, 2012a). In this study, we compare the host proteome profiles *in planta* challenged with CMV or its satRNA with an attempt to understand the mechanism of BRP1 regulated replication of CMV and its satRNA.

MATERIALS AND METHODS

CMV strain, Agroinfiltration and Confocal microscopy.

The construction of agroconstructs of genomic RNA of the Q strain of Cucumber mosaic virus, and QsatRNA is previously described(Choi et al., 2012a), BRP1 tagged with FLAG peptide (BRP1-FLAG) was kindly provided by Dr. Kriton Kalanditis(Kalantidis et al., 2007b). Wild type *Nicotiana benthamiana* leaves were infiltrated with agrocultures of GV 3101 strain containing the following inocula: BRP1-FLAG, or BRP1-FLAG + CMV, or BRP1-FLAG + satRNA. For analyzing the shift in the localization of BRP1 in the presence of CMV or satRNA, BRP1-GFP agrocultures (kindly obtained from Dr. Kalantidis) (Kalantidis et al., 2007b) were infiltrated to wild type *N. benthamiana* leaves along with QCMV or satRNA or CMV+satRNA, at 2dpi leaves were stained with DAPI (5 mg/ml in PBS buffer), and were subjected to confocal microscopy.

Protein extraction, co-immunoprecipitation, and LC MS/MS.

After 4dpi, agroinfiltrated leaves were ground in liquid nitrogen, and total protein was extracted in 3 volumes of extraction buffer (20 mM Tris-Cl [pH 7.5], 300 mM NaCl, 5 mM $MgCl_2$, 5 mM DTT, 1% plant protease inhibitor [Sigma, USA]). The liquid extract was centrifuged at 12,000 rpm for 15 minutes at 4°C,

and supernatant was used for co-immunoprecipitation, which was described previously (Chaturvedi et al., 2014). Briefly, total protein was subjected to immunoprecipitation using 25 µl of FLAG M2 agarose beads (Sigma, U.S.A) for every gram of starting material. The mixture was incubated at 4°C for 4 hours with gentle shaking. After precipitation, agarose beads were washed three times with extraction buffer, which was followed by a short spin at 4°C. LC MS/MS was performed on the protein eluted from agarose beads as described previously (Fig. 3.1)(Maor et al., 2007).

Protein identification, Panther classification and characterization.

Protein identification from peptide sequences from LC MS/MS samples was performed using MASCOT software(Perkins et al., 1999). Initially identified proteins were clustered on the basis of number of proteins interacting with BRP1 by itself, or in the presence of CMV or satRNA (Fig. 3.2). Further, the emPAI (Exponentially Modified Protein Abundance Index) value was calculated for every sample(Ishihama et al., 2005), and were plotted in the form of a graph (Fig. 3.3).

Subcellular localization and functionality prediction of the host proteins.

Number of host proteins interacting with BRP1 were classified on the basis of their subcellular localization using WoLF-PSORT (Fig. 3.4)(Horton et al., 2007), and functionality using PANTHER classification system (Fig. 3.5)(Mi et al., 2013).

RESULTS AND DISCUSSION

BRP1 is essential for CMV replication

satRNA is known to significantly interfere with the genome replication of CMV(Hu et al., 2009). We previously have demonstrated that BRP1 has a biological role in the infection cycle of satRNA(Chaturvedi et al., 2014). To verify whether a similar role exists for BRP1 in the infection cycle of CMV, transgenic *N, benthamianai* plants (ph5.2nb) defective in BRP1(Kalantidis et al., 2007a) were infiltrated with CMV agrotransformants and total RNA isolated at 4 dpi was subjected to Northern blot analysis. Results are shown in Fig. 3.1A. Compared to non-transgenic wild type lines, CMV replication in BRP1 defective lines was reduced by 70% (Fig. 3.1A). These observations suggest that BRP1 is an integral part of the CMV replication.

satRNA outcompetes CMV for BRP1

The data shown in Fig. 3.1A together with our previous observations(Chaturvedi et al., 2014) conclude that BRP1 is a commonly shared host protein between CMV and satRNA. If this were true, then we anticipate a competition for BRP1 in plants co-infected with CMV and satRNA. To test this possibility, *N benthamiana* leaves were agroinfiltrated with the following

agroconstructs: (i) GFP; (ii) BRP1-GFP; (iii) BRP1-GFP+CMV; (iv) BRP1-GFP+satRNA and (v) BRP1-GFP+CMV+satRNA. At 2 dpi, infiltrated leaves were stained with DAPI (5 mg/ml in PBS buffer) and observed under confocal microscope for GFP expression. Results are summarized in Fig. 3.1B. As expected, the distribution of GFP in control plants infiltrated only with GFP was confined to the cytoplasm (Fig. 3.1B, panel a). This GFP distribution pattern was de-directed to the nucleus when plants were infiltrated with BRP1-GFP construct (Fig. 3.1B, panel b). However, when CMV was co-expressed with BRP1-GFP, green fluorescence was re-located to the cytoplasm (Fig. 3.1B, panel c). Interestingly, co-expression of satRNA with either BRP1-GFP or BRP1-GFP+CMV, the distribution of green fluorescence was confined exclusively to the nucleus (Fig. 3.1B, panels d and e). Collectively, these results suggest that there is a competition between CMV and satRNA for BRP1, and clearly satRNA outcompetes CMV for BRP1 and changes its subcellular localization.

Distribution of BRP1 host proteome in planta challenged with CMV or satRNA

Given the biological significance of BRP1 in the infection cycle of CMV (Fig. 3.1A) and its satRNA(Chaturvedi et al., 2014), we seek to understand how the proteome interacting with BRP1 would shift *in planta* when challenged with CMV or satRNA. Thus, *N benthamiana* leaves were agroinfiltrated with agroconstructs

containing either BRP1-FLAG or BRP1-FLAG+CMV or BRP1-FLAG+satRNA (according to flow chart shown in Fig. 3.2). At 4dpi, infiltrated leaves were subjected to co-immunoprecipitation using anti-FLAG agarose beads, followed by MudPIT analysis. Initially we identified >600 host proteins using green plant database of MASCOT. These include orthologs of a given protein and different peptides of the same protein. From this list, we shortlisted 60 host proteins based on peptides that match *Solanum* sp using MASCOT program (Hirosawa et al., 1993). From this shortlist, we further delineated the number of host proteins that are either exclusive to BRP1 or those that interacted with BRP1 in the presence of CMV or satRNA. Results shown in Fig. 3.3 revealed that number of host proteins that exclusively interacted with either BRP1 is 37. However, this number was significantly increased to 60 and 41, respectively in the presence of CMV or satRNA (Fig. 3.3). Whereas, the number of host proteins that commonly shared between CMV and satRNA is 8, BRP1 and CMV is 4 and BRP1 and satRNA is 0 (Fig. 3.3). Finally the number of host proteins that are shared among BRP1, CMV and satRNA is 33 (Fig. 3.3). There are no host proteins that interacted with BRP1 exclusively in the presence of satRNA or BRP1 by it self, although there are 15 host proteins, which interacted with BRP1 exclusively in the presence of CMV (Fig. 3.3). It is possible that these 15 host proteins might paly an important role in controlling phenotypes other than replication such as symptom induction, movement or pathogenesis.

Above results shed light on how BRP1's ability to interact with other host proteins changes in the presence of CMV or satRNA. CMV is known to induce a wide-range of symptom phenotypes in different host plants, and satRNA has been shown to modulate disease symptoms by RNA-silencing based regulation of host genes (Shimura et al., 2011b; Smith et al., 2011a). However, the contribution of host proteome toward disease development by CMV or satRNA is poorly understood. Our observations showing a significant shift in plant proteome of BRP1 in the presence of CMV or satRNA might help us answer this question.

Differential binding affinity of BRP1 to screened host proteins in the presence of CMV or satRNA

To understand how the binding affinity of BRP1 to different host proteins changes in plants challenged with CMV or satRNA, we calculated the (emPAI) value using MASCOT(Ishihama et al., 2005) for the list of 60 host proteins. Result shown in Fig. 3.4 summarizes the binding affinity of different host proteins to BRP1 by itself or in the presence of CMV or satRNA. From these emPAI values, it is evident that a considerable shift occurred in the binding ability of BRP1 (with the shift of more than 0.5 in emPAI value) in the presence of CMV or satRNA for host proteins such as Glyceraldehyde 3 phosphate dehydrogenase (GAPDH), Ribulose bisphosphate carboxylase, elongation factor TuA (EF-TuA), H(+)- transporting ATP synthase, oxygen evolving enhancer protein 1, actin,

phosphoglycerate kinase, carbonyl anhydrase, ubiquitin precursor and elongation factor TuB (EF-TuB) (Fig. 3.4).

The above mentioned host proteins that displayed high affinity of binding to BRP1 have been previously observed to play an important role in the replication of positive sense RNA viruses(Nagy and Pogany, 2012b). For example, GAPDH has been shown to down regulate the replication of *Bamboo mosaic virus* (BaMV)(Prasanth et al., 2011) and strand asymmetry in *Tomato bushy stunt virus* (TBSV)(Huang and Nagy, 2011). Ribulose bisphosphate carboxylase (Rubisco) is involved in the Tobravirus movement and promote plant resistance to virus infection(Zhao et al., 2013). Translation elongation factor 1a (EF-TuA) has been shown to facilitate the assembly of replicase complex in Tombusvirus, and stimulate minus strand synthesis(Li et al., 2010).

Distribution of host proteins in cellular-organelle interacting with BRP1 challenged with CMV or satRNA

Tonoplast has been shown to be the subcellular localization site for CMV replication(Hatta and Francki, 1981),(Cillo et al., 2002). Since replication of satRNA is dependent on CMV, the site of CMV-dependent replication of satRNA is cytoplasm. However, recent evidence suggests that localization of nucleus (both in the presence and absence of CMV) is obligatory for CMV-dependent

replication. To shed a light on the distribution of identified host proteins with respect to subcellular localization, WoLF-PSORT(Horton et al., 2007) program was used (Fig. 3.5). Replication of positive sense RNA viruses takes place in different cell organelles, (Denison, 2008; Laliberte and Sanfacon, 2010). Analysis of the host protein profile of various cell organelle revealed that, distribution of proteins interacting with BRP1 in the presence of CMV or satRNA varied among several cell organelle (Fig. 3.5)(Horton et al., 2007). For example, in the cytoplasm, the number of host proteins interacting with BRP1 by itself is 19 (Fig. 3.5). Interestingly, the number was increased to 35 and 23 respectively in the presence of CMV and satRNA (Fig. 3.5). Similar trend was observed for other organelle such as mitochondria, chloroplasts, nucleus and cytoskeleton (Fig. 3.5). With respect to CMV, involvement of host proteins associated with chloroplast (involved in symptom phenotype) and cytoskeleton (involved in cell-to-cell movement) are justified (Caplan et al., 2008), (Reichel et al., 1999). Likewise, since satRNA has a propensity to localize in the nucleus (Choi et al., 2012a), an increase in number of host proteins in this cell organelle is justified, However, an unexpected result was an increase in the number of host proteins associated with mitochondria. Although there is no experimental evidence for the involvement of mitochondria in either in CMV or satRNA replication or pathogenesis, it is likely that this organelle might paly an indirect role. Thus, the functional significance of the host proteins associated with mitochondria requires further examination.

CONCLUSIONS

In conclusion, our study provides a preliminary identification of various host proteins involved in the replication and pathogenesis of CMV and its satRNA. The biological significance of each of these host proteins remains to be tested. For example, GAPDH has been shown to involve in several RNA viruses in strand asymmetry(Nagy and Pogany, 2012a). Likewise HSP 40 has been shown to involve in the assembly of viral replicase complex in flaviviruses, flock house virus and brome mosaic virus(Nagy and Pogany, 2012a). Whether these roles of GAPDH or HSP 40 are universally conserved among RNA viruses or not remains to be tested. These studies are in progress in our lab.
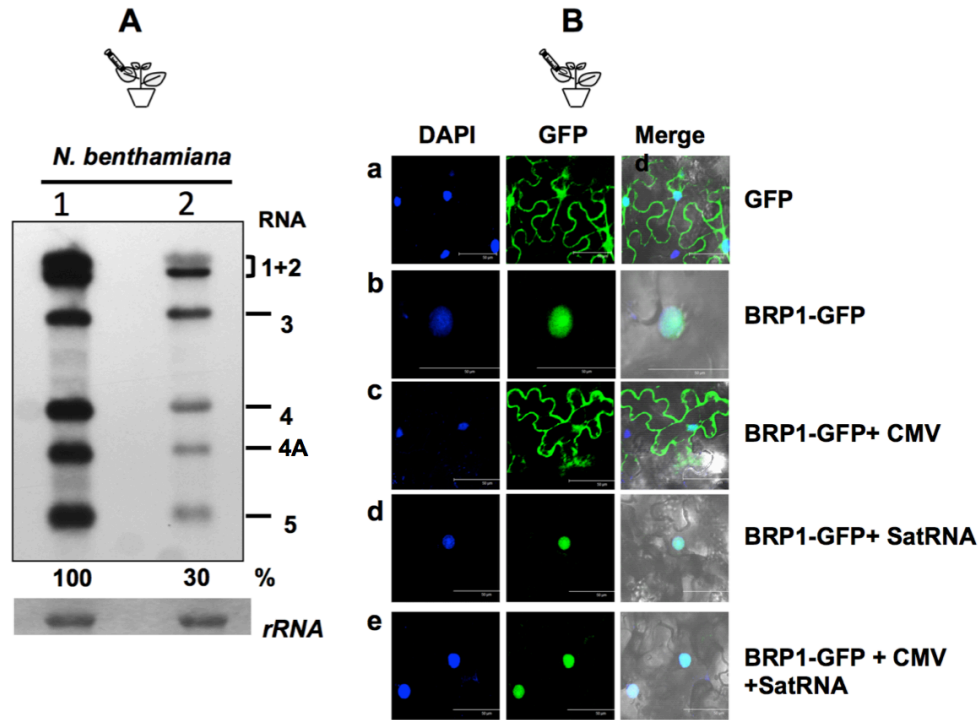
Figure 3.1 Role of BRP1 in CMV and its satRNA. (A) BRP1 is an essential host protein for CMV replication. Northern blot analysis of total RNA recovered from (1) wild type and (2) transgenic ph5.2nb (defective in BRP1) *N. benthamiana* plants following infiltration with agrotransformants of all three genomic RNAs of CMV. The position of CMV progeny RNA is shown to the right. Accumulation levels of CMV progeny RNA shown were normalized against wild type CMV as 100%. rRNA represents loading control. (B) satRNA outcompetes CMV for BRP1. *N. benthamiana* leaves were infiltrated with agrotransformants shown to the right. At 2 dpi, following DAPI staining to visualized the nucleus, leaves were subjected to confocal microscopy for green fluorescent signal detection. Bar= 50mm.

Flowchart for MudPIT analysis

Infiltrate agroculture of BRP1/BRP1+CMV/BRP1+SatRNA to wild type *N. benthamiana*

⬇

After 4 days of inoculation, coimmunoprecipitate the leaf extract with antiFLAG agarose beads

⬇

Elute agarose beads

⬇

Trypsin digestion

⬇

Multidimensional chromatography

⬇

Tandem Mass spectrometry

⬇

Spectrum/peptide matching using Mascot

⬇
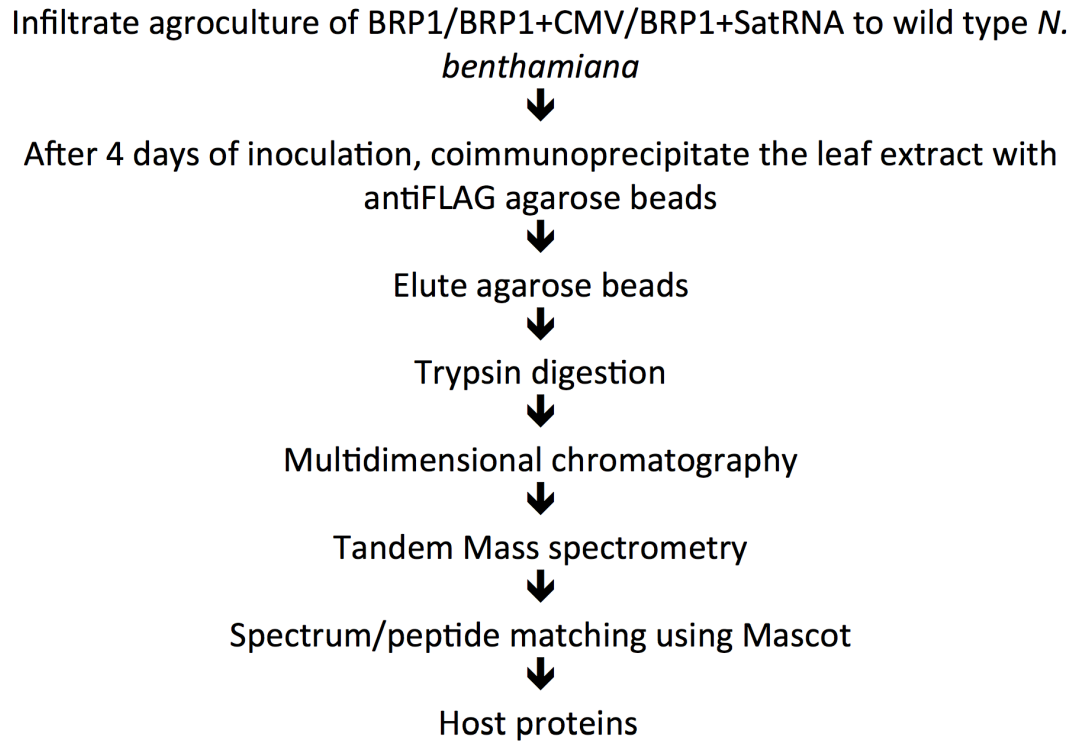
Host proteins

Figure 3.2 Flow chart showing various steps involved in the MudPIT analysis.
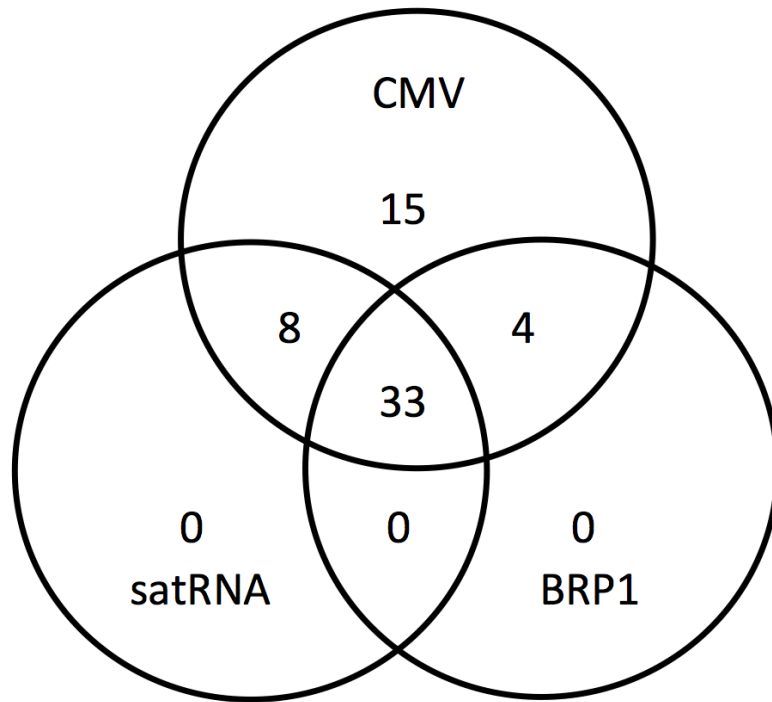
Figure 3.3 Venn diagram showing the number of host proteins shared among BRP1, CMV and satRNA.

Figure 3.4 Binding affinity of BRP1 to host proteins in the presence of CMV or sat RNA determined by MASCOT. Following MudPIT analysis (Fig. 3.2), MASCOT program was used to identify indicate host protein peaks (X-axis) and emPAI values were calculated (Y-axis) and plotted for indicated samples.
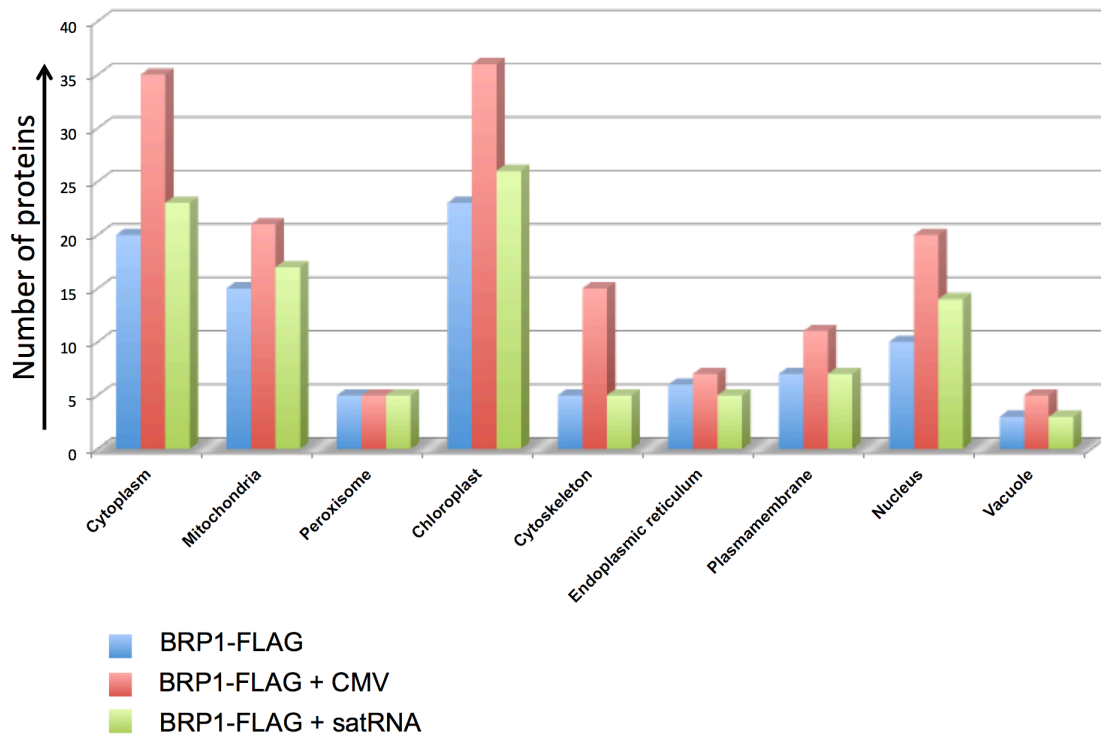
Figure 3.5 Subcellular distribution of number of host proteins interacting with either BRP1 alone or BRP1+CMV or BRP1+satRNA. Host proteins identified by MASOT were subjected to WoLF PSORT to classify them based on their subcellular distribution and plotted as shown.

REFERENCE

1.   **Palukaitis, P.; Garcia-Arenal, F., Cucumoviruses.** *Advances in virus research* **2003,** *62*, 241-323.

2.   **Ding, S. W.; Anderson, B. J.; Haase, H. R.; Symons, R. H.,** New overlapping gene encoded by the cucumber mosaic virus genome. *Virology* **1994,** *198* (2), 593-601.

3.   **Choi, S. H.; Seo, J. K.; Kwon, S. J.; Rao, A. L.,** Helper virus-independent transcription and multimerization of a satellite RNA associated with cucumber mosaic virus. *Journal of virology* **2012,** *86* (9), 4823-32.

4.   **de Wispelaere, M.; Rao, A. L.,** Production of cucumber mosaic virus RNA5 and its role in recombination. *Virology* **2009,** *384* (1), 179-91.

5.   **Hu, C.-C.; Hsu, Y.-H.; Lin, N.-S.,** Satellite RNAs and Satellite Viruses of Plants. *Viruses* **2009,** *1*, 1325-1350.

6.   **Seo, J. K.; Kwon, S. J.; Chaturvedi, S.; Choi, S. H.; Rao, A. L.,** Functional significance of a hepta nucleotide motif present at the junction of Cucumber mosaic virus satellite RNA multimers in helper-virus dependent replication. *Virology* **2013,** *435* (2), 214-9.

7.   **Chaturvedi, S.; Kalantidis, K.; Rao, A. L.,** A bromodomain-containing host protein mediates the nuclear importation of a satellite RNA of cucumber mosaic virus. *J Virol* **2014,** *88* (4), 1890-6.

8.   **Kalantidis, K.; Denti, M. A.; Tzortzakaki, S.; Marinou, E.; Tabler, M.; Tsagris, M.**, Virp1 is a host protein with a major role in Potato spindle tuber viroid infection in Nicotiana plants. *Journal of virology* **2007,** *81* (23), 12872-80.

9.   **Serva, S.; Nagy, P. D.,** Proteomics analysis of the tombusvirus replicase: Hsp70 molecular chaperone is associated with the replicase and enhances viral RNA replication. *Journal of virology* **2006,** *80* (5), 2162-9.

10.   **Huang, Y. P.; Chen, J. S.; Hsu, Y. H.; Tsai, C. H.**, A putative Rab-GTPase activation protein from Nicotiana benthamiana is important for Bamboo mosaic virus intercellular movement. *Virology* **2013,** *447* (1-2), 292-9.

11.   **Nagy, P. D.; Pogany, J.,** The dependence of viral RNA replication on co-opted host factors. *Nature reviews. Microbiology* **2012,** *10* (2), 137-49.

12.   **Maor, R.; Jones, A.; Nuhse, T. S.; Studholme, D. J.; Peck, S. C.; Shirasu, K.,** Multidimensional protein identification technology (MudPIT) analysis of ubiquitinated proteins in plants. *Molecular & cellular proteomics : MCP* **2007,** *6* (4), 601-10.

13.   **Perkins, D. N.; Pappin, D. J.; Creasy, D. M.; Cottrell, J. S.,** Probability-based protein identification by searching sequence databases using mass spectrometry data. *Electrophoresis* **1999,** *20* (18), 3551-67.

14.   Ishihama, Y.; Oda, Y.; Tabata, T.; Sato, T.; Nagasu, T.; Rappsilber, J.; **Mann, M.,** Exponentially modified protein abundance index (emPAI) for estimation of absolute protein amount in proteomics by the number of sequenced peptides per protein. *Molecular & cellular proteomics : MCP* **2005,** *4* (9), 1265-72.

15.   **Horton, P.; Park, K. J.; Obayashi, T.; Fujita, N.; Harada, H.; Adams-Collier, C. J.; Nakai, K**., WoLF PSORT: protein localization predictor. *Nucleic Acids Res* **2007,** *35* (Web Server issue), W585-7.

16.   **Mi, H.; Muruganujan, A.; Casagrande, J. T.; Thomas, P. D.,** Large-scale gene function analysis with the PANTHER classification system. *Nat Protoc* **2013,** *8* (8), 1551-66.

17.   **Kalantidis, K.; Denti, M. A.; Tzortzakaki, S.; Marinou, E.; Tabler, M.; Tsagris, M.,** Virp1 is a host protein with a major role in Potato spindle tuber viroid infection in Nicotiana plants. *Journal of Virology* **2007,** *81* (23), 12872-80.

18.   **Hirosawa, M.; Hoshida, M.; Ishikawa, M.; Toya, T.,** MASCOT: multiple alignment system for protein sequences based on three-way dynamic

programming. *Computer applications in the biosciences : CABIOS* **1993,** *9* (2), 161-7.

19 .   **Shimura, H.; Pantaleo, V.; Ishihara, T.; Myojo, N.; Inaba, J.; Sueda, K.; Burgyan, J.; Masuta, C.,** A viral satellite RNA induces yellow symptoms on tobacco by targeting a gene involved in chlorophyll biosynthesis using the RNA silencing machinery. *PLoS Pathogen* **2011,** *7* (5), e1002021.

20. **Smith, N. A.; Eamens, A. L.; Wang, M. B.**, Viral small interfering RNAs target host genes to mediate disease symptoms in plants. *PLoS Pathogen* **2011,** *7* (5), e1002022.

21.   **Prasanth, K. R.; Huang, Y. W.; Liou, M. R.; Wang, R. Y.; Hu, C. C.; Tsai, C. H.; Meng, M.; Lin, N. S.; Hsu, Y. H.,** Glyceraldehyde 3-phosphate dehydrogenase negatively regulates the replication of Bamboo mosaic virus and its associated satellite RNA. *Journal of virology* **2011,** *85* (17), 8829-40.

22.   **Huang, T. S.; Nagy, P. D.,** Direct inhibition of tombusvirus plus-strand RNA synthesis by a dominant negative mutant of a host metabolic enzyme, glyceraldehyde-3-phosphate dehydrogenase, in yeast and plants. *Journal of virology* **2011,** *85* (17), 9090-102.

23. **Zhao, J.; Liu, Q.; Zhang, H.; Jia, Q.; Hong, Y.; Liu, Y.,** The rubisco small subunit is involved in tobamovirus movement and Tm-2(2)-mediated extreme resistance. *Plant physiology* **2013,** *161* (1), 374-83.

24. **Li, Z.; Pogany, J.; Tupman, S.; Esposito, A. M.; Kinzy, T. G.; Nagy, P. D.,** Translation elongation factor 1A facilitates the assembly of the tombusvirus replicase and stimulates minus-strand synthesis. *PLoS pathogens* **2010,** *6* (11), e1001175.

25. **Hatta, T.; Francki, R. I.,** Cytopathic structures associated with tonoplasts of plant cells infected with cucumber mosaic and tomato aspermy viruses. *Journal of General Virology* **1981,** *53*, 343-345.

26. **Cillo, F.; Roberts, I. M.; Palukaitis, P.,** In situ localization and tissue distribution of the replication-associated proteins of Cucumber mosaic virus in tobacco and cucumber. *Journal of virology* **2002,** *76* (21), 10654-64.

27. **Denison, M. R.,** Seeking membranes: positive-strand RNA virus replication complexes. *PLoS biology* **2008,** *6* (10), e270.

28. Laliberte, J. F.; Sanfacon, H., Cellular remodeling during plant virus infection. *Annual review of phytopathology* **2010,** *48*, 69-91.

29.   Caplan, J. L.; Mamillapalli, P.; Burch-Smith, T. M.; Czymmek, K.; Dinesh-Kumar, S. P., Chloroplastic protein NRIP1 mediates innate immune receptor recognition of a viral effector. *Cell* **2008,** *132* (3), 449-62.

30.   Reichel, C.; Mas, P.; Beachy, R. N., The role of the ER and cytoskeleton in plant viral trafficking. *Trends in plant science* **1999,** *4* (11), 458-462.

Chapter 4

Evaluating the role of BRP1 and GAPDH in CMV replication

ABSTRACT

Viruses overcome their inability to code for large number of proteins by hijacking cellular proteins and lead to the replication of their genome by remodeling cellular membranes or utilizing host proteins in forming a functional replicase complex. RNA viruses in particular, utilize host proteins by protein-protein and protein-RNA interactions, and synthesize progeny RNAs. From the information garnered in previous chapters, two host proteins (BRP1 and GAPDH) were selected based on their indispensability in the replication of CMV and literature survey. For BRP1, performing MudPIT analysis using coimmunoprecipitated samples of BRP1-FLAG with CMV infected leaf extract suggested that BRP1 interacts with 1a protein of CMV, which was later confirmed by BiFC assay. For GAPDH, it was observed that in its absence viral replicase complex failed to form, as 1a-2a interactions did not take place in single gene knockout lines of GAPDH in *Arabidopsis thaliana* (Col-0), but rescued on addition of transiently expressing GAPDH to the knockout lines. This piece of data suggests the intricate role of host proteins in the replication of CMV.

INTRODUCTION

Virus usually encodes for a minimal set of proteins, which are necessary but not sufficient to lead a successful infection in the host. There is a dearth of information regarding how different host proteins interact with viral genome or proteins to successfully infect the cells. A widely expanding technique of proteomics has provided an insight in understanding the pivotal role of several host proteins in the infectivity of viruses, be it a role of HSP70 in the replication of *Tombusvirus* (Serva and Nagy, 2006), a putative Rab-GTPase activation protein for intracellular movement of *Bamboo mosaic virus* (Huang et al., 2013), and many others. Replication of a virus is dependent on plethora of host proteins forming a network during viral infection. There have been several reports demonstrating the role of host proteins in promoting the replication of a virus, along with many acting in the defense mechanism of plant against virus (Nagy and Pogany, 2012).

There have been different approaches by which role of host proteins in viral infection are been studied. The basic approach to study the shift in global proteins in plant cells on infection by plant viruses by comparing 2D- gel electrophoresis followed by mass spectrometry. Shift in plant proteome was observed for Cucumber mosaic virus (CMV) resistant transgenic tomato plant on infecting with CMV (Di Carli et al., 2010). There have been several reports where viral protein complexes were isolated by co-immunoprecipitation followed by 2D

gel electrophoresis and mass spectrometry, where an approach was made to delineate specific host proteins interacting with a particular complex. To understand which host protein is associated with a potyvirus RNA dependednt RNA polymerase, a tandem affinity purification (NTAPi)- tagged RdRP of Turnip mosaic virus (TuMV) was expressed in *Arabidopsis thaliana*, which was further subjected to tandem affinity purification, and host proteins interacting with RdRP were identified by Mass spectrometry (Dufresne et al., 2008).

After identification of proteins of interest, the list of host proteins can be narrowed down by employing mutant lines deficient for those proteins to study their effect on virus replication by the virtue of Genetic screening. There are several genetic approaches like (a) transiently silencing the host protein of interest e.g., VIGS (Virus Induced Gene Silencing) (Bachan and Dinesh-Kumar, 2012), CRISPR (Zhang et al., 2014), Zinc Finger Nuclease (ZFN) (Gaj et al., 2012), 2) Transcription activator like effector nuclease (TALENS) (Zhang et al., 2013). (b) By employing global gene knockout lines, which in case of *Arabidopsis thaliana* are available from "The Arabidopsis Information Resource, (TAIR)" (Lamesch et al., 2012).

In chapter 3, we pulled down plethora of host proteins interacting with BRP1. In this chapter, an attempt is made to understand the role of BRP1 in the replication of CMV. Furthermore, number of host proteins interacting with BRP1

were short listed on the basis of (a) Difference in emPAI value of host proteins interacting with BRP1, and (b) literature survey, where the role of particular host proteins have been demonstrated in the replication of a positive sense RNA virus. Total 15 shortlisted single gene knockout lines of Arabidopsis thaliana were obtained from **T**he **A**rabidopsis **I**nformation **R**esource (TAIR) (https://www.arabidopsis.org) (Lamesch et al., 2012), and number of single gene knockout lines were shortlisted based on inability of CMV to replicate in them. Further, ability of 1a-2a proteins of CMV to form a replicase complex in single gene knockout lines was determined, and it was observed that in the absence of Glyceraldehyde 3- phosphate dehydrogenase (GAPDH), 1a-2a replicase complex failed to assemble, which was able to form when GAPDH protein was exogenously provided.

MATERIAL AND METHODS

Agroinfiltration, single gene knockout lines, and progeny analysis.

Construction of infectious agroconstructs of Q strain of CMV is demonstrated previously (Choi et al., 2012). pKn-GAPDH construct for overexpression of GAPDH protein was kindly provided by Dr. Yau- Heiu Hsu (Prasanth et al., 2011). Single gene knockout lines of selected host proteins were obtained from **T**he **A**rabidopsis **I**nformation **R**esource (TAIR) (https://www.arabidopsis.org) (Lamesch et al., 2012). Agroinfiltration of genes in wild type and single gene knockout lines of Arabidopsis was performed as previously described (Lee and Yang, 2006; Oh et al., 2010). Progeny analysis of the samples was performed by extracting total RNA from infiltrated leaves at 4 days post infiltration (dpi) using Trizol (Sigma, U.S.A), and northern blot analysis of total RNA (10 µg) was performed and probed for CMV RNA (Choi et al., 2012). Construction of BiFC constructs and confocal microscopy

Agroconstructs for BRP1 and CMV 1a protein for BiFC assay were constructed as previously described (Seo et al., 2012). Briefly, sequence encompassing BRP1, CMV 1a or 2a protein was amplified using PCR, and ligated into pZPc-cYFP, pZPc-nYFP, pZPn-nYFP or pZPn-cYFP vectors. Constructs were transformed into GV3101 agrobacterium (Annamalai and Rao, 2008), and were mixed with their respective partners (as mentioned in figures),

and infiltrated to wild type *N. benthamiana* leaves (Chaturvedi et al., 2012). At 3 days post infiltration, epidermal cells of agroinfiltrated leaves were observed for fluorescence under Leica SP2 laser-scanning confocal microscope (Leica, Germany) to visualize YFP (excitation: 514 nm).

Co-immunoprecipitation and MudPIT analysis

N. benthamiana leaves were agroinfiltrated with agroculture containing CMV + BRP1-FLAG. After 4dpi, agroinfiltrated leaves were ground in liquid nitrogen, and total protein was extracted in 3 volumes of extraction buffer (20 mM Tris-Cl [pH 7.5], 300 mM NaCl, 5 mM $MgCl_2$, 5 mM DTT, 1% plant protease inhibitor [Sigma, USA]). The liquid extract was centrifuged at 12,000 rpm for 15 minutes at 4^oC, and supernatant was used for co-immunoprecipitation, which was described previously (Chaturvedi et al., 2014). Briefly, total protein was subjected to immunoprecipitation using 25 µl of FLAG M2 agarose beads (Sigma, U.S.A) for every gram of starting material. The mixture was incubated at 4^oC for 4 hours with gentle shaking. After precipitation, agarose beads were washed three times with extraction buffer, which was followed by a short spin at 4^oC. LC MS/MS was performed on the protein eluted from agarose beads as described previously (Maor et al., 2007).

RESULTS AND DISCUSSION

BRP1 interacts with 1a replicase protein of CMV

N. benthamiana leaves were infiltrated with BRP1-FLAG and CMV, and at 4dpi, leaf extract was immune precipitated with antiFLAG agarose beads (Sigma, U.S.A). LC MS/MS was performed on precipitated antiFLAG agarose beads, and using MASCOT program, peptides from mass spectrometry results were identified. It was observed from MASCOT identification, that BRP1 interacted with 1a replicase protein (Fig. 4.1) but not 2a. Results obtained from LC MS/MS were confirmed by performing BiFC assay for BRP1 and Q1a protein. Agroconstructs carrying BRP1 BiFC constructs (BRP1-pZPc-cYFP, BRP1-pZPc-nYFP, BRP1-pZPn-nYFP or BRP1n-cYFP) or Q1a BiFC constructs (Q1a-pZPc-cYFP, Q1a-pZPc-nYFP, Q1a-pZPn-nYFP, or Q1a-pZPn-cYFP) were mixed as shown in the figures 2 or 3 and infiltrated to wild type *N. benthamiana* leaves. At 3dpi, epidermal cells of agroinfiltrated leaves were observed for fluorescence under Leica SP2 laser-scanning confocal microscope (Leica, Germany) to visualize YFP (excitation: 514 nm). Using BiFC, it was observed that BRP1 or Q1a lead to homologous interactions (Fig. 4.2). Also, in three combinations, 1a-BRP1 heterologous interactions did take place (Fig. 4.3). This result provides with information that one of the reason why CMV or satRNA replication decreases in the absence of BRP1 is due to BRP1's ability to interact with 1a

protein of CMV. It suggests that BRP1 might play an important role in the activation of replicase complex, or might assist in binding of replicase complex to viral RNA, as BRP1 has an RNA binding domain.

Effect of host proteins on the replication of CMV in single gene knockout mutants of *Arabidopsis thaliana*

Single gene knockout lines of Arabidopsis thaliana ecotype Col-0 of shortlisted proteins (Fig. 4.4) were obtained from **T**he **A**rabidopsis **I**nformation **R**esource (TAIR) (https://www.arabidopsis.org) (Lamesch et al., 2012). Four weeks old single gene knockout lines were agroinfiltrated with 0.5 OD of CMV bacterial culture, and at 4 days post infiltration (dpi), total RNA was extracted using TRIZOL reagent (Sigma, U.S.A), and northern blot analysis was performed to detect CMV RNAs. It was observed that the replication level of CMV had reduced to be <1% for six host proteins (RNA Binding Glycine Rich Protein 1a, Elongation Factor 1 Gamma like Protein, Elongation Factor 2, Glyceraldehyde 3 Phosphate Dehydrogenase, Global Transcription Factor Group and Vacuolar H+ ATPase B subunit) (Fig. 4.4 and 4.5). These results suggest that six short listed host proteins might play an important role in the replication of CMV.

Protein-protein interactions in single gene knockout lines

Agroconstructs encompassing (BRP1-pZPc-cYFP, BRP1-pZPc-nYFP, BRP1-pZPn-nYFP or BRP1n-cYFP), Q1a BiFC constructs (Q1a-pZPc-cYFP, Q1a-pZPc-nYFP, Q1a-pZPn-nYFP, or Q1a-pZPn-cYFP) or Q2a BiFC constructs (Q2a-pZPc-cYFP, Q2a-pZPc-nYFP, Q2a-pZPn-nYFP, or Q2a-pZPn-cYFP) with their respective partners were infiltrated to single gene knockout lines of *Arabidopsis thaliana* (col-0) as demonstrated (Fig. 4.6 and 4.7), and at 3 dpi, epidermal cells of infiltrated leaves were visualized under Leica SP2 confocal microscope (Leica, Germany) using YFP filter (excitation: 514 nm). Single gene knockout lines for HSP-90 was used as a negative control (as the virus replicated in this knockout line (Fig. 4.4 and 4.5). It was observed that 1a-BRP1 interaction did take place in all the single gene knockout lines of *Arabidopsis thaliana* (col-0) along with wild type plant (Fig. 4.6). Though, it was observed that for 1a-2a BiFC assay, reconstitution of YFP did not take place in single gene knockout lines of GAPDH (Fig. 4.7). These results suggest that GAPDH plays an important role in formation or stabilization of 1a-2a replicase complex.

GAPDH trans-complementation assay

Wild type, GAPDH or HSP90 single gene knockout lines of A. thaliana were agroinfiltrated with QCMV RNA1+RNA2+RNA3, or QCMV

115

RNA1+RNA2+RNA3+pKn-GAPDH. At 4dpi, total RNA was extracted using Trizol (Sigma, U.S.A), and 10 mg of total RNA was subjected to northern blot analysis to detect CMV RNAs. Replication of CMV is rescued on providing GAPDH exogenously in single gene knockout line of GAPDH, though not much difference is observed in wild type, or single gene knockout line of HSP90 plants (Fig. 4.9). Further, it was assessed if 1a-2a replicase complex will reconstitute on trans-complementation of pKn-GAPDH, which did not take place in GAPDH single gene knockout line (Fig. 4.8). Agrobacterium containing a positive combination of 1a-2a construct (Q1a-nYFP+cYFP-Q2a) was infiltrated to wild type, single gene knockout line of HSP90, single gene knockout line of GAPDH, or single gene knockout line of GAPDH+pKn-GAPDH+P19. At 3dpi, epithelial cells of infiltrated leaves were subjected to confocal microscopy using Leica SP2 confocal microscope. Transient expression of GAPDH rescued YFP reconstitution, which is an indicative of 1a-2a interactions (Fig. 4.8). These results suggest that GAPDH plays an integral role in the replication of CMV by forming or stabilizing the replicase complex 1a-2a.
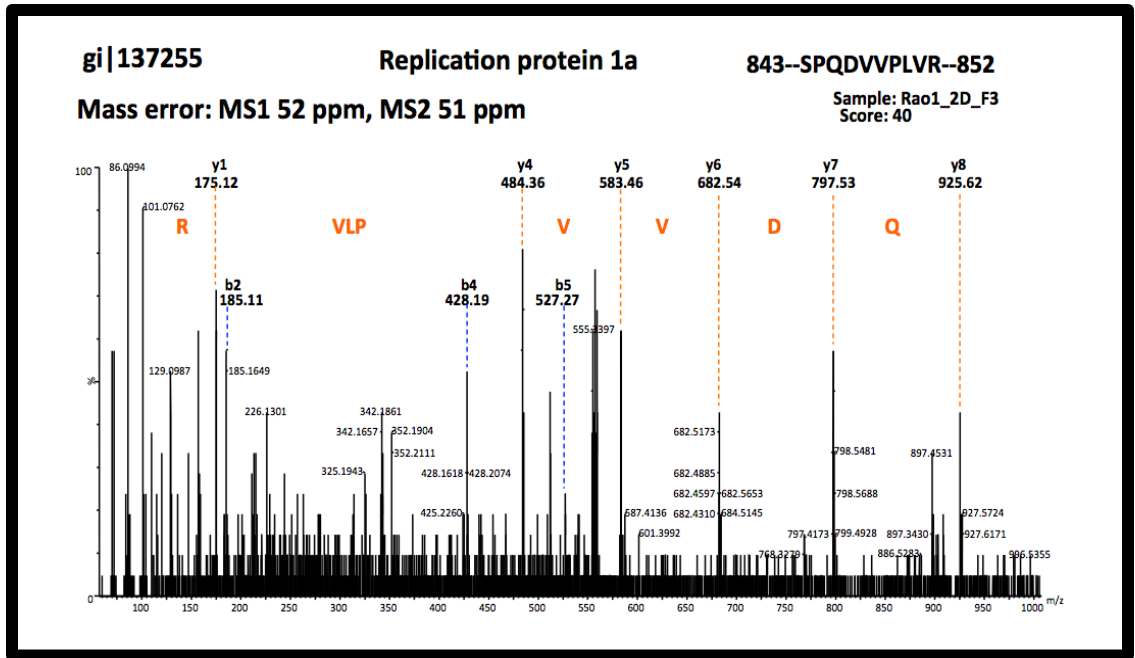
Figure 4.1 Co-IP of CMV proteins with BRP1-FLAG. Co-immunoprecipitation of CMV infected N. benthamiana leaves with BRP1-FLAG was performed using antiFLAG agarose beads and samples were subjected to LC MS/MS.

Q1a Self Interaction

BRP1 Self Interaction
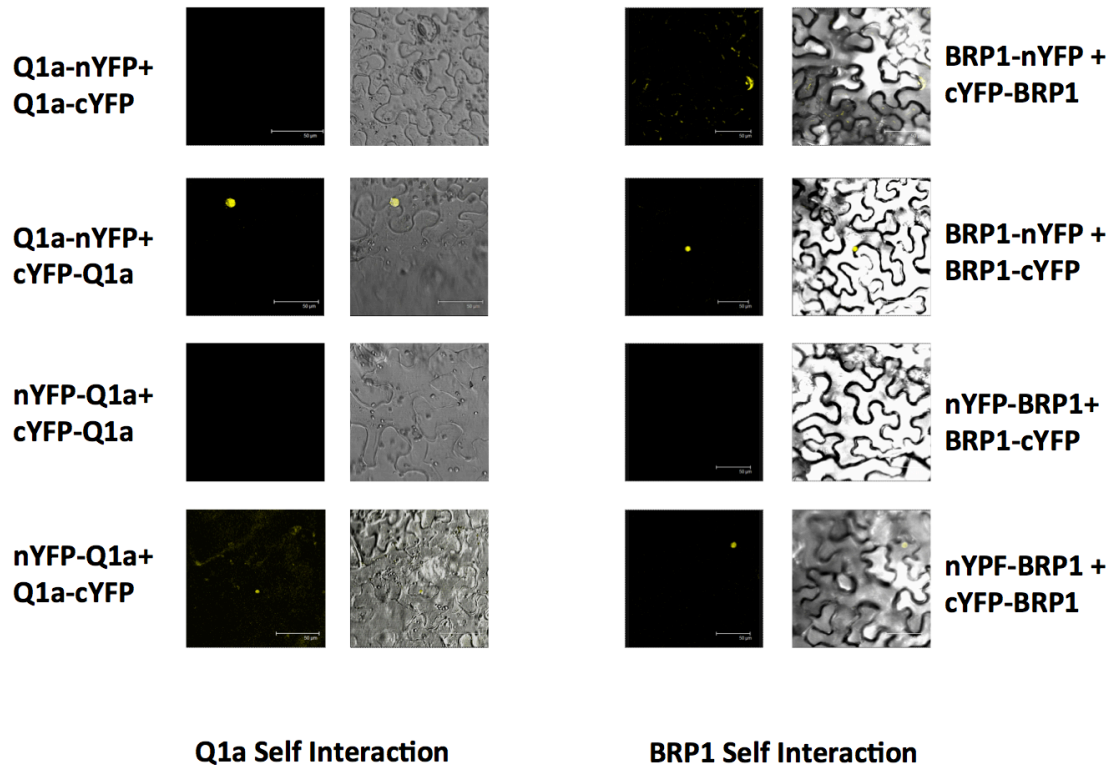
Figure 4.2 Self interaction of Q1a and BRP1 protein using BiFC. CMV 1a protein or BRP1 was cloned in pZP BiFC vectors and BiFC constructs were mixed in different combinations and infiltrated to *N. benthamiana* leaves. At 3dpi, epithelial cells were visualized under Leica SP2 confocal microscope for reconstitution of YFP signal.
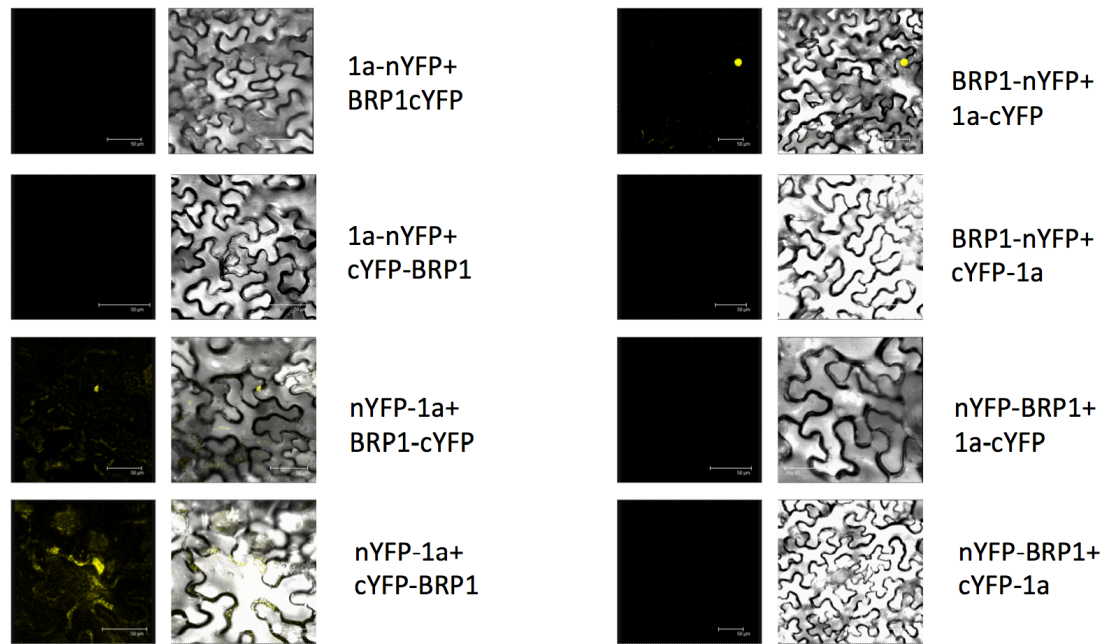
Figure 4.3 Heterologous interaction of Q1a and BRP1 protein using BiFC. CMV 1a protein or BRP1 was cloned in pZP BiFC vectors and BiFC constructs were mixed in different combinations and infiltrated to *N. benthamiana* leaves. At 3dpi, epithelial cells were visualized under Leica SP2 confocal microscope for reconstitution of YFP signal.

Sr. no.	Arabidopsis Single gene knockout lines	Gene number	Germplasm	Replication (%)
1	Wild type (Control)			100
2	HSP 90	AT5G56010.1	SALK_013240C	85
3	RNA Binding Glycine Rich Protein 1a	AT5G61030.1	SALK_007592	<1
4	Carbonyl Anhydrase	AT3G52720	SALK_082033C	85
5	Ferroxidin dependent glutamate synthase	AT5G04140	SALK_012180	76
6	Bifunctional enolase	AT2G36530	SALK_077784	89
7	Elongation Factor 1 Gamma Like Protein	AT1G57720.1	SALK_020191	<1
8	Elongation Factor 2	AT3G12915.1	SALK_015793	<1
9	Elongation Factor 4a	AT3G13920	SALK_038072	80
10	Citrate Synthase	AT3G58750	SALK_147925	77
11	Glyceraldehyde 3 Phosphate Dehydrogenase	AT1G13440.1	SALK_002909	<1
12	Global Transcription Factor Group	AT5G65630.1	SALK_006964	<1
13	Phosphoribulokinase	AT1G32060	CS411191	89
14	Ascorbate peroxidase	AT4G08390	SALK_083737	68
15	Vacuolar H+ ATPase B subunit	AT1G76030.1	SALK_015537	<1

Figure 4.4 Effect of host proteins on the replication of CMV in single gene knockout lines of A. thaliana (Col-0).
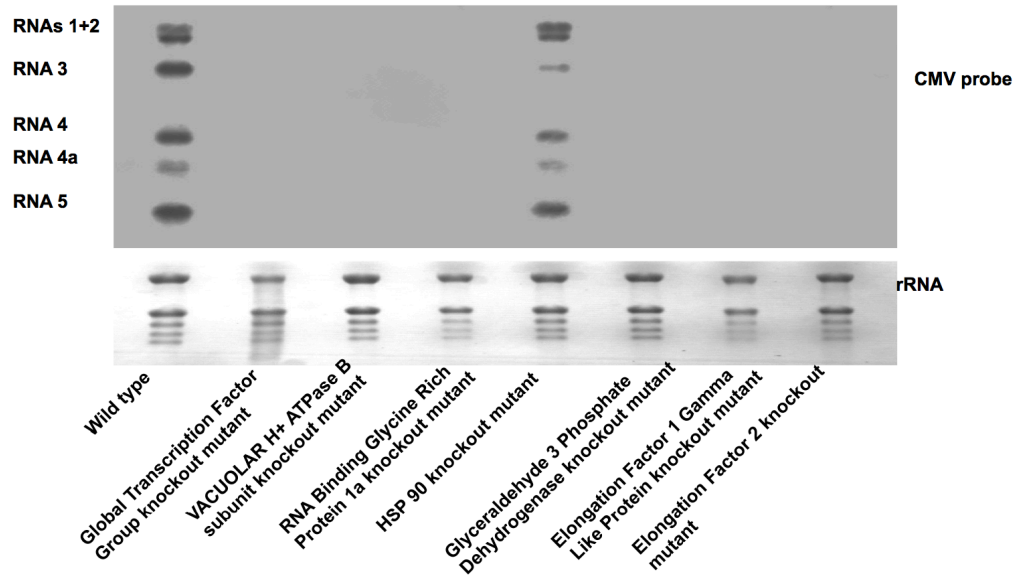
Figure 4.5 Northern blot analysis of replication level of CMV in shortlisted host proteins single gene knockout lines of *A. thaliana* (Col-0).
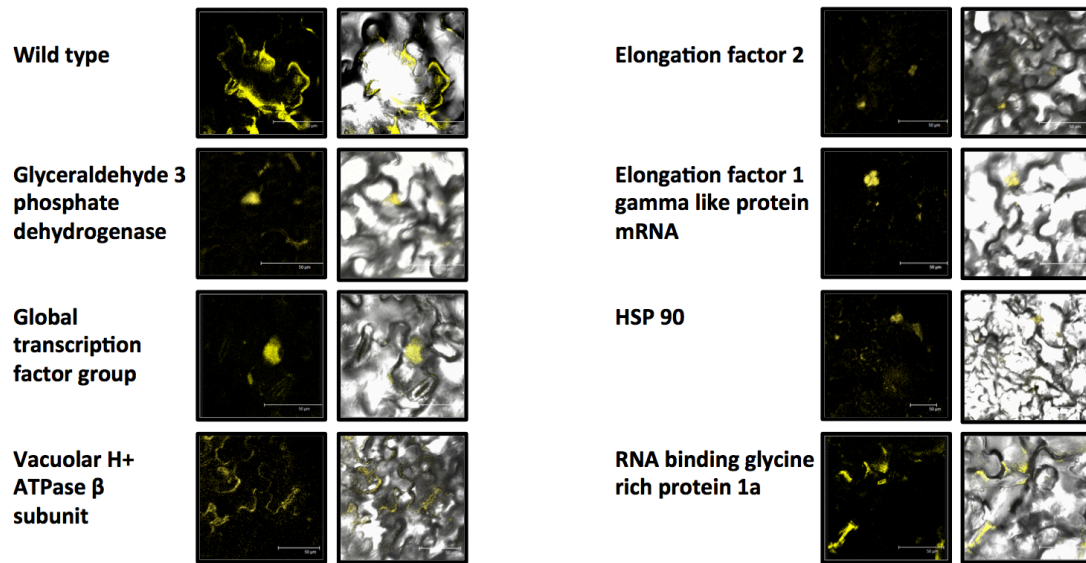
Figure 4.6 Heterologous interaction of Q1a and BRP1 protein in selected single gene knockout lines of *A. thaliana*. CMV 1a protein or BRP1 was cloned in pZP BiFC vectors and BiFC constructs were mixed in different combinations and infiltrated to single gene knockout lines of *A. thaliana*. At 3dpi, epithelial cells were visualized under Leica SP2 confocal microscope for reconstitution of YFP signal.
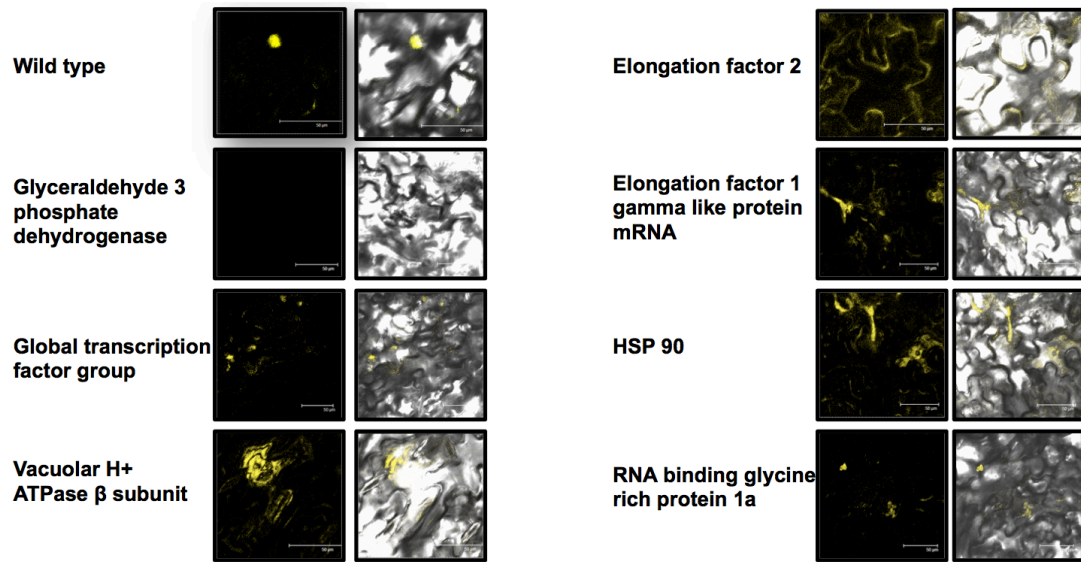
Figure 4.7 Heterologous interaction of Q1a and 2a protein in selected single gene knockout lines of *A. thaliana*. CMV 1a protein or 1a was cloned in pZP BiFC vectors and BiFC constructs were mixed in different combinations and infiltrated to single gene knockout lines of *A. thaliana*. At 3dpi, epithelial cells were visualized under Leica SP2 confocal microscope for reconstitution of YFP signal.
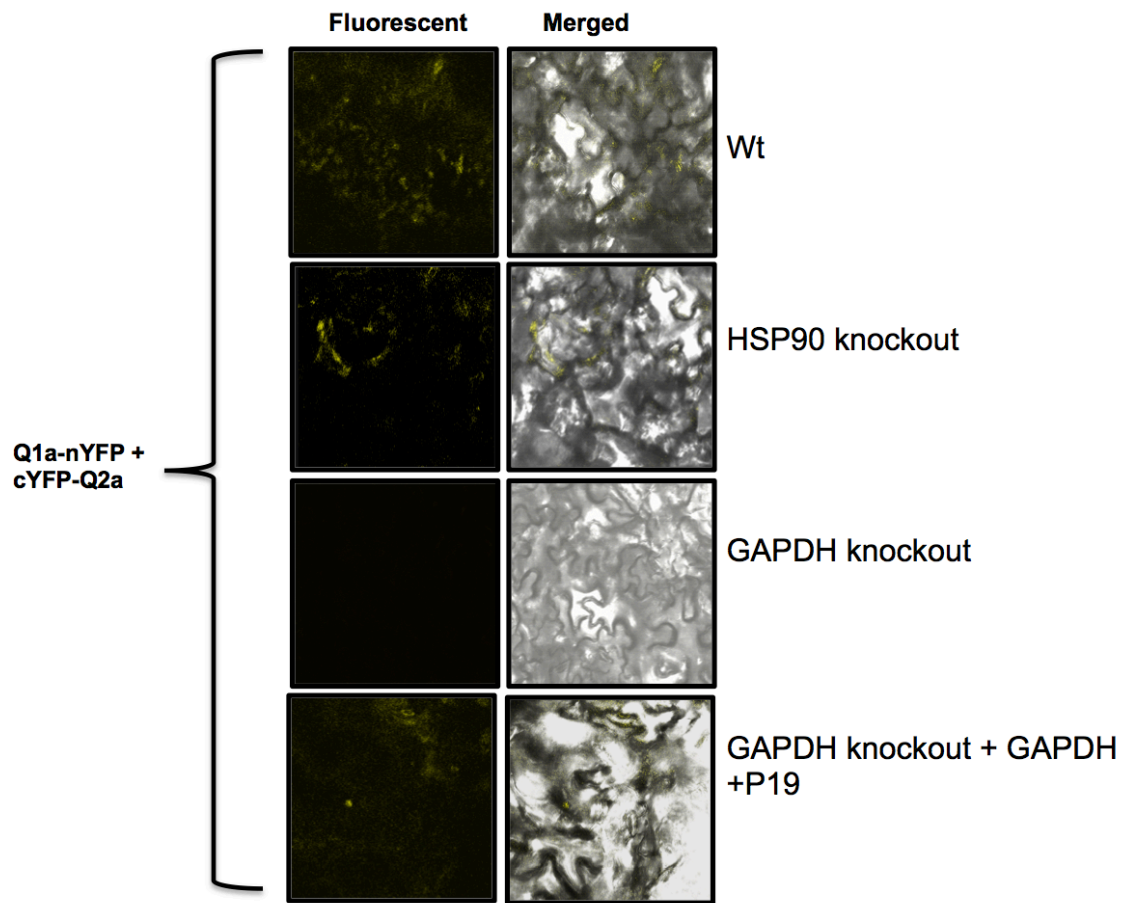
Figure 4.8 Transcomplementation assay for 1a -2a interaction in GAPDH knockout lines of *A. thaliana*. Representative 1a and 2a positive BiFC constructs were infiltrated to wt, ΔHSP90, ΔGAPDH or ΔGAPDH + pKn GAPDH+ P19 *A. thaliana* lines. At 3dpi, epithelial cells were visualized under Leica SP2 confocal microscope for reconstitution of YFP signal.
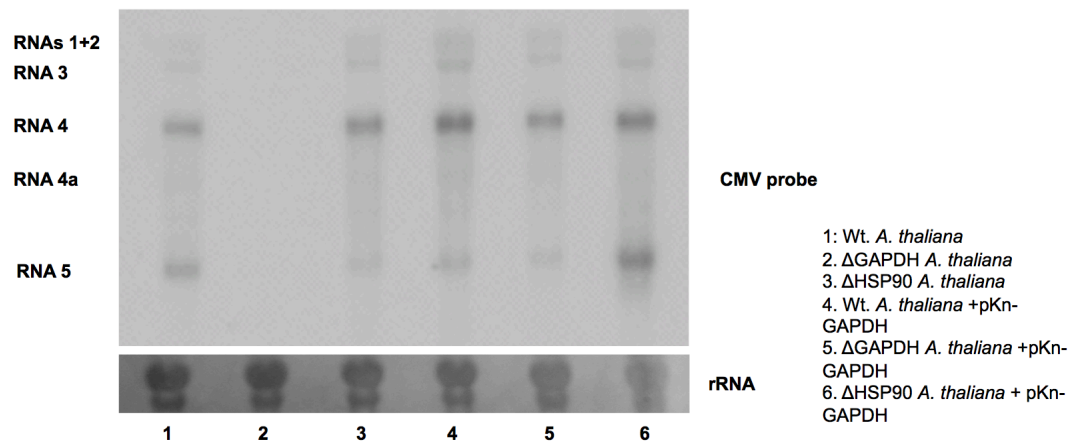
Figure 4.9 Transcomplementation of GAPDH rescued the replication of CMV. Infectious agroconstructs of QCMV were infiltrated to wt, ΔHSP90, ΔGAPDH or Wt+ pKn-GAPDH, ΔHSP90+ pKn-GAPDH or ΔGAPDH + pKn GAPDH *A. thaliana* lines. At 4dpi, total RNA was extracted, subjected to northern blot analysis and probed for CMV RNA.

REFERENCE

1.   **Annamalai, P., Rao, A.L., 2008.** RNA encapsidation assay. Methods in molecular biology 451, 251-264.

2.   **Bachan, S., Dinesh-Kumar, S.P., 2012.** Tobacco rattle virus (TRV)-based virus-induced gene silencing. Methods in molecular biology 894, 83-92.

3.   **Chaturvedi, S., Jung, B., Gupta, S., Anvari, B., Rao, A.L., 2012.** Simple and robust in vivo and in vitro approach for studying virus assembly. Journal of visualized experiments : JoVE.

4.   **Chaturvedi, S., Kalantidis, K., Rao, A.L., 2014.** A bromodomain-containing host protein mediates the nuclear importation of a satellite RNA of Cucumber mosaic virus. Journal of virology 88, 1890-1896.

5.   **Choi, S.H., Seo, J.K., Kwon, S.J., Rao, A.L., 2012.** Helper virus-independent transcription and multimerization of a satellite RNA associated with cucumber mosaic virus. Journal of virology 86, 4823-4832.

6.   **Di Carli, M., Villani, M.E., Bianco, L., Lombardi, R., Perrotta, G., Benvenuto, E., Donini, M., 2010.** Proteomic analysis of the plant-virus

126

interaction in cucumber mosaic virus (CMV) resistant transgenic tomato. Journal of proteome research 9, 5684-5697.

7.   **Dufresne, P.J., Thivierge, K., Cotton, S., Beauchemin, C., Ide, C., Ubalijoro, E., Laliberte, J.F., Fortin, M.G., 2008.** Heat shock 70 protein interaction with Turnip mosaic virus RNA-dependent RNA polymerase within virus-induced membrane vesicles. Virology 374, 217-227.

8.   **Gaj, T., Guo, J., Kato, Y., Sirk, S.J., Barbas, C.F., 3rd, 2012.** Targeted gene knockout by direct delivery of zinc-finger nuclease proteins. Nature methods 9, 805-807.

9.   **Huang, Y.P., Chen, J.S., Hsu, Y.H., Tsai, C.H., 2013.** A putative Rab-GTPase activation protein from Nicotiana benthamiana is important for Bamboo mosaic virus intercellular movement. Virology 447, 292-299.

10.   **Lamesch, P., Berardini, T.Z., Li, D., Swarbreck, D., Wilks, C., Sasidharan, R., Muller, R., Dreher, K., Alexander, D.L., Garcia-Hernandez, M., Karthikeyan, A.S., Lee, C.H., Nelson, W.D., Ploetz, L., Singh, S., Wensel, A., Huala, E., 2012.** The Arabidopsis Information Resource (TAIR): improved gene annotation and new tools. Nucleic acids research 40, D1202-1210.

11.   **Lee, M.W., Yang, Y., 2006.** Transient expression assay by agroinfiltration of leaves. Methods in molecular biology 323, 225-229.

12.   **Maor, R., Jones, A., Nuhse, T.S., Studholme, D.J., Peck, S.C., Shirasu, K., 2007.** Multidimensional protein identification technology (MudPIT) analysis of ubiquitinated proteins in plants. Molecular & cellular proteomics : MCP 6, 601-610.

13.   **Nagy, P.D., Pogany, J., 2012.** The dependence of viral RNA replication on co-opted host factors. Nature reviews. Microbiology 10, 137-149.

14.   **Oh, C.S., Pedley, K.F., Martin, G.B., 2010.** Tomato 14-3-3 protein 7 positively regulates immunity-associated programmed cell death by enhancing protein abundance and signaling ability of MAPKKK {alpha}. The Plant cell 22, 260-272.

15.   **Prasanth, K.R., Huang, Y.W., Liou, M.R., Wang, R.Y., Hu, C.C., Tsai, C.H., Meng, M., Lin, N.S., Hsu, Y.H., 2011.** Glyceraldehyde 3-phosphate dehydrogenase negatively regulates the replication of Bamboo mosaic virus and its associated satellite RNA. Journal of virology 85, 8829-8840.

16.   **Seo, J.K., Kwon, S.J., Rao, A.L., 2012.** A physical interaction between viral replicase and capsid protein is required for genome-packaging specificity in an RNA virus. Journal of virology 86, 6210-6221.

17.   **Serva, S., Nagy, P.D., 2006.** Proteomics analysis of the tombusvirus replicase: Hsp70 molecular chaperone is associated with the replicase and enhances viral RNA replication. Journal of virology 80, 2162-2169.

18.   **Zhang, F., Wen, Y., Guo, X., 2014.** CRISPR/Cas9 for genome editing: progress, implications and challenges. Human molecular genetics.

19.   **Zhang, Y., Zhang, F., Li, X., Baller, J.A., Qi, Y., Starker, C.G., Bogdanove, A.J., Voytas, D.F., 2013.** Transcription activator-like effector nucleases enable efficient plant genome engineering. Plant physiology 161, 20-27.

Chapter 5

Application of Riboproteomics for the identification of RNA-Protein interaction network in a Satellite RNA

ABSTRACT

Noncoding RNAs play an important role in host, where the secondary structure of RNA acts as a signal for many cellular processes. These RNAs interact with host proteins to form a ribonucleoprotein (RNP) complex, making study of this ribonucleoprotein complex imperative. Satellite RNA associated with Cucumber mosaic virus is a 336 nucleotides (nt) noncoding RNA, which is known to either ameliorate or intensify symptom expression by CMV. Hence, identificaltion of host proteins interacting with satRNA is of immense value. In this study, riboproteomics is employed to pull down host proteins interacting with satRNA. Cynogen bromide activated sepharose beads were tagged with satRNA in (+) or (-) polarity was used as RNA columns to pull down host proteins from healthy or CMV infected *N. benthamiana* leaves. Results from this study suggested difference in the proteome of N. benthamiana interacting with satRNA in (+) or (-) polarity, in the presence or absence of CMV, suggesting that the pulled down host proteins might play an important role in the life cycle of satRNA.

INTRODUCTION

Small noncoding RNAs (SnRNAs) play an important role in eukaryotic cells. These RNAs could be of host or non-host origin. RNAs might lead to various post- transcriptional mechanisms and regulate gene expression when are of host origin (Boyd, 2008), or successfully infect the eukaryotic cell, when it is of non-host origin (Kaper et al., 1981). Several small noncoding RNAs play an important role in the pathogenesis of plants, eg., Viroids (Ding, 2010), and satRNAs of viruses (Kaper et al., 1990). Satellite RNA (satRNA), plays an important role in the pathogenesis of CMV (Liao et al., 2007). It is a 336 nucleotides (nt) long noncoding RNA dependent on CMV for replication as well as encapsidation (Palukaitis and Garcia-Arenal, 2003b). satRNA has a 5'-terminal cap and a 3'-terminal-CCC which cannot be aminoacylated (Roossinck et al., 1992b). CMV satRNA is highly structured molecule, with a high percentage of bases (around 50%) base-paired, making satRNA highly stable and infectious (Roossinck et al., 1992b). CMV is one of the most important plant viruses, infecting more than 1200 species of plants, making it imperative to understand the biology of the virus and satRNA associated with it.

Replication of viruses or their subviral pathogens is closely associated with host proteins, which might either facilitate or curb disease spread by the virus. Different host proteins have been observed to play an important role in the

replication of several viruses, for example, in case of tombusvirus, HSP90 plays an important role in the assembly of functional replicase complex (Serva and Nagy, 2006). Change in global protein distribution in plants infected with the virus can be studied using 2D-gel electrophoresis followed by mass spectrometric analysis (Caplan et al., 2009; Casado-Vela et al., 2006; Kushner et al., 2003; Panavas et al., 2005).

In addition to studying global change in the plant proteome, plant RNA viruses or noncoding RNAs associated with them assemble ribo-nucleoproteins (RNPs) or protein complexes to mediate successful infection in plant. Precipitating protein complexes with viral proteins can be candidates, which might facilitate replication of the virus (Panavas and Nagy, 2003; Pantaleo et al., 2003; Pogany et al., 2008; Wang and Nagy, 2008; Wang et al., 2009).

In case of satRNA, where no protein is synthesized, studying host proteins involved in the life cycle of it can be a challenge. Study of RNA-protein interactome regulating the replication of satRNA can be studied using ribo-proteomics approach. Applying riboproteomics, number of host proteins interacting with viral RNAs has been previously identified for Norovirus life cycle (Vashist et al., 2012). In this report, we applied ribo-proteomics to pull down number of host proteins interacting with positive or negative sense satRNA in the presence or absence of CMV. Results demonstrate a drastic difference in the

enrichment of host proteins in each case, which might help one delineate the factors involved in the replication of satRNA, as well as might provide information regarding how the proteome of satRNA infected leaf changes when challenged with CMV.

MATERIALS AND METHODS

CMV strain, Agroinfiltration and preparation of cell extract

The construction of agroconstructs of genomic RNAs of the Q strain of CMV is previously described (Choi et al., 2012a). Wild type *Nicotiana benthamiana* leaves were infiltrated with GV3101 strain of CMV agrocultures. At 4 days post infiltration (dpi), healthy leaves or CMV infected leaves were used to prepare leaf extract.

Preparation of satRNA affinity column

satRNA (+) or (-) transcripts were synthesized by *in-vitro* transcription method using MEGAscript T7 Transcription kit (Invitrogen). Approximately 100 mg of each satRNA transcripts was covalently coupled to cynogen bromide (CNBR)-activated sepharose beads (Kaminski et al., 1995). 125 ml of packed preswollen CNBR activated sepharose beads (Sigma) were equilibrated with 200 mM MES (pH 6.0), and 100 mg of (+) or (-) satRNA transcripts were added to the solution, and further incubated overnight at 4°C with gentle mixing. Further, beads were washed three times with100 mM Tris (pH 8.0), and incubated for 1 hr at 4°C in 100 mM Tris (pH 8.0). satRNA column was washed three times in RNA binding buffer [50 mM HEPES (pH 7.6), 50 mM Kcl, 5 mM MgO-acetate, 125 mM

NaCl, 2 mM DTT, 10% glycerol] (Fig. 5.1) (Kaminski et al., 1995; Vashist et al., 2012).

Enrichment of RNA binding proteins by using RNA affinity column and MudPIT analysis

RNA affinity column for satRNA (+) or (-) was incubated with 10 mg of leaf extract from healthy *N. benthamiana* leaves or CMV infected *N. benthamiana* leaves along with 100 mg yeast RNA, 1 mM ATP, 1mM GTP and 100 U Ribonuclease inhibitor (Sigma, U.S.A) at $4^{o}C$ for 3 hours with gentle mixing. RNA affinity columns were washing three times with binding buffer at $4^{o}C$, and later proteins bound to RNA affinity columns were sent for MudPIT analysis. For protein identification, MASCOT MS/MS Ions Search tool (Koenig et al., 2008) was used to manually search against National Center of Biotechnology Information (NCBI) non redundant database (Fig. 5.1).

Classification of host proteins based on functionality and subcellular localization

Analysis of biological functionality of identified proteins was performed by Panther Classification (http://www.pantherdb.org) database (Mi et al., 2013). Gene ontology terms were identified for each protein, and statistical significance

was obtained by p values, where p values < 0.05 were considered significant. Functionalities, which were considered as significant, were based on several biological functions important for the replication of a positive sense RNA virus, like Nucleic acid binding, catalytic activity and others (Table 5.2 and Fig. 5.3). For subcellular localization, WoLF PSORT (http://www.wolfpsort.seq.cbrc.jp) program (Horton et al., 2007) was used (Fig. 5.4).

RESULTS AND DISCUSSION

Distribution of host proteins interacting with (+) or (-) satRNA by itself or in the presence of CMV

In the replication of positive sense RNA virus, an important intermediate step is synthesis of a negative sense RNA, which in turn synthesizes positive sense RNAs (Palukaitis and Garcia-Arenal, 2003b). Plethora of host proteins play cardinal role in the life cycle of a virus (Nagy and Pogany, 2012a). In case of a satRNA, which pays an important role in the replication of CMV, not much of literature is available for proteins interacting with (+) or (-) satRNA. To delineate number of host proteins interacting with (+) or (-) satRNA, satRNA affinity columns were prepared by covalently linking satRNA (+) or (-) transcripts to cynogen bromide activated sepharose beads. Further, leaf extract from healthy *N. benthamiana* was mixed with RNA affinity column for (+) or (-) satRNAs, followed by MuDPIT analysis to identify host proteins interacting with (+) or (-) satRNA. Using Ribo-proteomics approach (Fig. 5.1 A), number of host proteins interacting with satRNA (+)/(-) were delineated (Fig. 5.2 A, Table 1). The distribution of host proteins interacting with (+) satRNA was 29, which decreased to 15 in case of (-) satRNA, where 10 proteins were commonly shared between two.

Replication of CMV decreases in the presence of satRNA (Palukaitis and Garcia-Arenal, 2003b), suggesting there might be a competition between satRNA and CMV for host proteins. Hence, list of host proteins interacting with satRNA in isolation would not provide a complete picture of the biology of satRNA, as it is dependent on CMV for replication and encapsidation. To pull down host proteins interacting with (+) or (-) satRNA in the presence of CMV, *N. benthamiana* leaves were infiltrated with 0.1 OD of QCMV agrocultures (Chaturvedi et al., 2012b; Choi et al., 2012a). At 4 days post infiltration (dpi), leaves were ground in liquid nitrogen and leaf extract was prepared, followed by precipitation of host proteins using (+) or (-) satRNA affinity columns (Fig. 5.1B). The distribution of host proteins interacting with (+) or (-) satRNA affinity columns changed in the presence of CMV (Table 5.1, Fig. 5.2).

Above results suggest that the distribution of host proteins interacting with satRNA changed in (+) or (-) orientation, by itself or in the presence of CMV. The ratio of satRNA (+):(-) is 2-3:1 (Garcia-Arenal and Palukaitis, 1999a; Piazzolla et al., 1982), implying that the mechanism of synthesis of both the RNAs is different. Hence, exclusive host proteins pulled down in case of satRNA (+) or (-) might play an important role in the synthesis of respective RNAs (Fig. 5.2A). In presence of CMV, number of host proteins interacting with satRNA decreased to 18 for (+) satRNA and 10 for (-) satRNA, suggesting a shift in the proteome of

(+)/(-) satRNA in the presence of CMV. This might shed light on how there is a change in symptom expression of CMV in the presence of satRNA.

Functional classification and cellular distribution of proteome for (+) or (-) satRNA by itself or in the presence of CMV

To understand the biological relevance of host proteins pulled down by affinity columns of satRNA, PANTHER classification system was used to classify them according too the gene ontology and protein categories in which they are present. Host proteins were classified into ten biological processes groups (Fig. 5.3, Table 5.2). In the case of (+) satRNA, ~ 58% of enriched proteins had catalytic activity with only 3.4% of enriched proteins were involved in protein transport or chaperone activity, which in case of (-) satRNA was ~ 47% for catalytic activity, and no protein was pulled down with protein transport activity. In the presence of CMV, number of enriched host proteins with specific functionality changed. In case of (+) satRNA in the presence of CMV, none of the enriched host protein had transmembrane transport activity, transporter activity, nucleobase, nuceoside, nucleotide, and nucleic acid metabolic process, protein transport or chaperone activity, with ~50% of proteins had binding, or nucleic acid binding function (Table 5.2, Fig. 5.3). In case of (-) satRNA in the presence of CMV, enriched host proteins involved in binding, translation factor activity, or catalytic activity were ~50%, with none of them having a function in

transmembrane transport activity, transporter, protein transport, or chaperone activity (Table 5.2, Fig. 5.3).

Subcellular localization of proteins playing an important role in the replication of a virus plays an important role. For classifying proteins in terms of their localization sites, WoLF PSORT program was used. WoLF PSORT classifies proteins into more than 10 localization sites, along with dual localizations for proteins having localization signal for more than one site in the cell (Horton et al., 2007). Classification of proteins based on their localization suggests that more enriched proteins have a propensity to localize into cytoplasm for (+) satRNA by itself, or in the presence of CMV (Fig. 5.4) compared to (-) satRNA, though the localization of proteins interacting with (+) satRNA in the presence of CMV decreased. satRNA life cycle has a nuclear phase (Choi et al., 2012a), hence it is important to understand how many satRNA binding proteins have a nuclear localization signal. It was observed that out of total number of enriched proteins, 24% of proteins interacting with (+) satRNA had a nuclear localization signal, which in case of (-) satRNA was 53%. The percentage of host proteins interacting with satRNA in the presence of CMV remained unaltered, which for (+) satRNA was 38% and (-) satRNA 40%.
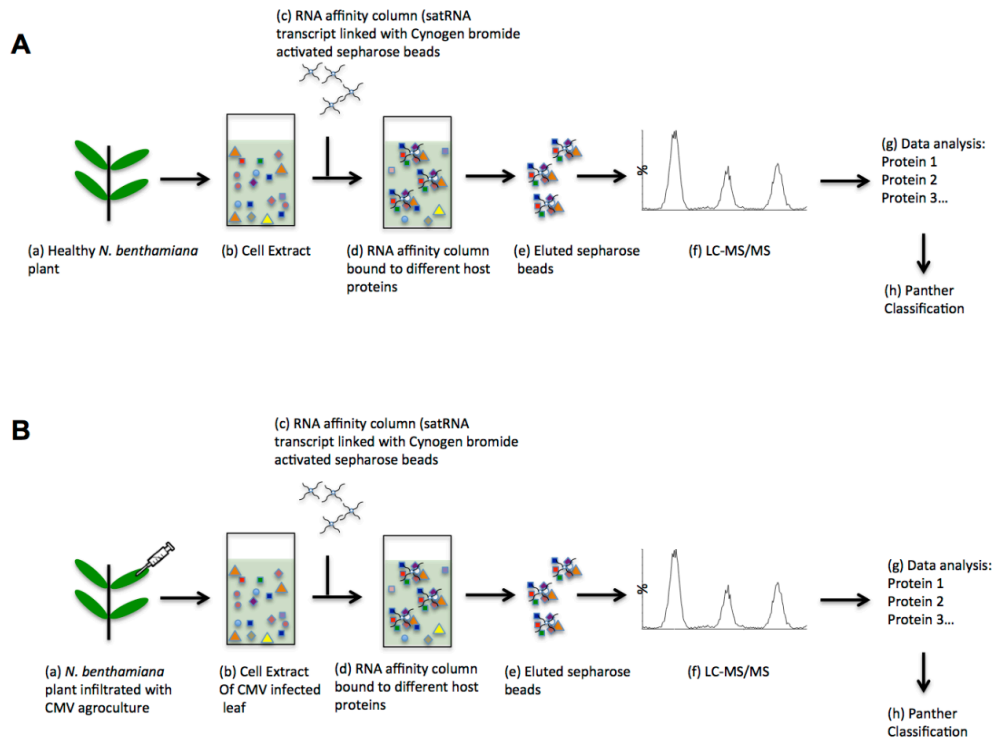
Figure 5.1 Schematic representation of riboproteomics approach. *N benthamiana* leaves were infiltrated with CMV or healthy leaves were used as control. At 4dpi, leaves extract was prepared for healthy (A) or CMV infected leaves (B), and coimmunoprecipitated with RNA affinity columns (satRNA (+) or satRNA (-) transcripts linked to cynogen bromide activated sepharose beads). Precipitated beads were washed three times with elution buffer and subjected to MudPIT analysis.

A. Venn Diagram of Host proteins interacting with (+)/(-) satRNA transcripts

19   10   5
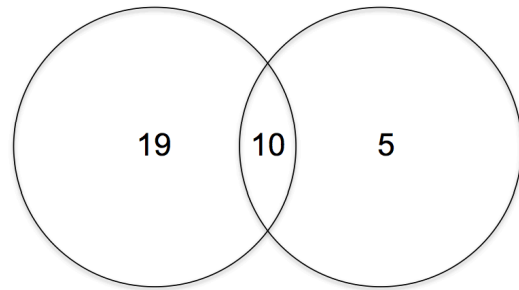
Host proteins interacting to (+) satRNA in the absence of CMV (29 proteins)

Host proteins interacting to (-) satRNA in the absence of CMV (15 proteins)

B. Venn Diagram of Host proteins interacting with (+)/(-) satRNA transcripts in the presence of Helper virus

12   6   4
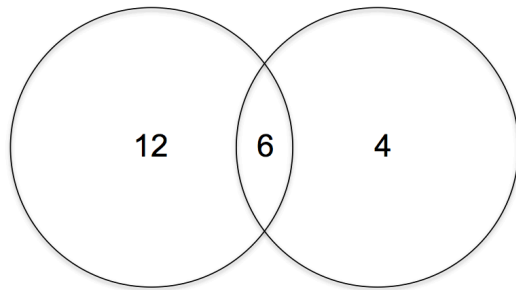
Host proteins interacting to (+) satRNA in the presence of CMV (18 proteins)

Host proteins interacting to (-) satRNA in the presence of CMV (10 proteins)

Figure 5.2 Distribution of host proteins interacting with satRNA affinity columns. (A) Venn Diagram of Host proteins interacting with (+)/(-) satRNA transcripts, where 29 host proteins interacted with (+) satRNA and 15 host proteins with (-) satRNA in the absence of CMV. (B) Venn Diagram of Host proteins interacting with (+)/(-) satRNA transcripts, where 18 host proteins interacted with (+) satRNA and 10 host proteins with (-) satRNA in the presence of CMV.
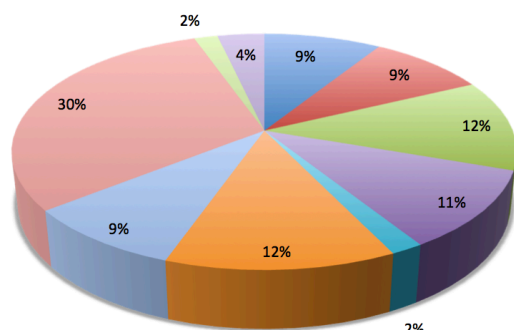
(i) (+)satRNA+ Healthy plant
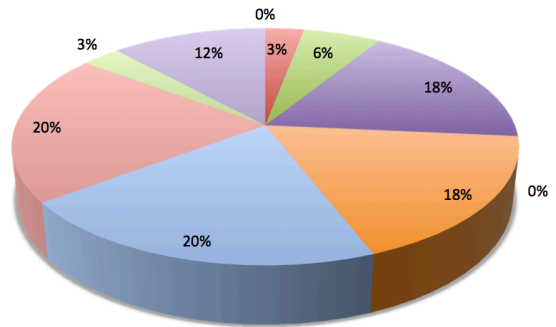
(ii) (-)satRNA+ Healthy plant
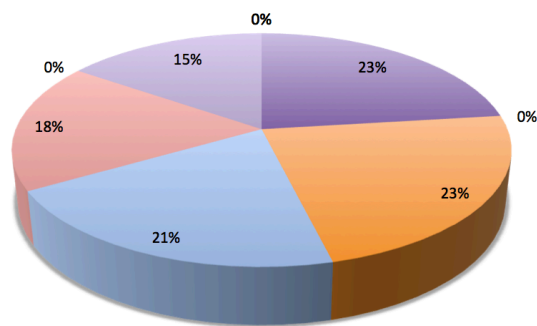
(iii) (+)satRNA+ CMV infected plant
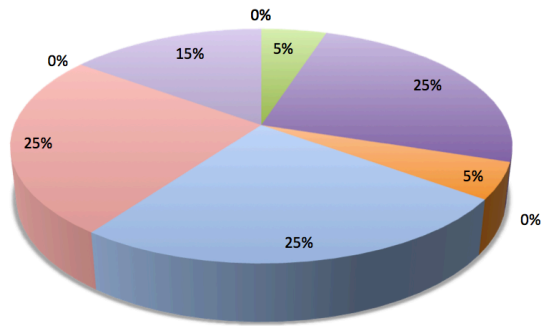
(iv) (-)satRNA+ CMV infected plant

Figure 5.3 Pie chart of classification of host proteins on the basis of their functions. See Table 2 for details.
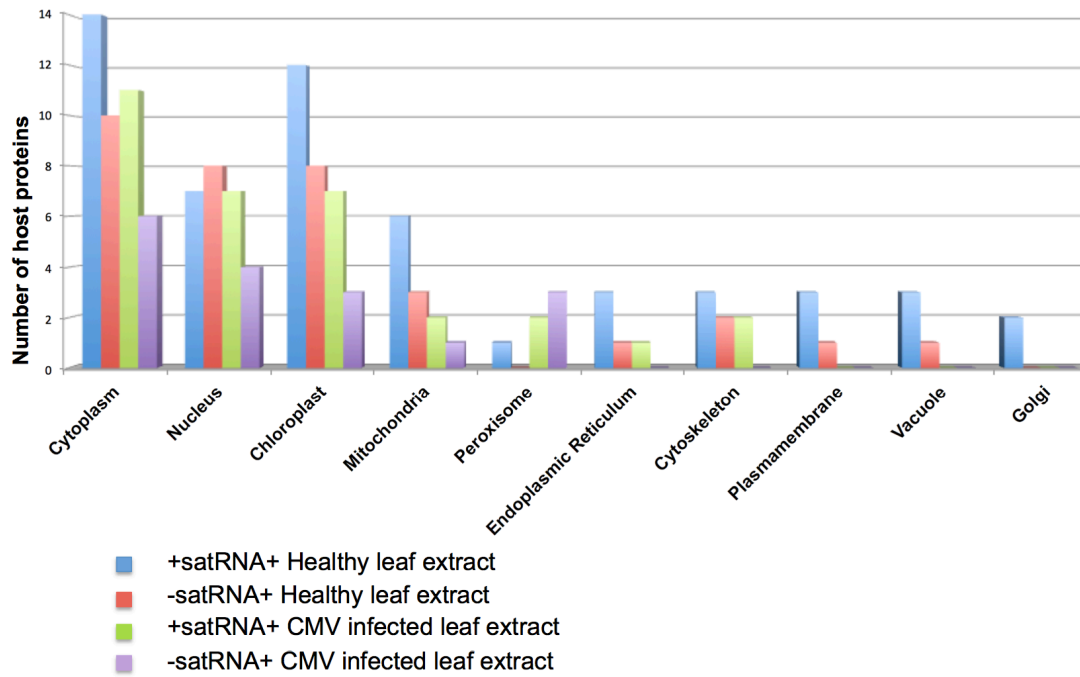
Figure 5.4 Subcellular distribution pattern of host proteins interacting with satRNA(+) or (-) affinity columns in the presence or absence of CMV. WoLF-PSORT program was used to find subcellular localization of host proteins interacting with satellite RNA.

A

Sat-RNA (+)	Sat-RNA (-)
ribulose-1,5-bisphosphate carboxylase	ribulose-1,5-bisphosphate carboxylase
glycolate oxidase	glycolate oxidase
serine hydroxymethyltransferase	elongation factor-1 alpha
elongation factor-1 alpha	putative ferredoxin-dependent glutamate synthase 1
putative ferredoxin-dependent glutamate synthase 1	S-adenosyl-L-homocysteine hydrolase
actin	carbonic anhydrase
Phosphoenolpyruvate carboxylase	40S ribosomal protein S6
ATP synthase beta subunit	cyc07-like
chloroplast photosynthetic oxygen-evolving protein 23 kDa subunit	s/s2
s/s2	plastidic aldolase NPALDP1
Glyceraldehyde-3-phosphate dehydrogenase A	40S ribosomal protein S6
40S ribosomal protein S6	Chaperonin
S-adenosylmethionine synthetase	hypothetical protein SORBIDRAFT
plastidic aldolase NPALDP1	
chloroplast elongation factor TuB (EF-TuB)	
glutamine synthetase	
hypothetical protein SORBIDRAFT	
High affinity sulfate transporter 1	
Eukaryotic initiation factor 4A-2	
alpha subunit of ATPase	
Phosphoribulokinase	
Chaperonin	
Cytochrome c	
Enolase	
chloroplast oxygen-evolving protein 16 kDa subunit	
kinase	
Phosphoribosylaminoimidazolecarboxamide formyltransferase	

B

Sat-RNA(+) + CMV	Sat-RNA(-) + CMV
ribulose-1,5-bisphosphate carboxylase	ribulose-1,5-bisphosphate carboxylase
elongation factor-1 alpha	40S ribosomal protein S6
40S ribosomal protein S6	elongation factor-1 alpha
Peroxisomal (S)-2-hydroxy-acid oxidase	Peroxisomal (S)-2-hydroxy-acid oxidase
60S ribosomal protein L13a-2, putative	cyc07-like
RNA binding / nucleic acid binding / structural constituent of ribosome	glutamine synthetase
chloroplast elongation factor TuB (EF-TuB)	putative Citrate synthase, glyoxysomal precursor (GCS)
cyc07-like	Eukaryotic initiation factor 4A-2
putative L24 ribosomal protein	
prepro-beta-1,3-glucanase precursor	
glutamine synthetase	
Beta-1,2-xylosyltransferase	
Putative retroelement	
UDP-glucosyltransferase	

Table 5.1 List of host proteins interacting with satRNA (+) or (-) in healthy *N. benthamiana* leaf extract (A), and CMV infected *N. benthamiana* leaf extract (B).

Sr No.	Function	Color annotation	(+)satRNA	(-) satRNA	(+)satRNA + CMV	(-) satRNA + CMV
1	TRANSMEMBRANE TRANSPORT ACTIVITY		5, 0	0	0	0
2	TRANSPORTER		5,0	1,0	0	0
3	NUCLEOBASE, NUCLEOSIDE, NUCLEPTODE AND NUCLEIC ACID METABOLIC PROCESS		7, 3.07E-182	2,0	0	1, 6.1E-177
4	BINDING		6, 4.16E-183	6, 3.5E-63	9, 1.33E-101	5, 1.18E124
5	PROTEIN TRANSPORT		1,0	0	0	0
6	NUCLEIC ACID BINDING		7,1.71E-105	6, 3.5E-62	9, 1.33E-101	1, 1.18E-124
7	TRANSLATION FACTOR ACTIVITY		5, 2.4E-105	7, 3E-63	8, 1.5E-101	5, 1.18E-124
8	CATALYTIC ACTIVITY		17, 4.41E-155	7, 1.12E-70	7, 1.18E-137	5, 1.22E-177
9	CHAPERONE		1, 1.1e-295	1,0	0	0
10	RIBOSOMAL PROTEIN		2, 6e-105	4, 5.25e-63	6, 2.0e-101	3, 1.96e-124

Table 5.2 Classification of host proteins pulled down by satRNA (+) or (-) in healthy or in CMV infected *N benthamiana* plants on the basis of their functionality using Panther Classification system.

REFERENCE

1.   **Boyd, S.D., 2008.** Everything you wanted to know about small RNA but were afraid to ask. Laboratory investigation; a journal of technical methods and pathology 88, 569-578.

2.   **Caplan, J.L., Zhu, X., Mamillapalli, P., Marathe, R., Anandalakshmi, R., Dinesh-Kumar, S.P., 2009.** Induced ER chaperones regulate a receptor-like kinase to mediate antiviral innate immune response in plants. Cell host & microbe 6, 457-469.

3.   **Casado-Vela, J., Selles, S., Martinez, R.B., 2006.** Proteomic analysis of tobacco mosaic virus-infected tomato (Lycopersicon esculentum M.) fruits and detection of viral coat protein. Proteomics 6 Suppl 1, S196-206.

4.   **Chaturvedi, S., Jung, B., Gupta, S., Anvari, B., Rao, A.L., 2012.** Simple and robust in vivo and in vitro approach for studying virus assembly. Journal of visualized experiments : JoVE.

5.   **Choi, S.H., Seo, J.K., Kwon, S.J., Rao, A.L., 2012.** Helper virus-independent transcription and multimerization of a satellite RNA associated with cucumber mosaic virus. Journal of virology 86, 4823-4832.

6.   **Ding, B., 2010.** Viroids: self-replicating, mobile, and fast-evolving noncoding regulatory RNAs. Wiley interdisciplinary reviews. RNA 1, 362-375.

7.   **Garcia-Arenal, F., Palukaitis, P., 1999.** Structure and functional relationships of satellite RNAs of cucumber mosaic virus. Current topics in microbiology and immunology 239, 37-63.

8.   **Horton, P., Park, K.J., Obayashi, T., Fujita, N., Harada, H., Adams-Collier, C.J., Nakai, K., 2007.** WoLF PSORT: protein localization predictor. Nucleic acids research 35, W585-587.

9.   **Kaminski, A., Hunt, S.L., Patton, J.G., Jackson, R.J., 1995.** Direct evidence that polypyrimidine tract binding protein (PTB) is essential for internal initiation of translation of encephalomyocarditis virus RNA. Rna 1, 924-938.

10.   **Kaper, J.M., Tousignant, M.E., Geletka, L.M., 1990.** Cucumber-mosaic-virus-associated RNA-5. XII. Symptom-modulating effect is codetermined by the helper virus satellite replication support function. Research in virology 141, 487-503.

11.   **Kaper, J.M., Tousignant, M.E., Thompson, S.M., 1981.** Cucumber mosaic virus-associated RNA 5, VIII. Identification and partial characterization of a CARNA 5 incapable of inducing tomato necrosis. Virology 114, 526-533.

12.   **Koenig, T., Menze, B.H., Kirchner, M., Monigatti, F., Parker, K.C., Patterson, T., Steen, J.J., Hamprecht, F.A., Steen, H., 2008.** Robust prediction of the MASCOT score for an improved quality assessment in mass spectrometric proteomics. Journal of proteome research 7, 3708-3717.

13.   **Kushner, D.B., Lindenbach, B.D., Grdzelishvili, V.Z., Noueiry, A.O., Paul, S.M., Ahlquist, P., 2003.** Systematic, genome-wide identification of host genes affecting replication of a positive-strand RNA virus. Proceedings of the National Academy of Sciences of the United States of America 100, 15764-15769.

14.   **Liao, Q., Zhu, L., Du, Z., Zeng, R., Peng, J., Chen, J., 2007.** Satellite RNA-mediated reduction of cucumber mosaic virus genomic RNAs accumulation in Nicotiana tabacum. Acta biochimica et biophysica Sinica 39, 217-223.

15.   **Mi, H., Muruganujan, A., Casagrande, J.T., Thomas, P.D., 2013.** Large-scale gene function analysis with the PANTHER classification system. Nature protocols 8, 1551-1566.

16.   **Nagy, P.D., Pogany, J., 2012.** The dependence of viral RNA replication on co-opted host factors. Nature reviews. Microbiology 10, 137-149.

17. **Palukaitis, P., Garcia-Arenal, F., 2003.** Cucumoviruses. Advances in virus research 62, 241-323.

18. **Panavas, T., Nagy, P.D., 2003.** Yeast as a model host to study replication and recombination of defective interfering RNA of Tomato bushy stunt virus. Virology 314, 315-325.

19. **Panavas, T., Serviene, E., Brasher, J., Nagy, P.D., 2005**. Yeast genome-wide screen reveals dissimilar sets of host genes affecting replication of RNA viruses. Proceedings of the National Academy of Sciences of the United States of America 102, 7326-7331.

20. **Pantaleo, V., Rubino, L., Russo, M., 2003.** Replication of Carnation Italian ringspot virus defective interfering RNA in Saccharomyces cerevisiae. Journal of virology 77, 2116-2123.

21. **Piazzolla, P., Tousignant, M.E., Kaper, J.M., 1982.** Cucumber mosaic virus-associated RNA 5. IX. The overtaking of viral RNA synthesis by CARNA 5 and dsCARNA 5 in tobacco. Virology 122, 147-157.

22. **Pogany, J., Stork, J., Li, Z., Nagy, P.D., 2008.** In vitro assembly of the Tomato bushy stunt virus replicase requires the host Heat shock protein 70.

Proceedings of the National Academy of Sciences of the United States of America 105, 19956-19961.

23.   **Roossinck, M.J., Sleat, D., Palukaitis, P., 1992.** Satellite RNAs of plant viruses: structures and biological effects. Microbiological reviews 56, 265-279.

24.   **Serva, S., Nagy, P.D., 2006.** Proteomics analysis of the tombusvirus replicase: Hsp70 molecular chaperone is associated with the replicase and enhances viral RNA replication. Journal of virology 80, 2162-2169.

25.   **Vashist, S., Urena, L., Chaudhry, Y., Goodfellow, I., 2012**. Identification of RNA-protein interaction networks involved in the norovirus life cycle. Journal of virology 86, 11977-11990.

26.   **Wang, R.Y., Nagy, P.D., 2008.** Tomato bushy stunt virus co-opts the RNA-binding function of a host metabolic enzyme for viral genomic RNA synthesis. Cell host & microbe 3, 178-187.

27.   **Wang, R.Y., Stork, J., Nagy, P.D., 2009.** A key role for heat shock protein 70 in the localization and insertion of tombusvirus replication proteins to intracellular membranes. Journal of virology 83, 3276-3287.

Chapter 6

Live Cell Imaging of Interactions Between Replicase and Capsid Protein of Brome Mosaic Virus using Bimolecular Fluorescence Complementation: Implications for Replication and Genome Packaging

ABSTRACT

In *Brome mosaic virus,* it was hypothesized that a physical interaction between viral replicase and capsid protein (CP) is obligatory to confer genome packaging specificity. Here we tested this hypothesis by employing Bimolecular Fluorescent Complementation (BiFC) as a tool for evaluating protein-protein interactions in living cells. The efficacy of BiFC was validated by a known interaction between replicase protein 1a (p1a) and protein 2a (p2a) at the endoplasmic reticulum (ER) site of viral replication. Additionally, co-expression *in planta* of a bona fide pair of interacting protein partners of p1a and p2a had resulted in the assembly of a functional replicase. Subsequent BiFC assays in conjunction with mCherry labeled ER as a fluorescent cellular marker revealed that CP physically interacts with p2a, but not p1a, and this CP:p2a interaction occurs at the cytoplasmic phase of the ER.. The significance of the CP:p2a interaction in BMV replication and genome packaging is discussed.

INTRODUCTION

The biological function of a given protein is determined by the formation of stable or transient protein complexes and networks. Consequently, disruption of protein complex formation or network leads to abnormal development of the host or may lead to disease induction. Thus, evaluation and identification of protein-protein interactions (PPI) often provides novel insight into their regulatory function in several signaling processes. Techniques such as Yeast Two-Hybrid (YTH), Fluorescence Resonance Energy Transfer (FRET) and Co-Immuno Precipitation (Co-IP) are frequently used for evaluating PPI (Khan et al., 2011). YTH analyses have provided invaluable information about interacting proteins in stable or transient complex formation, but an inherent disadvantage of YTH is that a large number of interactions are predicted to be false positives. Although FRET is ideal for visualizing PPI in real time, determination of protein interactions by FRET requires ratio-metric image analysis to subtract background signals. Despite their usefulness, YTH and FRET do not monitor the dynamics of interaction and localization *in vivo* in real time. This information is necessary in order to understand protein function at the cellular, tissue and organism levels. In recent years, the Bimolecular Fluorescent Complementation assay (Citovsky et al., 2006; Kerppola, 2008) has gained momentum in evaluating PPI *in vivo*. When combined with fluorescently labeled cellular marker proteins, BiFC offers the advantage of precisely determining the subcellular localization of PPI.

Availability of vectors amenable for engineering fusion proteins followed by their expression *in planta* (Citovsky et al., 2006) is particularly attractive for testing PPI in plant viruses.

Brome mosaic virus (BMV) is the type species of the genus *Bromovirus* (King et al., 2011), and belongs to the *Bromoviridae* family of plant viruses. The genome of BMV is divided among three RNA components. Viral replication is dependent on two non-structural proteins, p1a (containing a RNA-helicase-like domain and a capping domain) and p2a (containing a polymerase domain) encoded respectively by genomic RNAs 1 and 2 (Ahlquist, 2006). Genomic RNA3 is dicistronic, encoding a non-structural movement protein (MP) and the capsid protein (CP) which is expressed via a subgenomic RNA (RNA4) produced during replication (Ahlquist, 2006). Replication of BMV has been studied in detail at the molecular and subcellular level using natural plant hosts (Bamunusinghe et al., 2011b; Kao and Sivakumaran, 2000) and non-host, surrogate yeast system (Ahlquist, 2006).

Macromolecular interactions (eg. PPI, protein-RNA interactions) have been shown to be intimately involved in the establishment of a successful infection by an RNA viral pathogen (Hunter, 1994; Kujala et al., 2001). Although virus-encoded proteins are envisioned to perform a specific function (eg. viral replicase

in catalyzing the synthesis of progeny RNA), accumulated information over the past two decades revealed otherwise (Laliberte and Sanfacon, 2010). For example, in addition to synthesizing viral progeny RNA, viral replicases have been shown to be intimately associated with many important functions such as RNA silencing (Ding et al., 2004), symptom modulation and movement (Creager et al., 1999), genome packaging and translation (Sanz et al., 2007). Another important multifunctional macromolecular entity is the CP. The primary function of the CP is to encapsidate the infectious genome progeny and form stable virions (Rao, 2006). Several factors such as CP-CP interactions, sequence-independent RNA-protein interactions (involved in stabilization of encapsidated virions), sequence-dependent RNA-protein interactions (origin of assembly sequences), auxiliary factors such as cellular tRNAs, viral replicase and scaffolding protein contribute to the assembly of infectious virions (Rao, 2006). Experimental evidence suggested that packaging specificity in BMV and *Flock house virus* (FHV) is regulated not only by synchronized co-expression of homologous replicase and CP, but also the translation of CP from replication derived mRNA (Rao, 2006). In addition, we for BMV (Bamunusinghe et al., 2011b) and others for FHV (Venter et al., 2009) showed that the subcellular localization sites of CP and replication overlap. Subsequent follow up studies further revealed that, in FHV, a physical interaction between replicase and CP is obligatory to confer packaging specificity (Seo et al., 2012a). However, in BMV, unlike FHV, functional replicase is a complex of two non-structural proteins, p1a

157

and p2a (Kao and Sivakumaran, 2000). If packaging specificity in BMV, like in FHV, requires a replicase-CP interaction, the question that needs to be addressed would be: *which of the two proteins interact with CP?* Thus, to find an answer to this question, in the present investigation, we opted to employ BiFC in conjunction with endoplasmic reticulum (ER) labeled with mCherry as a cellular marker protein. Our results underscore a previously undisclosed interaction between BMV replicase p2a and CP. This observation when integrated into the existing data (Annamalai and Rao, 2006c; Marsh et al., 1991; Yi et al., 2009a) provides insight to explain how the interaction between these two macromolecules regulates the overall replication and packaging in BMV.

RESULTS AND DISCUSSION

Live cell visualization of ER rearrangement in BMV infected plants

In plants, as a part of the endomembrane system, all ER membranes (rough ER, smooth ER, and nuclear envelopes) are physically linked and enclose a single, continuous lumen that extends beyond the boundaries of individual cells via the plasmodesmata (PD) (Staehelin, 1997). In several plant viral systems, membrane rearrangements involving ER have been observed (Laliberte and Sanfacon, 2010). Previous high resolution studies using electron microscopy revealed that wt BMV infection in *N. benthamiana* leaves is characterized by the accumulation of a large collection of vesicles derived from the ER. Since sites of viral RNA replication and CP synthesis overlap (Bamunusinghe et al., 2011b), prior to evaluating PPI in living cells, we sought to compare the morphology of the ER in non-infected and BMV infected *N. benthamiana* leaves under a confocal microscope using mCherry-HDEL (Nelson et al., 2007) as a fluorescent luminal ER marker (ER-mCherry). For infecting *N. benthamiana* plants with wt BMV we used either agroinfiltration or mechanical inoculation. Prior to examination under a confocal microscope, leaves were stained with DAPI to visualize the nucleus. Results are shown in Fig. 6.1 (A-C). In plant cells, the nucleus and ER can be distinguished based on their appearance. Nuclei are predominantly globular in appearance, whereas ER forms an extensive network

throughout the cytoplasm and surrounding the nucleus. In control samples, DAPI staining specifically identified the nucleus as globular structures emitting blue fluorescence (Fig. 6.1A). As expected, red fluorescence emitted by ER-mCherry was uniformly distributed throughout the cell periphery (Fig. 6.1A) and perinuclear area (Fig. 6.1A; inset). Confocal microscopic analysis of the ER phenotype in *N. benthamiana* leaves infected with BMV either via agroinfiltration or mechanical inoculation appeared to be identical (Fig. 6.1 B, C). For example, distinct from control samples (Fig. 6.1A), in BMV infected leaves, the distribution of red fluorescence appeared to be compacted, displaying large red fluorescent punctate bodies (indicated by arrows in Fig. 6.1B, C). Since BMV infection modifies ER to induce large cluster of vesicles (Bamunusinghe et al., 2011b), we conclude that these punctate bodies represent the vesicle collection. Furthermore, unlike in surrogate yeast system, the distribution of red fluorescence in peri-nuclear area was indistinguishable in BMV infected vs health plants (Fig. 6.1A-C, compare insets).

Efficacy of BiFC assay

For evaluating the interaction between replicase proteins (p1a and p2a) and CP, the N-terminal and C-terminal fragments of YFP were fused to ORFs of p1a, p2a and CP (Fig. 6.2A, B), generating a set of four fusion proteins for each virus-encoded protein under study (Fig. 6.2C). Prior to testing the interaction between

replicase and CP, we first evaluated the efficacy of BiFC assay. Results shown in Fig. 6.3 exemplify the specificity of the BiFC assay. For example, unlike free YFP that was distributed throughout the cytoplasm (Fig. 6.3), co-expression of either a N- or C-terminal fusion of the target protein (eg. p2a-nYFP or p2a-cYFP or CP-nYFP) with a counterpart of a non-fused fragment of YFP (eg. nYFP or cYFP) in all possible combinations failed to reconstitute YFP and hence no yellow fluorescence was detected (Fig. 6.3). In BMV, p1a and p2a are known to interact to assemble a functional replicase (Kao and Ahlquist, 1992). Therefore, we applied BiFC to verify such an interaction and to identify a set of bona fide interacting partners of p1a and p2a fusions. Consequently, four pairs of nYFP and cYFP terminal fusions of p1a (p1a-nYFP+p1a-cYFP; p1a-nYFP+cYFP-p1a; nYFP-p1a+p1a-cYFP and nYFP-p1a+cYFP-p1a) and p2a (p2a-nYFP+p2a-cYFP; p2a-nYFP+cYFP-p2a; nYFP-p2a+p2a-cYFP and nYFP-p2a+cYFP-p2a) were infiltrated into *N. benthamiana* leaves and the reconstituted YFP signal was monitored by confocal microscopy. Results are summarized in Fig. 6.4A and representative confocal images are shown in Fig. 6.4B. Among the eight possible pairs, a bona fide interaction resulting in the YFP fragment complementation was observed for five pairs (Fig. 6.4A, B; p1a-nYFP+p2a-cYFP; nYFP-p1a+p2a-cYFP; nYFP-p1a+cYFP-p2a; p1a-cYFP+p2a-nYFP and cYFP-p1a+p2a-nYFP).

The intensity of YFP emission, relative to negative control, in each of these five bona fide interacting partners was measured and shown in the interactive 3-

D surface plot image (Fig. 6.4C). Among these five positive interactions, maximum YFP intensity was observed for the pair nYFP-p1a+p2a-cYFP while lowest for the pair cYFP-p1a+p2a-nYFP (Fig. 6.4C). Previous confocal and electron microscopy studies performed with surrogate yeast and *N. benthamiana* plants showed that BMV replication occurs on ER (Bamunusinghe et al., 2011b). Therefore, to verify the subcellular localization of p1a:p2a interactions, five bona fide interacting partners of p1a and p2a were co-expressed with ER-mCherry. Results shown in Fig. 6.4B confirmed the co-localization of p1a:p2a interactions on ER. Furthermore, as observed with wt BMV infections (Fig. 6.1), each p1a:p2a interaction had resulted in the re-arrangement of ER, and was exemplified by the appearance of red fluorescent punctate bodies (Fig. 6.4B). Quantification of YFP and mCherry co-localization (see Materials and Methods section) revealed that majority of YFP emitted by each bona fide interacting partners co-localized on ER (Fig. 6.5). Consistent with our recent high-resolution EM data (Bamunusinghe et al., 2013a; Bamunusinghe et al., 2011b), a closer examination revealed little or no localization of reconstituted YFP signal around peri-nuclear area. Collectively, these observations validate the efficacy of BiFC as an ideal tool for not only evaluating the PPI *in vivo,* but also the subcellular localization sites of interactions.

Products of bona fide pair of interacting partners of p1a and p2a are
biologically active

To test the biological activity of five bona fide interacting fusion protein partners of p1a:p2a the following experiment was performed. Since synthesis of CP mRNA (i.e. B4) is contingent on the replication of genomic B3, *N. benthamiana* plants were co-infiltrated with an agroculture of a biologically active agroconstruct of wild type B3 (Annamalai and Rao, 2005b) and each pair of the bona fide interacting partners of p1a and p2a. Control plants were infiltrated with cultures of all three wild type BMV agroconstructs. At 4 dpi, total protein extracts were subjected to Western blot analysis using anti-CP antibody. Results shown in Fig. 6.6 confirm that each product of interaction resulting from all five bona fide interacting fusion protein partners of p1a:p2a is biologically active and catalyzes the complete replication of genomic B3. These observations further suggest that addition of N- or C- terminal YFP did not impair the functionality of p1a and p2a. Hence the observed p1a:p2a interactions and their subcellular localization sites are authentic.

Self-interactions in p1a, p2a and CP

Having confirmed the appropriateness of BiFC in evaluating PPI *in vivo*, we first verified the self-interaction in the fusion proteins of p1a, p2a and CP. Four

pairs of nYFP and cYFP terminal fusions of p1a (p1a-nYFP+p1a-cYFP; p1a-nYFP+cYFP-p1a; nYFP-p1a+p1a-cYFP and nYFP-p1a+cYFP-p1a), p2a (p2a-nYFP+p2a-cYFP; p2a-nYFP+cYFP-p2a; nYFP-p2a+p2a-cYFP and nYFP-p2a+cYFP-p2a) and CP (CP-nYFP+CP-cYFP; CP-nYFP+cYFP-CP; nYFP-CP+CP-cYFP and nYFP-CP+cYFP-CP) were infiltrated into *N. benthamiana* leaves and the reconstituted YFP signal was monitored by confocal microscopy. Results are summarized in Fig. 6.7 (A-C). Self-interaction was evident for each protein. For p1a, among four pairs, infiltration of three pairs resulted in the reconstitution of YFP (Fig. 6.7A). Whereas for p2a and CP, two of the four pairs for each protein resulted in YFP reconstruction (Fig. 6.7B, C). In each reconstituted YFP, unlike free YFP (Fig. 6.3), the subcellular distribution of YPF signal was distinct. It is interesting to note that among three positive self-interacting partners of p1a, the pattern of YFP distribution for nYFP-p1a+cYFP-p1a is distinct from the other two (Fig. 6.7A). However, no such variation in the reconstituted YFP distribution was observed for positive self-interacting partners of p2a (Fig. 6.7B) or CP (Fig. 6.7C).

CP interacts with p2a but not p1a

To verify which of the two replicase proteins interact with CP, we used two independent assays. In the first assay, four fusion proteins of CP (Fig. 6.2C) were co-expressed with each fusion protein of either p1a or p2a in *N.*

benthamiana plants. Following DAPI staining, infiltrated leaf samples were evaluated for YFP complementation by confocal microscopy. Results are summarized in Fig. 6.8 (A and B) and representative confocal images are shown in Fig. 6.8C. Absence of any YFP signal in plants infiltrated with all four possible pairs of fusion partners between p1a and CP (Fig. 6.8B) suggested these two proteins do not interact (Fig. 6.8C). By contrast, among four pairs of fusion partners of p2a and CP, infiltration of two pairs (p2a-cYFP+nYFP-CP and cYFP-p2a+nYFP-CP) resulted in a detectable YFP signal (Fig. 6.8D). Subsequent subcellular localization assays involving co-expression of two bona fide interacting partners of p2a and CP in conjunction with ER-mCherry suggested that each positive interaction between p2a and CP occurs on the ER (Fig. 6.8D). In BMV, p1a and CP but not p2a mediate induction of ER rearrangement (Bamunusinghe et al., 2013a; Bamunusinghe et al., 2011b). Thus, It is important to note that red fluorescent punctate bodies seen in Fig. 6.8C are mediated by p1a and CP while those seen in Fig. 6.8D are mediated by CP only. 3-D surface plot analysis showed that between the two positive interacting partners of p2a and CP, maximum intensity was observed for the pair containing cYFP-p2a+nYFP-CP (Fig. 6.8E). Despite weak YFP emission for the pair containing p2a-cYFP+nYFP-CP, quantification of YFP and mCherry co-localization was almost identical for both pairs of bona fide interacting partners of p2a-CP (Fig. 6.8F).

Co-immunoprecipitation assay confirms p2a and CP interaction

In the second assay, co-immunoprecipitation was used to confirm the interaction of CP with p2a (Fig. 6.8). Total protein preparations isolated from *N. benthamiana* leaves agroinfiltrated with two pairs of bona fide interacting partners of CP and p2a YFP fusions (i.e. p2a-cYFP+nYFP-CP and cYFP-p2a+nYFP-CP) were incubated with either anti-p2a or anti-CP antibody followed by the precipitation of the complex with anti-rabbit agrose beads. Western blotting with anti-CP or anti-p2a antibody was performed to detect the p2a or CP in the co-immunoprecipitated products. Results are shown in Fig. 6.9. Expression of each protein and antibody specificity for respective protein is evident from data shown in Fig. 6.9A. Consistent with the BiFC assay (Fig. 6.8), both CP and p2a was co-precipitated with heterologous antibodies (Fig. 6.9B, C). These results validate our BiFC assays showing that CP specifically interacts with p2a. Furthermore, the fact that the observed interaction between CP and p2a was not disrupted by RNase A treatment suggest that no RNA was involved in CP and p2a interaction. These results were consistently reproduced in three independent Co-IP assays.

A previous study evaluating interactions between BMV proteins by YTH failed to detect any interaction between replicase and CP (O'Reilly et al., 1997). These authors concluded that the absence of an interaction between replicase

166

and CP in YTH does not necessarily mean the interaction does not occur, since such interactions may require additional factors that are not duplicated in YTH. Having proved the specificity and validity of the BiFC assay in testing PPI in several plant and non-plant viral systems (Atanasiu et al., 2010; Hemerka et al., 2009; Seo et al., 2012a) in conjunction with the results presented in this study, below we offer two major mechanistic roles played by CP:p2a interaction in the regulation of replication and genome packaging in BMV.

Molecular analysis of p1a and p2a revealed that unlike p2a which is required in catalytic amounts (Rao and Hall, 1990), sustained synthesis of p1a is obligatory (Kroner et al., 1990; Rao and Hall, 1990). Membrane fraction studies performed with BMV and the genetically related *Cucumber mosaic* virus (CMV) revealed that p2a exists in two forms: one associated with p1a and the other as a free form in the cytoplasm (Chen and Ahlquist, 2000; Seo et al., 2009). Furthermore, in BMV and CMV, although p1a is functional only when co-assembled with p2a, p2a alone can initiate the synthesis of (+)-strand on a transiently expressed (-)-strand template (Kwon and Rao, 2012; Seo et al., 2009). These observations in conjunction with the fact that sites of RNA synthesis and CP overlap (Bamunusinghe et al., 2011b), it is reasonable to assume that (+)-synthesis occurs in the cytoplasm. Although RNA replication in BMV is entirely catalyzed by p1a:p2a complex (Kao and Ahlquist, 1992), CP has been shown to have a profound influence on BMV replication, specifically in up

regulating (+)-strand synthesis. For example, experiments performed in the early 1990's in studying the effect of B3 on BMV progeny accumulation showed that the ratio of (+):(-)-strand progeny in the absence of B3 was 1:1 compared to 1:100 in its presence (Marsh et al., 1991). However, a more recent study revealed that CP could regulate BMV RNA accumulation in a concentration dependent manner by binding to Box B located in the 5'end of B2 (Yi et al., 2009a; Yi et al., 2009b). Integration of these past results into those obtained in the current study provide a mechanistic role played by CP:p2a interaction in the up-regulation of (+)-strand synthesis in BMV.

Genome packaging in BMV and other (+)-strand RNA viruses is functionally coupled to replication (Rao, 2006). Replication-independent expression of BMV CP resulted in the assembly of polymorphic virions packaging cellular RNA in addition to non-replicating viral RNAs, and complementation with viral replicase significantly enhanced packaging specificity (Annamalai and Rao, 2005b). However, experiments performed with chimeric RNAs between BMV and FHV engineered to express CP using a heterologous replication system (i.e. B1+B2+B3/FHV-CP; F1+F2/BMV-CP) exhibited non-specific packaging phenotypes and complementation with homologous replicase (with respect to CP) failed to enhance packaging specificity, suggesting that transcription of CP mRNA from homologous replication machinery and its translation must be synchronized (Annamalai et al., 2008b). From these observations it was

hypothesized that an interaction with replicase renders the CP more specific in packaging viral progeny RNA (Annamalai et al., 2008b; Rao, 2006). Dissecting the components of BMV replicase interacting with CP, this study has identified that p2a, but not p1a, exclusively interacts with CP. Sub-cellular co-localization of replication and CP (Bamunusinghe et al., 2011b) and exclusive involvement of p2a in the (+)-strand synthesis (Kwon and Rao, 2012; Seo et al., 2009) collectively justify the p2a:CP interaction observed in this study. In conclusion our data provide the first convincing evidence for the existence of a physical interaction between BMV CP and p2a. Further work is needed not only to identify the interacting domains of p2a and CP but also to test whether additional host proteins are required to promote CP:p2a interaction.

MATERIALS AND METHODS

Construction of YFP fusion proteins for ectopic expression

Agrobacterium-based binary vectors PZPc-nYFP, PZPc-cYFP, PZPn-nYFP, or PZPn-cYFP for BiFC assay in *N. benthamiana* plants were constructed as previously described (Seo et al., 2012a). BMV ORFs p1a, p2a or CP were amplified by PCR using sequence specific primers and Vent Polymerase (Sigma). The resulting PCR products were inserted into PZPc-nYFP, PZPc-cYFP, PZPn-nYFP or PZPn-cYFP utilizing *Stu*I and *Spe*I sites (Fig. 6.2). The orientation of each insert was confirmed by sequencing.

Mechanical inoculation, Agroinfiltration and Confocal Microscopy

For mechanical inoculation, *N. benthamiana* plants were dusted with Carborundum and purified virions of BMV (1 mg/ml) were mechanically spread on the leaf followed by washing of the excess inoculum with water. For agroinfiltration, after transformation of, N- or C-terminal YFP fusion constructs of p1a, p2a or CP were transformed into *Agrobacterium* strain GV3101. Similar agrotransformation was performed with a binary vector harboring ER organelle fluorescently labeled with mCherry (ER-mCherry; obtained from Dr. Andreas Nebenfuhr) (Nelson et al., 2007). Agrocultures (OD 0.5_{600}) containing single or

170

pairwise combinations of each YFP fusion construct were infiltrated into the abaxial side of *N. benthamiana* leaves as described previously (Chaturvedi et al., 2012a). At 3 dpi (days post infiltration), leaves were stained with DAPI (5 μg/ml; Sigma, USA), and epidermal cells of agroinfiltrated leaves were observed for emission of fluorescence using a Leica SP2 confocal microscope equipped with a specific laser/filter combination to detect DAPI (excitation at 345 nm), YFP (excitation at 514 nm), and mCherry (excitation at 587 nm).

Image analysis

Yellow fluorescence in test samples and background fluorescence in control samples captured by Leica TCS SP2 microscope was further processed using NIH ImageJ software (Schneider et al., 2012). Mean of three measurements of yellow fluorescence was taken and subtracted from the background fluorescence in the negative control. Surface plot for confocal images were created by using Interactive three-dimensional (3D) Surface Plot plugin (v2.33) software developed for ImageJ (Collins, 2007). Quantification of co-localization of YFP (from reconstituted N and C terminus of YFP) and mCherry (ER localization signal) was analyzed with the co-localization function of Huygen Professional software (8.5.9) from SVI (Scientific Volume Imaging), where graphical representation of the Pearson correlation coefficient values between YFP signals

with corresponding ER-mCherry was represented graphically (Dupuis et al., 2007). Absolute threshold was set to 1 for both YFP and mCherry.

Western blot analysis

Bona fide pair of interacting partners of p1a and p2a were mixed with a biologically agroconstruct harboring full-length B3 (Annamalai and Rao, 2005b) transformed into *Agrobacterium* GV3101 and infiltrated to *N. benthamiana* leaves. At 4dpi, infiltrated leaves were ground using liquid nitrogen, and homogenized with 3 volumes of protein extraction buffer (50 mM Tris-HCl [pH 8.0], 150 mM NaCl, 0.5% Triton x-100, 0.2% 2-mercaptoethanol, 5% glycerol, proteinase inhibitor cocktail [Sigma, USA]). Samples were then centrifuged at 12,000 rpm for 10 min at $4^{o}C$ and the supernatant was recovered as total protein. Total protein samples of wt BMV (4 μg) and test samples (20 μg) were resolved on 12% SDS-PAGE, and CP was detected using anti-CP antibody (Annamalai and Rao, 2005b).

Co-immunoprecipitation assays

Total proteins were extracted from healthy and agroinfiltrated *N. benthamiana* plants as described previously (Fujioka et al., 2007; Seo et al., 2012a). Briefly, after grinding the healthy or agroinfiltrated leaf material in liquid

nitrogen with 3 volumes of protein extraction buffer (50mMTris-HCl [pH 8.0], 150 mM NaCl, 0.5% Triton X-100, 0.2% 2-mercaptoethanol, 5% glycerol, proteinase inhibitor cocktail [Sigma, USA]), cell debris was removed by centrifugation at 18,000 x g for 20 min at 4°C. The resulting supernatant was incubated with either anti-protein p1a or p2a antibody at 1:100 dilution for 4 h at 4°C. A 30 μl aliquot of anti-rabbit agarose beads (Sigma, USA) was added to each tube, followed by incubation for 2 h at room temperature. The immune-complexes were then precipitated by centrifugation for 1 min at 10,000 x g and washed three times in 1 ml of PBS buffer. The precipitated proteins were then treated with RNase A (50 μg/ ml) for 2 h at 25°C and eluted from the beads by boiling in SDS-PAGE sample buffer for 3 min. Equal volumes of protein samples were subjected SDS-PAGE, followed by immunoblot analysis with anti-CP antibody.

ACKNOWLEDGMENTS
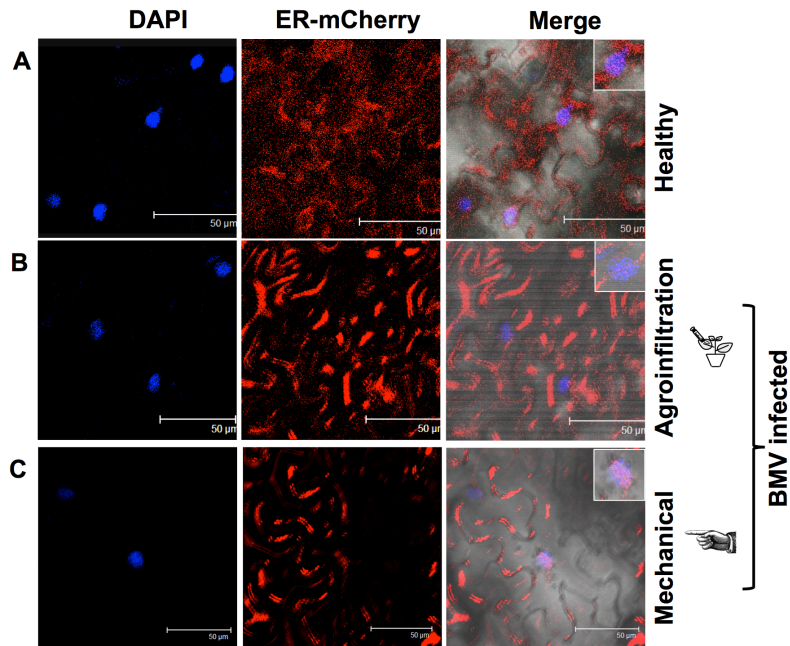
Figure 6.1 Visualizing ER rearrangement by confocal microscopy using mCherry labeled ER marker protein. *N. benthamiana* plants were agroinfiltrated (A) with a binary construct of ER-mCherry or (B) with a mixture containing binary constructs of all three wild type BMV RNA and ER-mCherry or (C) with ER-mCherry at 1 day post mechanical inoculation with purified BMV virions. At 4dpi, infiltrated leaves were stained with DAPI as a nuclear marker and observed under a confocal microscope equipped with a specific laser/filter combination to detect blue fluorescence emitted by DAPI (excitation at 345 nm) and red fluorescence emitted by mCherry (excitation at 587 nm). Insets (A-C): A magnified view of ER localization in the peri-nuclear area, Bar, 50 μm. In panels B and C, arrows indicate rearranged ER.
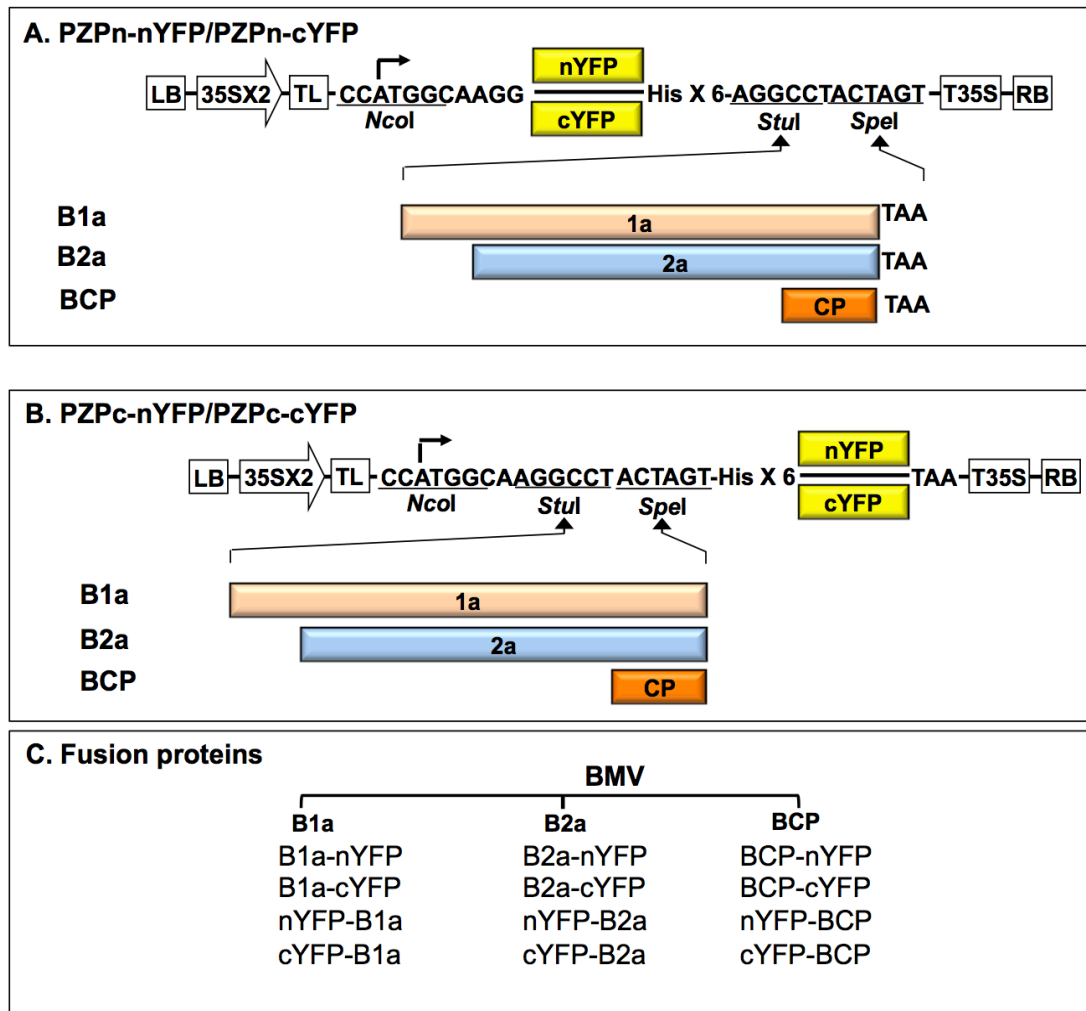
Figure 6.2 Schematic representation of fluorescent protein fusion constructs used in the present study. Two pairs of basal BiFC binary vectors were used. Constructs shown in panels A and B were engineered respectively for generating N-terminal (PZPn-nYFP and PZPn-cYFP) and C-terminal fusions (PZPc- nYFP and PZPc-cYFP). Open reading frames (ORFs) of BMV p1a, p2a and CP were fused in-frame to each pair of binary vectors using *Stu*I and *Spe*I sites. Each binary vector contained in sequential order, a left border of T-DNA (LB); a double 35S promoter (35Sx2); a tobacco etch virus (TEV) translation enhancer leader sequence (TL), multiple cloning site, a fragment of N-terminal 157 residues of yellow fluorescent protein (nYFP), a fragment of C-terminal 83 residues of YFP (nYFP), six-histidine tag (Hisx6), a 35S terminator (T35S), and a right border of T-DNA (RB). (C) Four possible fusion constructs for p1a, p2a and CP tested in this study are shown.

175
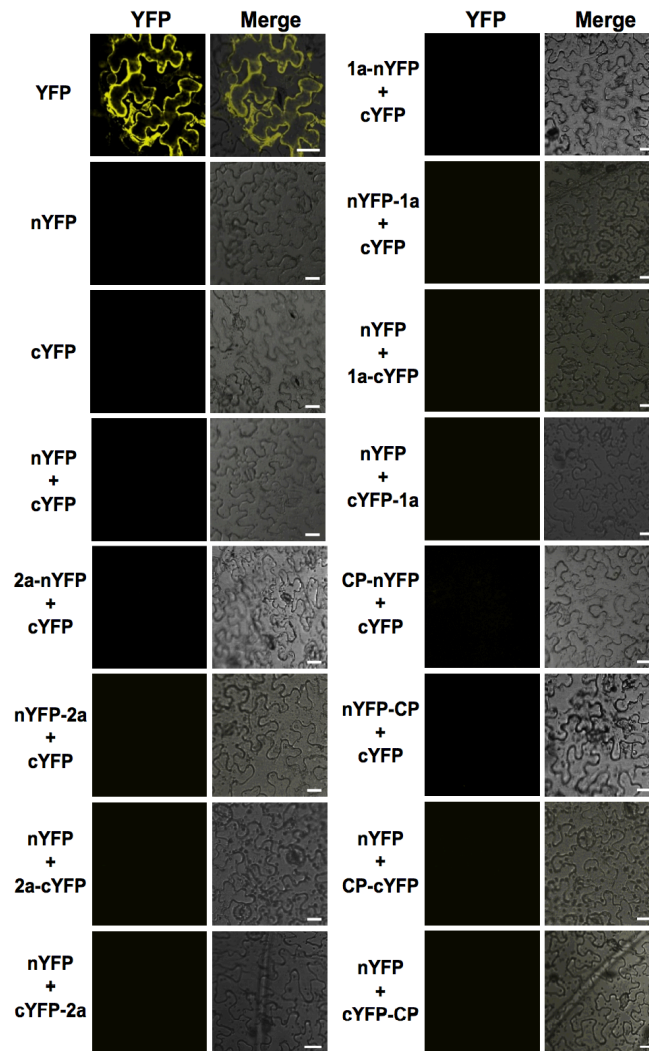
Figure 6.3 Specificity of BiFC. To test the specificity of the BiFC assay, binary constructs of either N or C-terminal YFP fusion proteins were transformed into *Agrobacterium* strain GV3101 and infiltrated into the abaxial side of *N. benthamiana* in either single or pairwise combinations as indicated on the left and right side of each panel. At 4 dpi, the reconstituted YFP signal was observed in the epidermal cells using a confocal microscope equipped with a specific laser/filter combination to detect YFP (excitation at 514 nm). Subcellular images for yellow fluorescence emitted by YFP and the merged images under the transmitted-light mode are shown. Bar, 15 μm.

A

1a-1a self interaction

1a-nYFP + 1a-cYFP

1a-nYFP + cYFP-1a

nYFP-1a + 1a-cYFP

nYFP-1a + cYFP-1a

1a \ 1a	1a-cYFP	cYFP-1a
1a-nYFP	+	−
nYFP-1a	+	+

B

2a-2a self interaction

2a-nYFP + 2a-cYFP

2a-nYFP + cYFP-2a

nYFP-2a + 2a-cYFP

nYFP-2a + cYFP-2a

2a \ 2a	2a-cYFP	cYFP-2a
2a-nYFP	+	−
nYFP-2a	−	+

C

CP-CP self interaction

CP-nYFP + CP-cYFP

CP-nYFP + cYFP-CP

nYFP-CP + CP-cYFP

nYFP-CP + cYFP-CP

CP \ CP	CP-cYFP	cYFP-CP
CP-nYFP	+	−
nYFP-CP	+	−
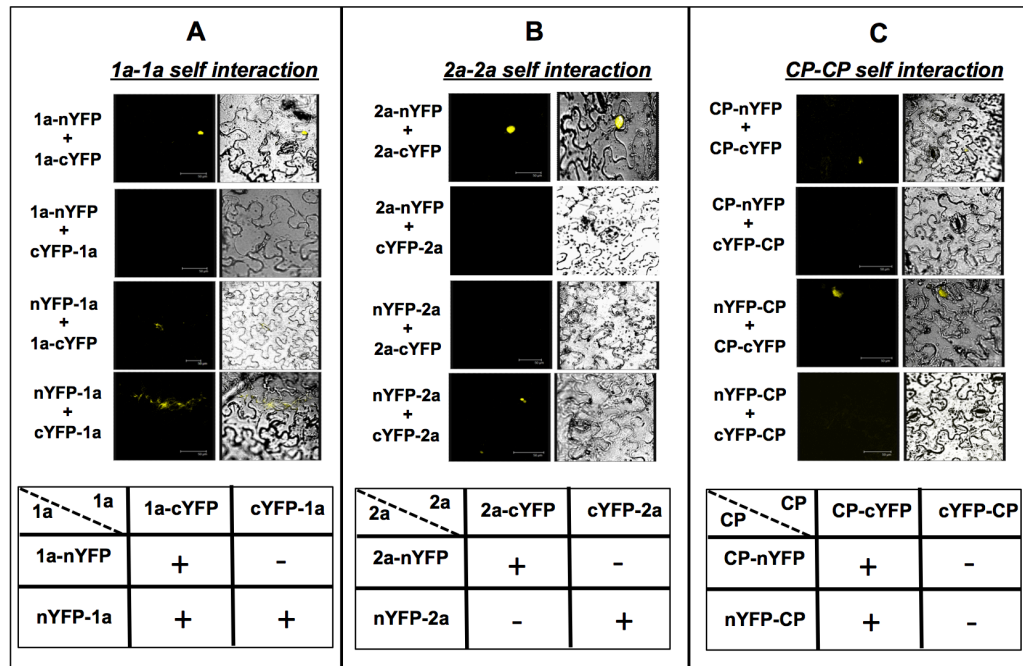
Figure 6.4 Efficacy of BiFC. A binary construct of ER-mCherry was mixed with binary constructs of N or C-terminal YFP fusion proteins of p1a and p2a in all possible pairwise combinations and infiltrated into *N. benthamiana* leaves. Prior to visualizing under confocal microcopy, each infiltrated leaf was stained with DAPI for visualizing the nucleus as a sub cellular marker organelle. (A) Summary of interactions between p1a and p2a. The presence or absence of yellow fluorescence was indicated by "+" and "-" symbols, respectively. (B) Representative confocal images of five positively interacting bona fide partners of p1a and p2a are shown. The fluorescent signals were observed in the epidermal cells using confocal microscope at 4 dpi. Nuclei and ER emit blue and red fluorescence respectively. Bar, 50 μm. (C) Surface plot images for the indicated samples were generated using Interactive 3-D Surface Plot plugin. The numbers indicate the mean intensity of YFP.
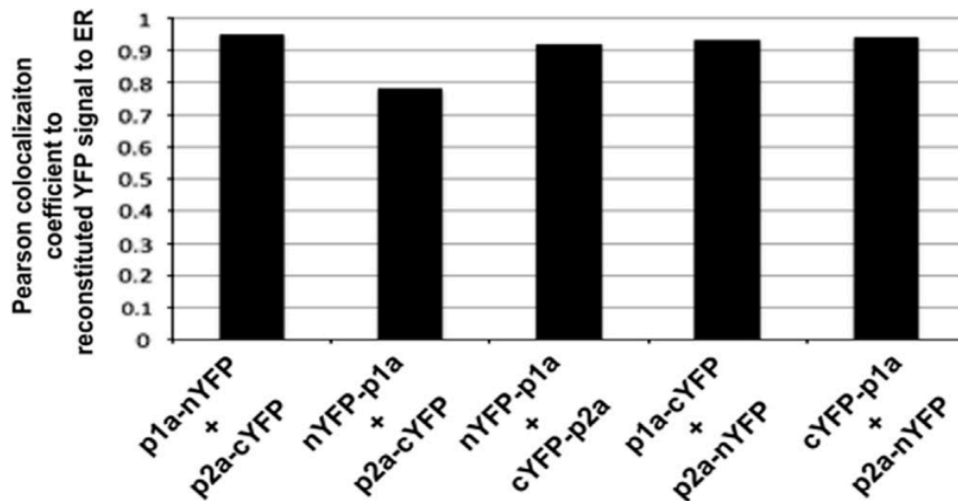
Figure 6.5 Co-localization analysis of YFP and mCherry for p1a-p2a interacting partners. Digital images showing YFP for five pairs of bona fide interacting fluorescent protein partners of p1a and p2a and red fluorescence for ER-mCherry shown in 6.4B were analyzed for co-localization as described under Materials and Methods section. A coefficient of 0 means no co-localization while coefficient of 1 signifies perfect co-localization.
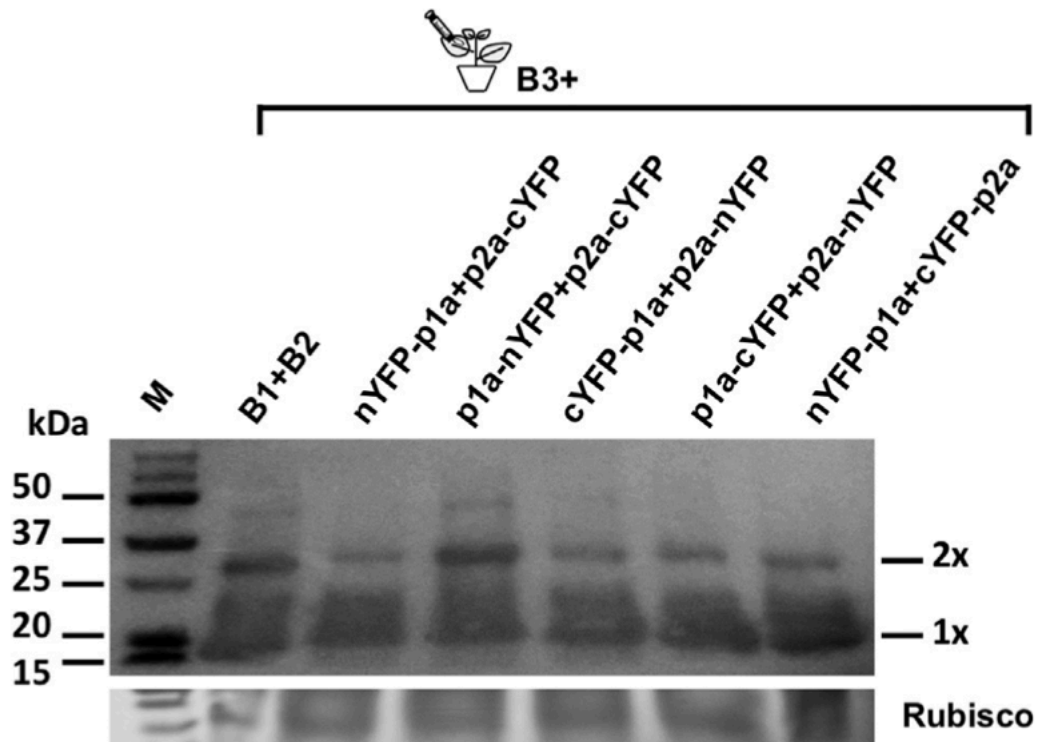
Figure 6.6 Biological activity of products of bona fide pair of interacting partners of p1a ad p2a. A binary construct of wt B3 was mixed with five pairs of bona fide interacting partners of p1 and p2a (shown in 6. 4) and infiltrated into *N. benthamiana* plants. Plants infiltrated with all three wt binary constructs of BMV RNA served as controls. At 4 dpi, total protein extracts were isolated and subjected to Western blot analysis using anti-BMV CP antibody. The positions of marker proteins (M) and monomeric (1x) and dimeric (2x) forms of BMV CP are shown to the left and right, respectively.
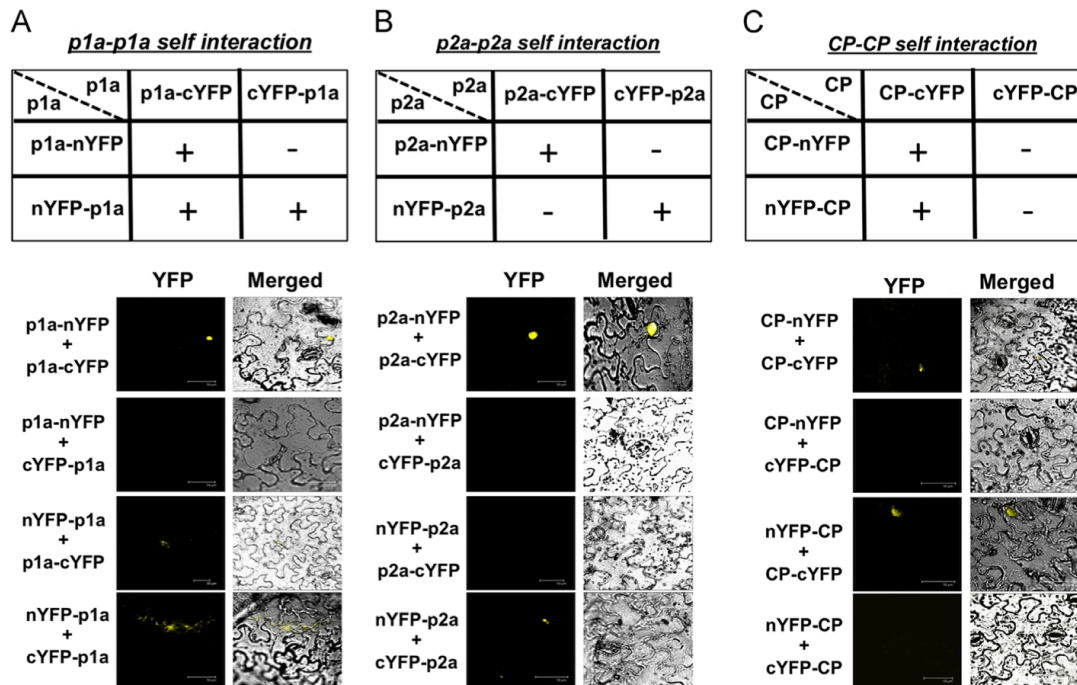
Figure 6.7 Self-interaction of p1a, p2 and CP fusion constructs. Agrocultures containing a binary plasmid of ER-mCherry and a pair of N- or C-terminal fusion constructs for p1a or p2a or CP were infiltrated into *N. benthamiana* plants and visualized for YFP signal by confocal microscopy. Summary of self-interactions (top panels) and representative confocal images showing self-interaction between a bon fide interacting partners (bottom panels) of (A) p1a, (B) p2a and (C) CP. Confocal microscopy was performed as described under Fig. 6.3 legend. The presence or absence of yellow fluorescence is indicated by "+" and "-" symbols, respectively. Bar, 50 μm.

A

p1a –CP interaction

p1a \ CP	CP-nYFP	nYFP-CP	CP-cYFP	cYFP-CP
p1a-nYFP	-	-	-	-
p1a-cYFP	-	-	-	-
nYFP-p1a	-	-	-	-
cYFP-p1a	-	-	-	-

B

p2a-CP Interaction

p2a \ CP	CP-nYFP	nYFP-CP	CP-cYFP	cYFP-CP
p2a-nYFP	-	-	-	-
p2a-cYFP	-	+	-	-
nYFP-p2a	-	-	-	-
cYFP-p2a	-	+	-	-
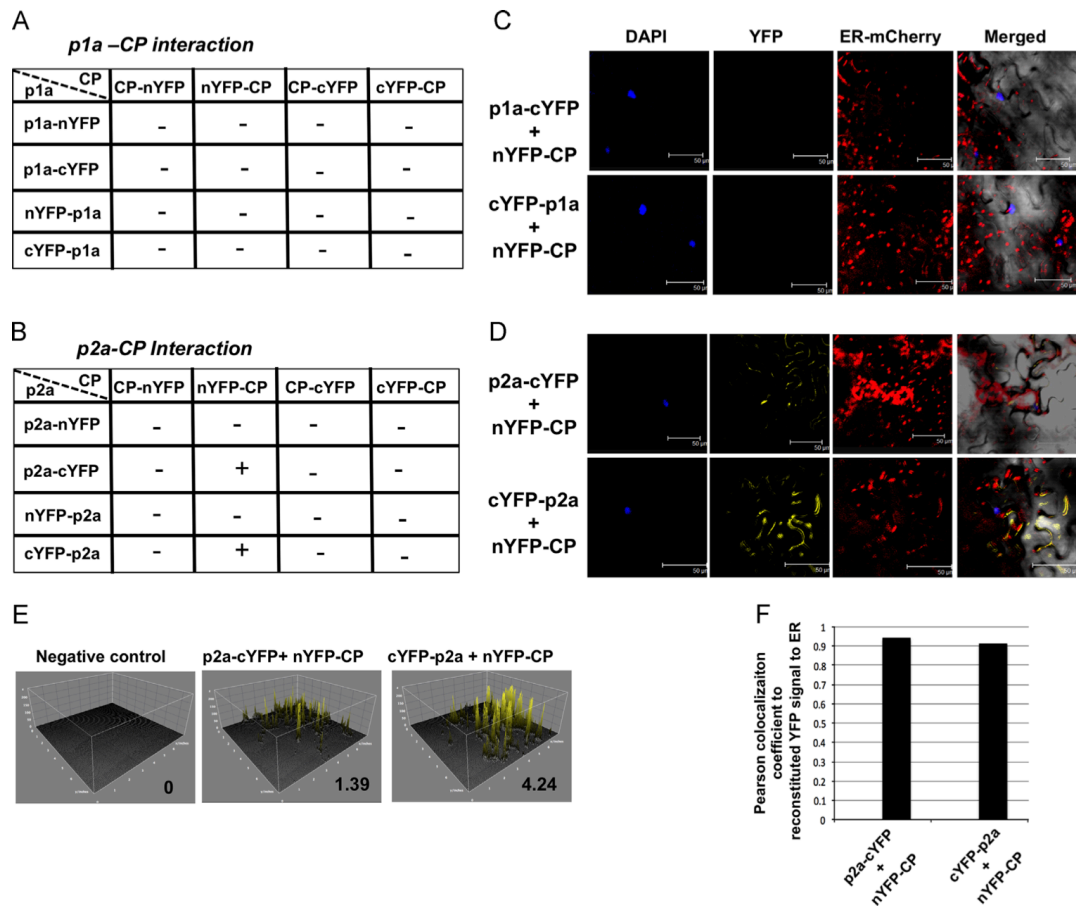
Figure 6.8 Interaction of CP with either p1a or p2a. Agrocultures containing a binary plasmid of ER-mCherry and binary constructs N or C terminal fusion proteins of CP were mixed with similar constructs of p1a or p2a and co-infiltrated into *N. benthamiana* plants. Summary of interactions between (A) p1a and CP and (B) p2a and CP are shown. The presence or absence of yellow fluorescence is indicated by "+" and "-" symbols, respectively. (C, D) Representative confocal images showing the interactions between (C) either p1a and CP or (D) p2a and CP. Confocal microscopy with a specific laser/filter combination to detect DAPI (excitation at 345 nm), YFP (excitation at 514 nm), and mCherry (excitation at 587 nm) was used. Bar, 50 μm. (E) 3-D surface intensity plot images for the indicated samples are prepared as described under Fig. 6.4C legend. (F) Co-localization of YFP and mCherry for the two pairs of bona fide interacting fluorescent protein partners of p2a and CP was quantitated as described under Fig. 6.5 legend.

181
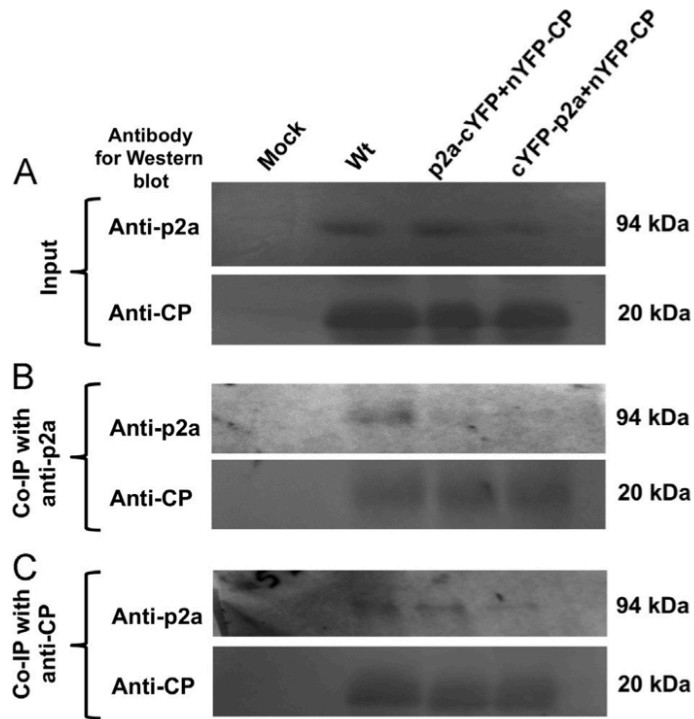
Figure 6.9 Co-immunoprecipiation (Co-IP) assay. (A) Expression of p2a and CP in RNase A treated total protein extracts recovered from the indicated experimental samples was confirmed by Western blotting with anti-p2a and anti-CP antibodies, respectively. Total protein extracts from healthy (mock) or leaves infiltrated with a mixture containing all three BMV genomic RNA binary constructs (wt) served as controls. (B, C). Co-IP assay. Agrocultures containing two pairs of bona fide interacting partners of p2a and CP (p2acYFP+nYFP-CP and cYFP-p2a+nYFP-CP) were co-infiltrated into *N. benthamiana*. Total protein extracts of each sample were incubated with either anti-p2a or anti-CP antibodies, treated with RNase A and the complex was precipitated with anti-rabbit agarose beads. The final products were subjected to Western blotting using anti-p2a and anti-CP antibodies.

REFERENCE

1.   **Ahlquist, P., 2006**. Parallels among positive-strand RNA viruses, reverse-transcribing viruses and double-stranded RNA viruses. Nat Rev Microbiol 4, 371-382.

2.   **Annamalai, P., Rao, A.L., 2005**. Replication-independent expression of genome components and capsid protein of brome mosaic virus in planta: a functional role for viral replicase in RNA packaging. Virology 338, 96-111.

3.   **Annamalai, P., Rao, A.L., 2006.** Packaging of brome mosaic virus subgenomic RNA is functionally coupled to replication-dependent transcription and translation of coat protein. J Virol 80, 10096-10108.

4.   **Annamalai, P., Rofail, F., Demason, D.A., Rao, A.L., 2008**. Replication-coupled packaging mechanism in positive-strand RNA viruses: synchronized coexpression of functional multigenome RNA components of an animal and a plant virus in Nicotiana benthamiana cells by agroinfiltration. Journal of Virology 82, 1484-1495.

5.   **Atanasiu, D., Whitbeck, J.C., de Leon, M.P., Lou, H., Hannah, B.P., Cohen, G.H., Eisenberg, R.J., 2010.** Bimolecular complementation defines

functional regions of Herpes simplex virus gB that are involved with gH/gL as a necessary step leading to cell fusion. J Virol 84, 3825-3834.

6.   **Bamunusinghe, D., Chaturvedi, S., Seo, J.K., Rao, A.L., 2013.** Mutations in the Capsid Protein of Brome Mosaic Virus Affecting Encapsidation Eliminate Vesicle Induction In Planta: Implications for Virus Cell-to-Cell Spread. Journal of Virology 87, 8982-8992.

7.   **Bamunusinghe, D., Seo, J.K., Rao, A.L., 2011.** Subcellular localization and rearrangement of endoplasmic reticulum by Brome mosaic virus capsid protein. Journal of virology 85, 2953-2963.

8.   **Chaturvedi, S., Jung, B., Gupta, S., Anvari, B., Rao, A.L., 2012**. A Simple and robust in vivo and in vitro approach for studying virus assembly. J Vis Exp 61, e3645.

9.   **Chen, J., Ahlquist, P., 2000.** Brome mosaic virus polymerase-like protein 2a is directed to the endoplasmic reticulum by helicase-like viral protein 1a. J Virol 74, 4310-4318.

10.   **Citovsky, V., Lee, L.Y., Vyas, S., Glick, E., Chen, M.H., Vainstein, A., Gafni, Y., Gelvin, S.B., Tzfira, T., 2006.** Subcellular localization of interacting proteins by bimolecular fluorescence complementation in planta. Journal of molecular biology 362, 1120-1131.

11.   **Collins, T.J., 2007.** ImageJ for microscopy. Biotechniques 43, 25-30.

12.   **Creager, A.N., Scholthof, K.B., Citovsky, V., Scholthof, H.B., 1999.** Tobacco mosaic virus. Pioneering research for a century. Plant Cell 11, 301-308.

13.   **Ding, S.W., Li, H., Lu, R., Li, F., Li, W.X., 2004.** RNA silencing: a conserved antiviral immunity of plants and animals. Virus Res 102, 109-115.

14.   **Dupuis, J., Prefontaine, A., Villeneuve, L., Ruel, N., Lefebvre, F., Calderone, A., 2007.** Bone marrow-derived progenitor cells contribute to lung remodelling after myocardial infarction. Cardiovascular pathology : the official journal of the Society for Cardiovascular Pathology 16, 321-328.

15.   **Fujioka, Y., Utsumi, M., Ohba, Y., Watanabe, Y., 2007.** Location of a possible miRNA processing site in SmD3/SmB nuclear bodies in Arabidopsis. Plant Cell Physiol 48, 1243-1253.

16.   **Hemerka, J.N., Wang, D., Weng, Y., Lu, W., Kaushik, R.S., Jin, J., Harmon, A.F., Li, F., 2009.** Detection and characterization of influenza A virus PA-PB2 interaction through a bimolecular fluorescence complementation assay. J Virol 83, 3944-3955.

17.   **Hunter, E., 1994.** Macromolecular interactions in the assembly of HIV and other retroviruses. Seminars in virology 5.

18. **Kao, C.C., Ahlquist, P., 1992.** Identification of the domains required for direct interaction of the helicase-like and polymerase-like RNA replication proteins of brome mosaic virus. J Virol 66, 7293-7302.

19. **Kao, C.C., Sivakumaran, K., 2000**. Brome mosaic virus, good for an RNA virologist's basic needs. Mol Plant Pathol 1, 91-97.

20. **Kerppola, T.K., 2008.** Bimolecular fluorescence complementation: visualization of molecular interactions in living cells. Methods Cell Biol 85, 431-470.

21. **Khan, S.H., Ahmad, F., Ahmad, N., Flynn, D.C., Kumar, R., 2011.** Protein-protein interactions: principles, techniques, and their potential role in new drug development. J Biomol Struct Dyn 28, 929-938.

22. **King, A.M.Q., Adams, M.J., Carstens, E.B., Lefkowitz, 2011.** Virus Taxonomy: Ninth Report of the International Committee on Taxonomy of Viruses 1ed. Elsevier.

23. **Kroner, P.A., Young, B.M., Ahlquist, P., 1990.** Analysis of the role of brome mosaic virus 1a protein domains in RNA replication, using linker insertion mutagenesis. J Virol 64, 6110-6120.

24.   **Kujala, P., Ikaheimonen, A., Ehsani, N., Vihinen, H., Auvinen, P., Kaariainen, L., 2001.** Biogenesis of the Semliki Forest virus RNA replication complex. J Virol 75, 3873-3884.

25.   **Kwon, S.J., Rao, A.L., 2012.** Emergence of distinct brome mosaic virus recombinants is determined by the polarity of the inoculum RNA. Journal of Virology 86, 5204-5220.

26.   **Laliberte, J.F., Sanfacon, H., 2010.** Cellular remodeling during plant virus infection. Annual review of phytopathology 48, 69-91.

27.   **Marsh, L.E., Huntley, C.C., Pogue, G.P., Connell, J.P., Hall, T.C., 1991**. Regulation of (+):(-)-strand asymmetry in replication of brome mosaic virus RNA. Virology 182, 76-83.

28.   **Nelson, B.K., Cai, X., Nebenfuhr, A., 2007.** A multicolored set of in vivo organelle markers for co-localization studies in Arabidopsis and other plants. The Plant journal : for cell and molecular biology 51, 1126-1136.

29.   **O'Reilly, E.K., Paul, J.D., Kao, C.C., 1997.** Analysis of the interaction of viral RNA replication proteins by using the yeast two-hybrid assay. J Virol 71, 7526-7532.

30. **Rao, A.L., 2006.** Genome packaging by spherical plant RNA viruses. Annu Rev Phytopathol 44, 61-87.

31. **Rao, A.L., Hall, T.C., 1990.** Requirement for a viral trans-acting factor encoded by brome mosaic virus RNA-2 provides strong selection in vivo for functional recombinants. J Virol 64, 2437-2441.

32. **Sanz, M.A., Castello, A., Carrasco, L., 2007.** Viral translation is coupled to transcription in Sindbis virus-infected cells. J Virol 81, 7061-7068.

33. **Schneider, C.A., Rasband, W.S., Eliceiri, K.W., 2012.** NIH Image to ImageJ: 25 years of image analysis. Nat Methods 9, 671-675.

34. **Seo, J.K., Kwon, S.J., Choi, H.S., Kim, K.H., 2009.** Evidence for alternate states of Cucumber mosaic virus replicase assembly in positive- and negative-strand RNA synthesis. Virology 383, 248-260.

35. **Seo, J.K., Kwon, S.J., Rao, A.L., 2012.** A Physical Interaction between Viral Replicase and Capsid Protein Is Required for Genome-Packaging Specificity in an RNA Virus. Journal of Virology 86, 6210-6221.

36. **Staehelin, L.A., 1997.** The plant ER: a dynamic organelle composed of a large number of discrete functional domains. The Plant journal : for cell and molecular biology 11, 1151-1165.

37.   **Venter, P.A., Marshall, D., Schneemann, A., 2009.** Dual roles for an arginine-rich motif in specific genome recognition and localization of viral coat protein to RNA replication sites in flock house virus-infected cells. J Virol 83, 2872-2882.

38.   **Yi, G., Letteney, E., Kim, C.H., Kao, C.C., 2009a.** Brome mosaic virus capsid protein regulates accumulation of viral replication proteins by binding to the replicase assembly RNA element. RNA 15, 615-626.

39.   **Yi, G., Vaughan, R.C., Yarbrough, I., Dharmaiah, S., Kao, C.C., 2009b.** RNA binding by the brome mosaic virus capsid protein and the regulation of viral RNA accumulation. Journal of molecular biology 391, 314-326.

Chapter 7

Protein-Protein Interaction in Cucumber Mosaic Virus

ABSTRACT

Replication of a positive sense RNA virus is dependent on Protein-Protein and Protein-RNA interactions, which in turn leads to a successful infection in the host. Cucumber mosaic virus (CMV) is one of the most important plant viruses based on its wide host range; still the interacting patterns of proteins encoded by CMV have not been studied elaborately. Bi-molecular Fluorescence Complementation (BiFC) assay in conjunction with cellular markers demonstrated the interacting partners of CMV in live cell imaging. Along with previously known 1a and 2a replicase protein interactions, we were able to observe 1a-CP, 2a-CP and CP-MP interactions. Co-localization of positive interacting partners of CMV proteins with nuclear (DAPI) and Endoplasmic Reticulum (ER-mCherry) markers demonstrated the localization site of these interactions to be Endoplasmic reticulum (ER). Further, remodeling of ER network in the presence of CMV suggests that it plays an important role in the replication of the virus.

INTRODUCTION

Cucumber Mosaic Virus (CMV) is a tripartite positive sense RNA virus, belonging to the genus Cucumovirus (Palukaitis and Garcia-Arenal, 2003b). Genome of CMV is divided into three single stranded RNAs. Genomic RNAs 1 and 2 encode for nonstructural replicase proteins, 1a (encoding for methyltransferase and helicase domain), and 2a (encoding for RNA dependent RNA replicase) (Jacquemond, 2012a), along with a subgenomic RNA 4A, which encodes for 2b protein, which acts as a silencing suppressor (Ding et al., 1996). RNA 3 is bicistronic RNA, encoding for a nonstructural movement protein (MP) and a subgenomic capsid protein (CP) (Palukaitis and Garcia-Arenal, 2003b). Along with three genomic RNAs, several strains of CMV encapsidate satellite RNA, size of which in strain Q is 336 nucleotides. Satellite RNA uses CMV's replication as well as encapsidation machinery, and in turn either ameliorates or intensifies symptom expression (Kaper et al., 1990).

All five proteins encoded by CMV have been analyzed at a genetic level, where 1a protein has been demonstrated to localize on vacuolar membrane. Yeast two hybrid analysis has demonstrated that the N- terminal methyltransferase domain and a C terminal helicase domain interact *in-vitro* (O'Reilly et al., 1998). Also, C terminus of 1a protein interacts with the N terminal region of 2a protein *in vitro,* rendering N and C terminus of 1a protein to loose

functionality by addition of six hisitidine residues or GFP (Gal-On et al., 2000; Kim et al., 2002; Palukaitis and Garcia-Arenal, 2003b). Movement protein is required for the movement of unencapsidated RNA or encapsidated virion particle from one cell to another, but is dispensable for replication (Boccard and Baulcombe, 1993). Movement protein localizes to plasmadesmata and large aggregates accumulated in sieve elements (Blackman et al., 1998).

Most of the above-mentioned studies have been performed *in vitro*, or are visualized *in-vivo* in the absence of other components of viral replication machinery. Recent development of Bi-molecular Fluorescent Complementation assay has availed us with the ability to visualize interaction of two different proteins *in vivo*, where the localization of interactions can also be delineated (Seo et al., 2012b). In this study, a successful attempt is made to observe live cell imaging of interacting partners of CMV proteins using BiFC. Further, the site of localization of interacting partners is deciphered to be Endoplasmic reticulum. Also, detailed observation of *Nicotiana benthamiana* plants infected with the wild type CMV suggests a global remodeling of ER network throughout the leaf, indicating a pivotal role of ER network in the replication of Cucumber mosaic virus.

RESULTS AND DISCUSSION

Efficacy of BiFC assay for CMV proteins

To study the interaction between CMV proteins, N-terminal and C-terminal fragments of YFP were engineered to N terminus or C terminus of p1a, p2a, MP and CP leading to a set of four fusion proteins for every virus encoded protein (7. 1). Before interaction study between viral proteins, we confirmed the efficiency of BiFC constructs by performing BiFC between control samples, where it was observed that unlike free YFP signal, co-expressing one of the N- or C- terminal fusion protein of CMV with un-fused YFP fragment (N- or C- terminus) did not reconstitute to full length YFP, and hence no yellow fluorescence was observed (Fig. 7.2).

Homo-oligomerization of CMV proteins

Rationale for this study emerged from the fact that Cucumber mosaic virus's protein-protein interaction hasn't been studied elaborately, this function plays a very important role in the replication, movement and genome packaging of a positive sense RNA virus (Kao et al., 1992), (Annamalai et al., 2008a; Hwang et al., 2005). Replicase protein 1a-1a interaction in CMV was previously demonstrated using yeast two hybrid assay (O'Reilly et al., 1997), which has an

efficiency to screen 50% reliable PPI(s) (Deane et al., 2002). Hence, we employed BiFC, where two split fragments of YFP, N-terminal (1-156) residues and C-terminal (157-239) residues were fused to N terminus or C terminus of target proteins (Q1a, Q2a, MP or CP). Homologous interactions of Q1a, Q2a, MP or CP were tested by using four different pairs of nYFP and cYFP fusion proteins of Q1a (Q1a-nYFP+ Q1a-cYFP, Q1a-nYFP+ cYFP-1a, nYFP-1a+ 1a-cYFP, and nYFP-1a+ cYFP-1a) or Q2a (Q2a-nYFP+ Q2a-cYFP, Q2a-nYFP+ cYFP-2a, nYFP-2a+ 2a-cYFP, and nYFP-2a+ cYFP-2a), or MP (MP-nYFP+ MP-cYFP, MP-nYFP+ cYFP-MP, nYFP-MP+ MP-cYFP, and nYFP-MP+ cYFP-MP), or CP(CP-nYFP+ CP-cYFP, CP -nYFP+ cYFP-CP, nYFP-CP+ CP-cYFP, and nYFP-CP+ cYFP-CP). All the combinations were infiltrated into abaxial side of *N. benthamiana* leaves, and after 3 days post infiltration (dpi), epidermal cells of infiltrated leaves, after staining with DAPI, were observed for reconstitution of YFP signal under confocal microscope. For Q1a protein homologous interaction, two out of four combinations led to reconstitution of YFP signal, confirming self-interaction of Q1a in-vivo (Fig. 7.3A). These results bolster the previous research where Q1a-1a protein interaction was demonstrated (O'Reilly et al., 1997).

For Q2a protein, among the four pairs tested, three combinations confirmed Q2a self-interaction (Fig. 7.3B). In the case of MP, the reconstitution of YFP was observed in one combination out of four, where YFP signal was spread

throughout the periphery of infiltrated cells (Fig. 7.3C). In case of CP, two out of four combinations were observed to reconstitute full length YFP (which unlike MP was localized at the periphery of the cell) (Fig. 7.3D).

Heterologous interaction takes place between CMV proteins

Interaction between 1a-2a proteins constitutes to a functional replicase. 1a-2a interactions for BMV and CMV have been previously demonstrated using yeast two hybrid assays (O'Reilly et al., 1995) (Kim et al., 2002). There has not been any *in-vivo* interaction study for CMV, or demonstration of site of interactions in the cell.

Agrocultures encompassing BiFC constructs of replicase proteins 1a and 2a were mixed, as described (Fig. 7.4A), agroinfiltrated to *N. benthamiana* leaves, and were observed under confocal microscope at 3dpi. It was observed that five out of eight different combinations of 1a-2a interacting partners led to the reconstitution of YFP signal, providing first *in-vivo* evidence of CMV 1a-2a interaction (Fig 7.4A, C). Further, 1a-CP and 2a-CP, and MP-CP interactions were also scored in the similar fashion to 1a-2a interactions, and it was observed that five out of eight in case of 1a-CP interaction (Fig. 7.5A, C), six out of eight in case of 2a-CP (Fig. 7.6A, C), and seven out of eight of MP-CP (Fig. 7.7A, B) interacting partners led to reconstitution of YFP. When comparing results to that

of BMV BiFC (Chapter 6), it was observed that in case of BMV, none of the BiFC combinations for 1a-CP interact, whereas for CMV, 1a-CP leads to a positive interaction. This piece of data suggests how two members of Bromoviridae family differ in terms of interacting partners.

MATERIALS AND METHODS:

Construction of YFP fusion proteins for ectopic expression

Agrobacterium-based binary vector PZPc-nYFP, PZPc-cYFP, PZPn-nYFP, or PZPn-cYFP for BiFC assay in *N. benthamiana* plants were used as previously described (Seo et al., 2012b). QCMV 1a, 2a, MP or CP were amplified using the primers as mentioned (Table 1) with Vent Polymerase (Sigma). Amplified 1a, 2a, MP or CP open reading frames (ORF) were inserted into PZPc-nYFP, PZPc-cYFP, PZPn-nYFP or PZPn-cYFP utilizing StuI and SpeI sites.

Primers	Sequence
Q1A (STU1-FW)	5' ATATATAGGCCTATGGCAACGTCCTCATTCAA 3'
Q1A (SPE1-RW)	5'CGACTAGTTCAGACTAACGGAATACAAT 3'
Q1A (SPE1-RWΔTCA)	5'AACGACTAGTGACTAACGGAATACAAT 3'
Q2A (STU1-FW)	5' ATATATAGGCCTATGATAAGTCCTCCACCCACTTTCTCAT 3'
Q2A (SPE1-RW)	5' CGACTAGTTCAGGAAACCAATCCACGGGATCTACTCC 3'
Q2A (SPE1-RWΔTCA)	5' CGACTAGTGGAAACCAATCCACGGGATCTACTCC 3'
Q3a FW-STU1:	5'ATATATAGGCCTATGGCTTTCCAAGGTCCCAG 3'

Q3A(SPE1-RW):	5'ACGACTAGTTTAAAACTGTGATGTGTACTTACTAACC 3'
Q3A(SPE1-RWΔTCA)	5'AACGACTAGTAAACTGTGATGTGTACTTACTAACC 3'
Q4A(STU1-FW):	5' ATATATAGGCCTATGGACAAATCTGGC3'
Q4A(SPE1-RW)	5'AAATACTAGTTCAGCACTCGCGATTGAGAG 3'
Q4A(SPE1-RWΔTCA)	5'AAATACTAGTGCACTCGCGATTGAGAG 3'

Agroinfiltration and Confocal Microscopy

CMV 1a, 2a, MP or CP PZP YFP constructs were transformed into Agrobacterium strain GV3101, as previously described (Annamalai and Rao, 2006b). Different combinations of agrocultures at OD 0.5 (as shown in figures) were infiltrated into abaxial side of *N. benthamiana* leaves, as previously described (Chaturvedi et al., 2012b), stained with DAPI (Sigma, U.S.A), and visualized under Leica SP2 confocal microscopy equipped with a specific laser to detect YFP (excitation at 514 nm).
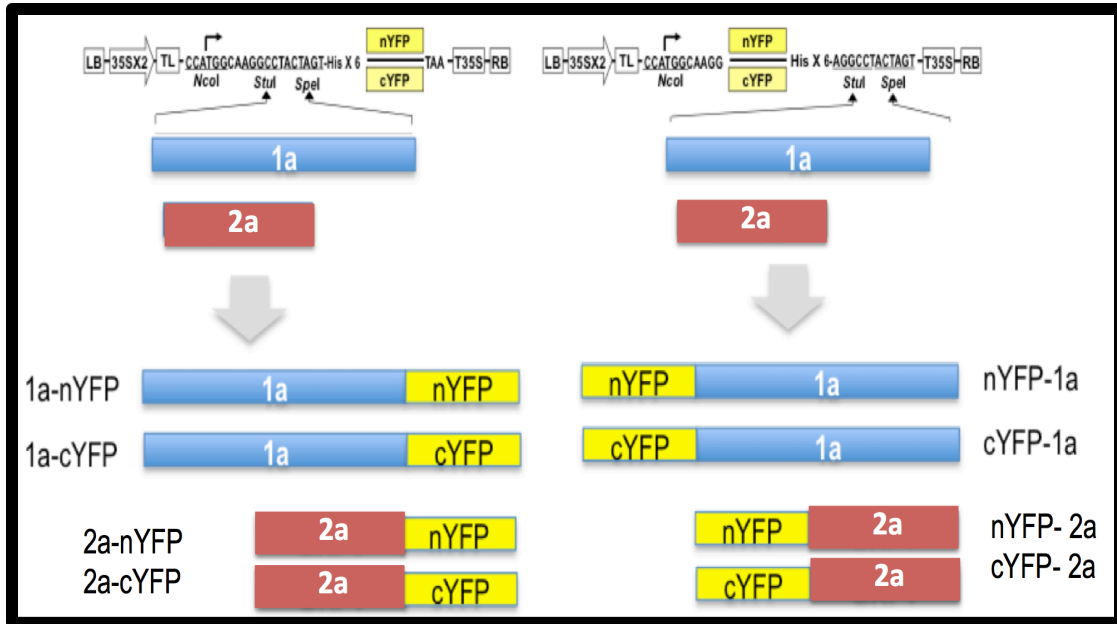
Figure 7.1 Schematic representation of fluorescent protein fusion constructs used in the study.
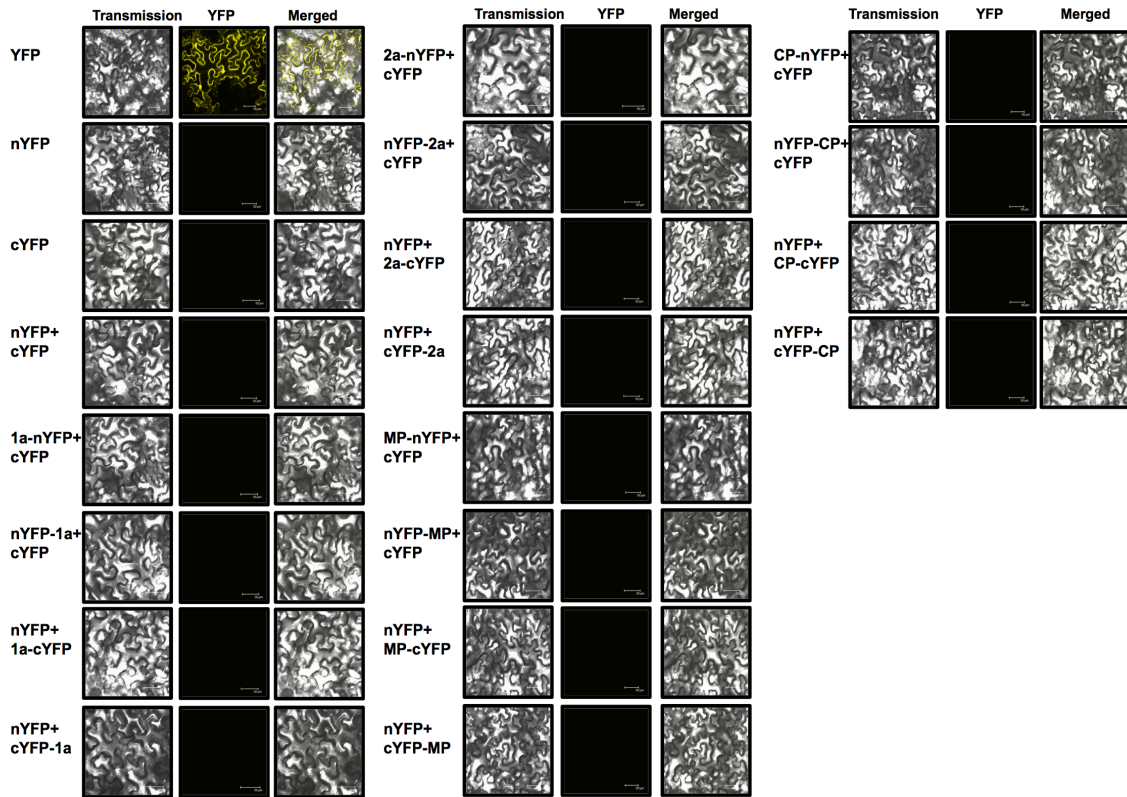
Figure 7.2 Specificity of BiFC. To test the specificity of the BiFC assay for CMV, binary constructs of either N or C-terminal YFP fusion proteins were transformed into *Agrobacterium* strain GV3101 and infiltrated into the abaxial side of *N. benthamiana* in either single or pairwise combinations as indicated. At 3 dpi, the reconstituted YFP signal was observed in the epidermal cells using a confocal microscope equipped with a specific laser/filter combination to detect YFP (excitation at 514 nm). Subcellular images for transmission, yellow fluorescence emitted by YFP, and the merged images under the transmitted-light mode are shown. Bar, 50 μm.
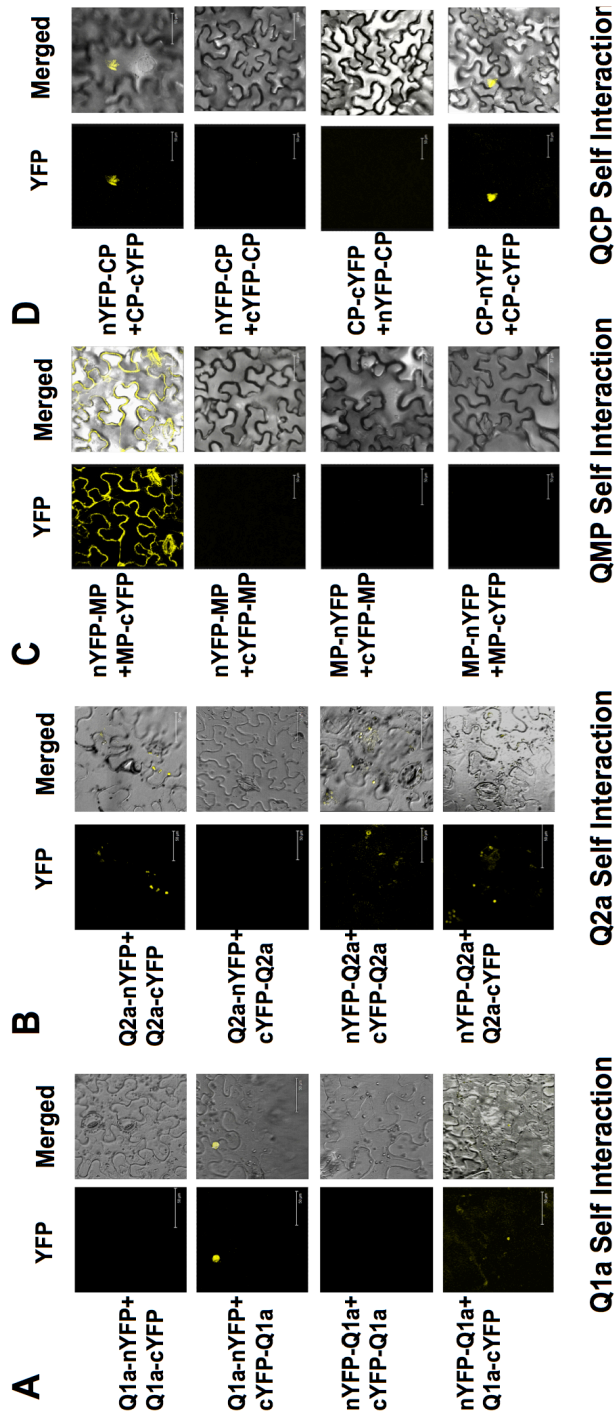
Figure 7.3 Self interaction of CMV proteins. Labeled agrobacterium cultures were transformed to GV3101 cells and combinations mentioned above were infiltrated to the abaxial side of *N. benthamiana* leaves. Epidermal cells were visualized for YFP signal at 3 days post infiltration using confocal microscopy, where (A) represents 1a self interaction, (B) represents 2a self interaction, (C) represents movement protein self interaction, and (D) Capsid protein self interactions.

(A)

	YFP	Merged		YFP	Merged
Q1a-nYFP+ Q2a-cYFP			Q2a-nYFP+ Q1a-cYFP		
Q1a-nYFP+ cYFP-Q2a			Q2a-nYFP+ cYFP-Q1a		
nYFP-Q1a+ cYFP-Q2a			nYFP-Q2a+ cYFP-Q1a		
nYFP-Q1a+ Q2a-cYFP			nYFP-Q2a+ Q1a-cYFP		

(B)
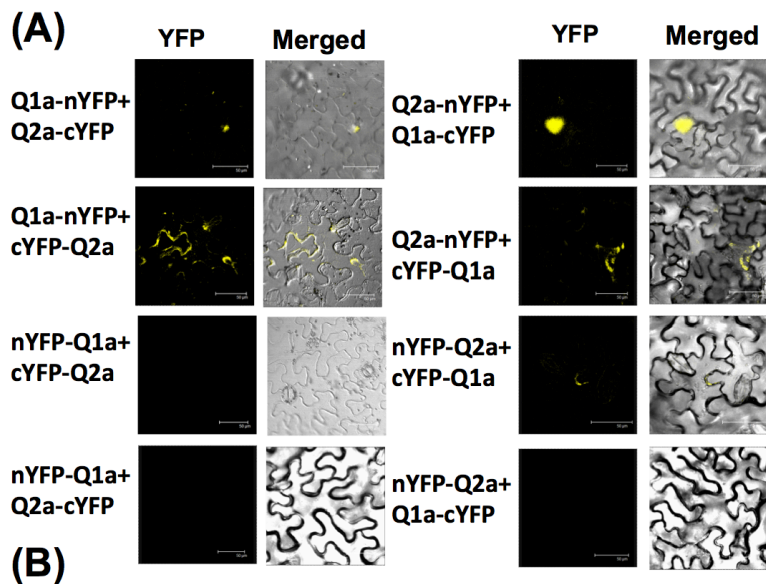
	cYFP	Q1a-cYFP	cYFP-Q1a	Q2a-cYFP	cYFP-Q2a
nYFP	-	-	-	-	-
Q1a-nYFP	-	-	+	+	+
nYFP-Q1a	-	+	-	-	-
Q2a-nYFP	-	+	+	+	-
nYFP-Q2a	-	-	+	+	+

Figure 7.4 Heterologous interaction of CMV 1a and 2a replicase proteins. Each of the labeled binary construct was transformed in Agrobacterium strain GV3101 and infiltrated into the abaxial side of N. benthamiana leaves in the pairwise combination mentioned above. The reconstitution of YFP signal was observed using confocal microscopy at 3dpi. The heterologous interactions of CMV 1a and 2a proteins are shown (A). (B) Represents summary of self and heterologous interactions between 1a and 2a, where (+) represent yellow fluorescence, and (-) represent absence of it.

(A)

| | YFP | Merged | | YFP | Merged |

1a-nYFP+CP-cYP / 1a-nYFP+cYFP-CP / CP-nYFP+1a-cYFP / CP-nYFP+cYFP-1a

nYFP-CP+1a-cYFP / nYFP-CP+cYFP-1a / nYFP-1a+cYFP-CP / nYFP-1a+CP-cYFP

(B)
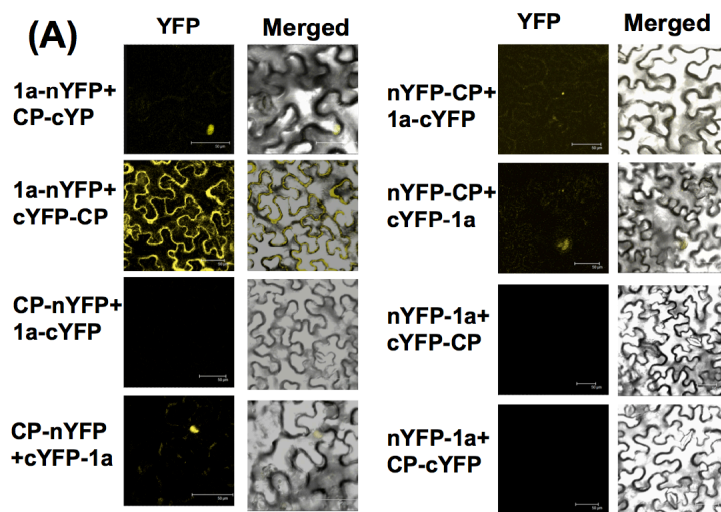
	cYFP	Q2a-cYFP	cYFP-Q2a	QCP-cYFP	cYFP-QCP
nYFP	-	-	-	-	-
Q2a-nYFP	-	+	+	+	-
nYFP-Q2a	-	+	+	+	+
QCP-nYFP	-	-	+	+	+
nYFP-QCP	-	+	+	+	+

Figure 7.5 Heterologous interaction of CMV 1a replicase protein and CP (Capsid protein). Each of the labeled binary construct was transformed in Agrobacterium strain GV3101 and infiltrated into the abaxial side of N. benthamiana leaves in the pairwise combination mentioned above. The reconstitution of YFP signal was observed using confocal microscopy at 3dpi. The heterologous interactions of CMV 1a and CP are shown (A). (B) Represents summary of self and heterologous interactions between 1a and CP, where (+) represent yellow fluorescence, and (-) represent absence of it.

(A)

	YFP	Merged		YFP	Merged
2a-nYFP+ CP-cYFP			CP-nYFP+ 2a-cYFP		
2a-nYFP+ cYFP-CP			CP-nYFP+ cYFP-2a		
nYFP-2a+ CP-cYFP			nYFP-CP+ 2a-cYFP		
nYFP-2a+ cYFP-CP			nYFP-CP+ cYFP-2a		

(B)

	cYFP	Q2a-cYFP	cYFP-Q2a	QCP-cYFP	cYFP-QCP
nYFP	-	-	-	-	-
Q2a-nYFP	-	+	+	+	-
nYFP-Q2a	-	+	+	+	+
QCP-nYFP	-	-	+	+	+
nYFP-QCP	-	+	+	+	+

Figure 7.6 Heterologous interaction of CMV 2a replicase protein and CP (Capsid protein). Each of the labeled binary construct was transformed in Agrobacterium strain GV3101 and infiltrated into the abaxial side of N. benthamiana leaves in the pairwise combination mentioned above. The reconstitution of YFP signal was observed using confocal microscopy at 3dpi. The heterologous interactions of CMV 2a and CP are shown (A). (B) Represents summary of self and heterologous interactions between 2a and CP, where (+) represent yellow fluorescence, and (-) represent absence of it.
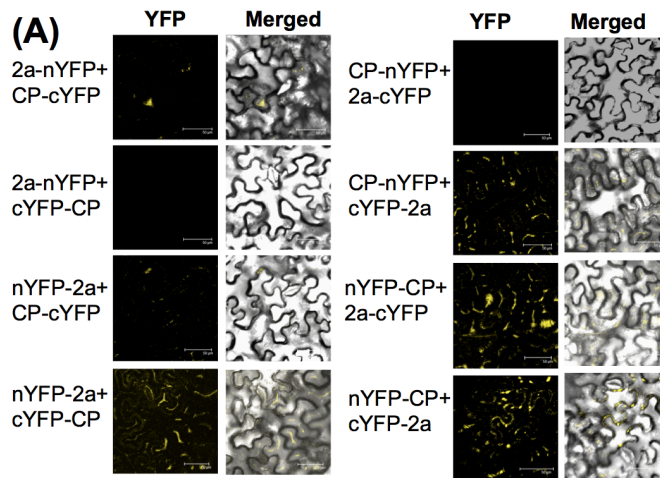
(A)

(B)

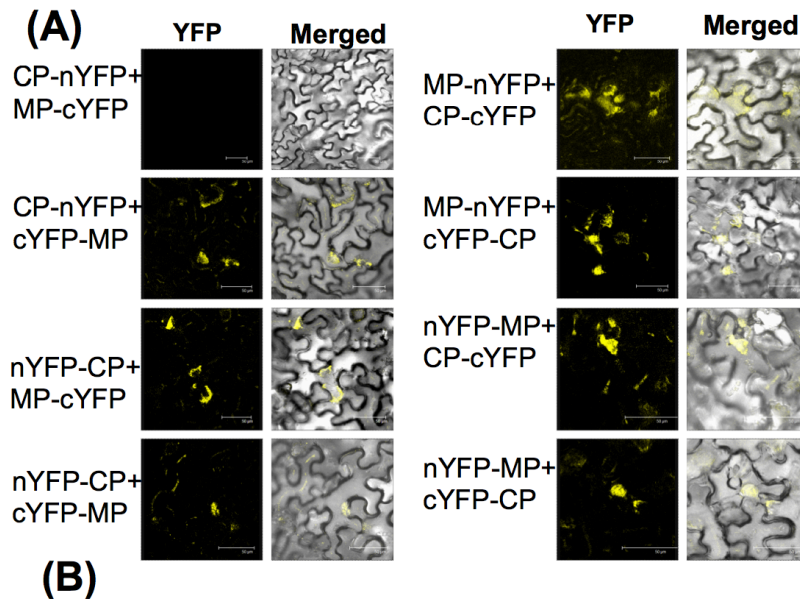|	cYFP	QMP-cYFP	cYFP-QMP	QCP-cYFP	cYFP-QCP
nYFP	-	-	-	-	-
QMP-nYFP	-	+	+	+	+
nYFP-QMP	-	+	+	+	+
QCP-nYFP	-	-	+	+	+
nYFP-QCP	-	+	+	+	+

Figure 7.7 Heterologous interaction of MP replicase protein and CP (Capsid protein). Each of the labeled binary construct was transformed in Agrobacterium strain GV3101 and infiltrated into the abaxial side of N. benthamiana leaves in the pairwise combination mentioned above. The reconstitution of YFP signal was observed using confocal microscopy at 3dpi. The heterologous interactions of CMV MP and CP are shown (A). Positive candidates for reconstitution of YFP signals were observed. (B) Represents summary of self and heterologous interactions between MP and CP, where (+) represent yellow fluorescence, and (-) represent absence of it.

206

REFERENCE

1.   **Annamalai, P., Rao, A.L., 2006.** Delivery and expression of functional viral RNA genomes in planta by agroinfiltration. Current protocols in microbiology Chapter 16, Unit16B 12.

2.   **Annamalai, P., Rofail, F., Demason, D.A., Rao, A.L., 2008**. Replication-coupled packaging mechanism in positive-strand RNA viruses: synchronized coexpression of functional multigenome RNA components of an animal and a plant virus in Nicotiana benthamiana cells by agroinfiltration. Journal of virology 82, 1484-1495.

3.   **Bamunusinghe, D., Seo, J.K., Rao, A.L., 2011.** Subcellular localization and rearrangement of endoplasmic reticulum by Brome mosaic virus capsid protein. Journal of virology 85, 2953-2963.

4.   **Blackman, L.M., Boevink, P., Cruz, S.S., Palukaitis, P., Oparka, K.J., 1998.** The movement protein of cucumber mosaic virus traffics into sieve elements in minor veins of nicotiana clevelandii. The Plant cell 10, 525-538.

5.   **Boccard, F., Baulcombe, D., 1993.** Mutational analysis of cis-acting sequences and gene function in RNA3 of cucumber mosaic virus. Virology 193, 563-578.

6.   **Chaturvedi, S., Jung, B., Gupta, S., Anvari, B., Rao, A.L., 2012.** Simple and robust in vivo and in vitro approach for studying virus assembly. Journal of visualized experiments : JoVE.

7.   **Deane, C.M., Salwinski, L., Xenarios, I., Eisenberg, D., 2002.** Protein interactions: two methods for assessment of the reliability of high throughput observations. Molecular & cellular proteomics : MCP 1, 349-356.

8.   **Ding, S.W., Shi, B.J., Li, W.X., Symons, R.H., 1996.** An interspecies hybrid RNA virus is significantly more virulent than either parental virus. Proceedings of the National Academy of Sciences of the United States of America 93, 7470-7474.

9.   **Gal-On, A., Canto, T., Palukaitis, P., 2000.** Characterisation of genetically modified cucumber mosaic virus expressing histidine-tagged 1a and 2a proteins. Archives of virology 145, 37-50.

10.   **Grangeon, R., Agbeci, M., Chen, J., Grondin, G., Zheng, H., Laliberte, J.F., 2012.** Impact on the endoplasmic reticulum and Golgi apparatus of turnip mosaic virus infection. Journal of virology 86, 9255-9265.

11.   **Hwang, M.S., Kim, S.H., Lee, J.H., Bae, J.M., Paek, K.H., Park, Y.I., 2005.** Evidence for interaction between the 2a polymerase protein and the 3a movement protein of Cucumber mosaic virus. The Journal of general virology 86, 3171-3177.

12.   **Jacquemond, M., 2012.** Cucumber mosaic virus. Advances in virus research 84, 439-504.

13.   **Kao, C.C., Quadt, R., Hershberger, R.P., Ahlquist, P., 1992.** Brome mosaic virus RNA replication proteins 1a and 2a from a complex in vitro. Journal of virology 66, 6322-6329.

14.   **Kaper, J.M., Tousignant, M.E., Geletka, L.M., 1990.** Cucumber-mosaic-virus-associated RNA-5. XII. Symptom-modulating effect is codetermined by the helper virus satellite replication support function. Research in virology 141, 487-503.

15.   **Kim, S.H., Palukaitis, P., Park, Y.I., 2002.** Phosphorylation of cucumber mosaic virus RNA polymerase 2a protein inhibits formation of replicase complex. The EMBO journal 21, 2292-2300.

16.   **Nelson, B.K., Cai, X., Nebenfuhr, A., 2007.** A multicolored set of in vivo organelle markers for co-localization studies in Arabidopsis and other plants. The Plant journal : for cell and molecular biology 51, 1126-1136.

17. **O'Reilly, E.K., Paul, J.D., Kao, C.C., 1997.** Analysis of the interaction of viral RNA replication proteins by using the yeast two-hybrid assay. Journal of virology 71, 7526-7532.

18.   **O'Reilly, E.K., Tang, N., Ahlquist, P., Kao, C.C., 1995.** Biochemical and genetic analyses of the interaction between the helicase-like and polymerase-like proteins of the brome mosaic virus. Virology 214, 59-71.

19. **O'Reilly, E.K., Wang, Z., French, R., Kao, C.C., 1998.** Interactions between the structural domains of the RNA replication proteins of plant-infecting RNA viruses. Journal of virology 72, 7160-7169.

20.   **Palukaitis, P., Garcia-Arenal, F., 2003.** Cucumoviruses. Advances in virus research 62, 241-323.

21.   **Seo, J.K., Kwon, S.J., Rao, A.L., 2012.** A physical interaction between viral replicase and capsid protein is required for genome-packaging specificity in an RNA virus. Journal of virology 86, 6210-6221.

CONCLUSIONS AND FUTURE DIRECTIONS

The research presented in this dissertation is directed in understanding the replication mechanism of a member of Bromoviridae family, *Cucumber mosaic virus* and a satellite RNA (satRNA) associated with it and the role of host proteins involved therein. In **chapter 1**, using agrotransformants of *Brome mosaic* virus (BMV), various physiological conditions affecting virus replication and gene expression during agroinfiltration was evaluated. Some of the examined physiological conditions include the extent of necrosis induced in *N.benthamiana* by density (OD_{600}) of bacterial suspension, effect of various concentrations of *trans-* complemented viral genes such as capsid protein on replication etc. To this end, it was observed that, infiltration of bacterial suspensions of empty vector into *N. benthamiana* with densities above $OD_{600}=$ 1.0 often resulted in tissue yellowing. This yellowing correlated with degradation and poor quality of total RNA. Northern blot analysis of BMV replication assays indicated that optimal bacterial density for infiltration was between OD_{600} 0.1-0.5. Co-infiltration of empty vector with bacterial suspensions exceeding $OD_{600=}$ 0.1 significantly down regulated BMV replication. Similar down regulation of BMV replication was observed when bacterial suspensions of B4 (i.e. designed to express CP *in trans*) exceeding OD_{600} 0.1 were added. Taken together the results argue against previous conclusions that overexpression of BMV CP down regulates replication (Yi et al. 2009). Our results accentuate that an optimal

density of bacterial suspension of a given viral agrotransformant designed for either evaluating replication or for *tans*-complementation must be optimized.

In **chapter 2**, experiments were formulated to understand the mechanism of nuclear import of satRNA. A premise for this was based on a recent observation that satRNA has a propensity to enter nucleus either in the presence or absence of its helper CMV (Choi et al., 2012). A previous study involving *Potato Spindle Tuber* Viroid (PSTVd) has shown that Bromodomain containing RNA binding protein 1 (BRP 1) is intimately involved in transporting PSTVd to nucleus. An RNA tagging assay for satRNA in transgenic lines suppressed in BRP1 suggested nuclear import of satRNA is mediated by as BRP1. Further biochemical and cell biology experiments confirmed that BRP1 physically interacts with satRNA, and plays an integral role in the replication of satRNA (Chaturvedi et al., 2014). satRNA of CMV being a serious pathogen for economically important crops like tomato (Kaper et al., 1988), future experiments should evaluate the functionality of BRP1 in tomato using genome editing approach such as CRISPR (Zhang et al., 2014) followed by testing replication and pathogenesis of CMV and its satRNA in BRP1 suppressed tomato lines.

In **chapter 3**, an attempt is made to understand the change in plant proteome interacting with BRP1 when challenged with CMV or satRNA. Plants infected with CMV or its satRNA were co-immunoprecipitated with BRP 1-FLAG

and subjected to MudPIT analysis. The results indicated that a shift in the host protein interactome of BRP1 was observed when plants were challenged with CMV or its satRNA. Future research directions include evaluating the functionality of host proteins selected on the basis of their binding ability to BRP 1 in the replication of CMV and its satRNA.

Chapter 4 focuses on the role of two important host proteins in the replication of CMV. As summarized in chapters 2 and 3, replication of satRNA and CMV was down regulated in BRP1 suppressed lines of *N. benthamiana*. To understand the mechanism involved therein, co-immunoprecipitation followed by MuDPIT analysis of BRP1-FLAG with leaf extract infected with CMV was performed. The results suggested that BRP1 interacted with p1a of CMV, which was further confirmed by BiFC assay. This result suggests that BRP1 is an essential host protein in the replication of CMV and satRNA. It will be of interest to test, after interacting with p1a, whether BRP1 would promote interacting with other host proteins in assembling a functional replicase complex. Glyceraldehyde 3 phosphate dehydrogenase (GAPDH) has been found to play an important role in the replication of *Tomato bushy stunt virus* (Huang and Nagy, 2011) and Bamboo mosaic virus (Prasanth et al., 2011). From data obtained in chapter 3, GAPDH was selected based on the literature survey. To shed alight on the role of GAPDH in CMV replication, *Arabidopsis thaliana* (Col-0), lines defective in GAPDH were tested. The results accentuate that GAPDH is obligatory to support

CMV replication. Additional BiFC assays performed in GAPDH defective *A. thaliana* lines indicated that GAPDH plays an important role in either forming or stabilizing the p1a-p2a replicase complex. Further research can be carried out to understand if GAPDH directly interacts with 1a and/or 2a, or leads to this complex formation by interacting with some other host protein. This is the first attempt made in our lab to delineate role of host proteins in the replication of CMV. Hence, these results need to be confirmed by a thorough genotyping of single gene knockout lines, and determining expression level of the transiently expressed genes in the same.

In **chapter 5**, a riboproteomics approach was used to identify the host proteome interacting with satRNA. Ribo-proteomic allowed isolation and identification of host factors interacting with satRNA (+) or (-) polarity, in the presence or absence of helper virus (CMV). Evaluating the functionality of these host proteins in the replication of satRNA would be the topic for future study.

In **chapter 6 and 7**, live cell imaging of protein-protein interactions in BMV and CMV was performed using BiFC. For BMV, in addition to self-interactions, an interaction of CP with replicase protein p2a, but not p1a, was observed. By contrast, for CMV, CP was found to interact with both p1a and p2a. Future studies should focus in identifying the subcellular localization sites of each of

these with an eventual aim of understanding how these protein interactions would regulate overall biology and pathogenesis.

REFERENCE

1.   **Chaturvedi, S., Kalantidis, K., Rao, A.L., 2014.** A bromodomain-containing host protein mediates the nuclear importation of a satellite RNA of Cucumber mosaic virus. Journal of virology 88, 1890-1896.

2.   **Chaturvedi, S., RAO, A.L.N, 2014.** Live Cell Imaging of Interactions Between Replicase and Capsid Protein of Brome Mosaic Virus using Bimolecular Fluorescence Complementation: Implications for Replication and Genome Packaging. Virology.

3.   **Choi, S.H., Seo, J.K., Kwon, S.J., Rao, A.L., 2012.** Helper virus-independent transcription and multimerization of a satellite RNA associated with cucumber mosaic virus. Journal of virology 86, 4823-4832.

4.   **Elena, S.F., Dopazo, J., de la Pena, M., Flores, R., Diener, T.O., Moya, A., 2001.** Phylogenetic analysis of viroid and viroid-like satellite RNAs from plants: a reassessment. Journal of molecular evolution 53, 155-159.

5.   **Huang, T.S., Nagy, P.D., 2011**. Direct inhibition of tombusvirus plus-strand RNA synthesis by a dominant negative mutant of a host metabolic enzyme, glyceraldehyde-3-phosphate dehydrogenase, in yeast and plants. Journal of virology 85, 9090-9102.

6.   **Kalantidis, K., Denti, M.A., Tzortzakaki, S., Marinou, E., Tabler, M., Tsagris, M., 2007.** Virp1 is a host protein with a major role in Potato spindle tuber viroid infection in Nicotiana plants. Journal of virology 81, 12872-12880.

7.   **Kaper, J.M., Tousignant, M.E., Steen, M.T., 1988.** Cucumber mosaic virus-associated RNA 5. XI. Comparison of 14 CARNA 5 variants relates ability to induce tomato necrosis to a conserved nucleotide sequence. Virology 163, 284-292.

8.   **Prasanth, K.R., Huang, Y.W., Liou, M.R., Wang, R.Y., Hu, C.C., Tsai, C.H., Meng, M., Lin, N.S., Hsu, Y.H., 2011.** Glyceraldehyde 3-phosphate dehydrogenase negatively regulates the replication of Bamboo mosaic virus and its associated satellite RNA. Journal of virology 85, 8829-8840.

9.   **Yi, G., Letteney, E., Kim, C.H., Kao, C.C., 2009.** Brome mosaic virus capsid protein regulates accumulation of viral replication proteins by binding to the replicase assembly RNA element. Rna 15, 615-626.

10.   **Zhang, F., Wen, Y., Guo, X., 2014.** CRISPR/Cas9 for genome editing: progress, implications and challenges. Human molecular genetics.